

## **Response to Referee Comment 1 (RC1) on “Rapid transition in winter aerosol composition in Beijing from 2014 to 2017: response to clean air actions” by H. Li et al.**

In past publications, the authors have reported on the effects of emission controls on China’s air quality. This paper focuses on how those emission changes affect aerosol chemical composition. The authors present a comprehensive analysis involving measurements and models to assess the role of just emissions, apart from transport and meteorological differences. The results are interesting and the topic appropriate for this journal, however some details were missing and in many cases the analysis or description of processes was not of sufficient technical detail, such as the thermodynamic analysis. Also, strong conclusions are made with limited analysis to support them. For example, a major finding seems to be that these changes in emissions altered the aerosol formation mechanisms. It is stated in the Abstract and Conclusions that lower SO<sub>2</sub> suppressed rapid sulfate formation through heterogeneous reactions. But it is not clear that this is really shown or tested in a quantitative way, instead it seems to be mostly speculation, based mainly on this hypotheses being consistent with the observations. Line 324 simply states: the results here imply that: : : Could not a chemical transport model, or maybe a simpler 0-D or 1D box model be run to further test this hypothesis? Overall, my recommendation is that the authors check closely if their reported findings are truly supported in the manuscript by quantitative analyses, and if only based on a consistency with expectations, that this clearly be stated. More detailed comments are provided below.

We would like to thank Rodney Weber for giving the constructive and helpful comments and suggestions, especially for the discussions on thermodynamic analysis. In the revised manuscript, more technical details about the thermodynamic analysis have been added according to the comments. One finding that the decrease in SO<sub>2</sub> emissions suppressed the rapid sulfate formation through heterogeneous reactions was speculated based on the ambient observations. We found that compared to the fast SO<sub>2</sub>-to-sulfate formation starting from a RH threshold of ~50% in 2014, the promptly increased sulfate formation through heterogeneous reactions was observed to delay to a higher RH of 70% in 2017. Therefore, this is one hypothesis based on the consistency with ambient observations. We have clearly stated it in the Abstract, Sect. 3.2.4, and Conclusions in the manuscript.

In the following, we will answer the comments point by point.

Specific Comments:

Line 59-60; I would think atmospheric chemical reactions (secondary aerosol) and deposition would also be a major contributor to PM<sub>2.5</sub> composition.

Agreed. We slightly modified the sentence to “The chemical composition of PM<sub>2.5</sub> is mainly affected by the following factors: precursor emissions, meteorological conditions, atmospheric chemical reactions, and regional transport and deposition”.

Line 136 to 137, in giving the ambient data vs model comparison, state the integration time, ie 24 hr average data?

It has been clearly stated that the data are 24-hour averages.

ISORROPIA calculations: In this paper the model is run without considering nonvolatile cations. Maybe a few words should be added why this is ok, ie, it may be argued that for PM<sub>1</sub> this is reasonable. As another example, the nitrate considered in the paper is all semivolatile nitrate (ie, NH<sub>4</sub>NO<sub>3</sub>), but it is possible that nonvolatile nitrate also exists in the ambient PM<sub>2.5</sub> (eg, Ca(NO<sub>3</sub>)<sub>2</sub>). Thus if Ca<sup>2+</sup> was considered in the thermodynamic calculations, it could affect predicted pH and NO<sub>3</sub><sup>-</sup> concentrations. Most of this Ca<sup>2+</sup> would likely be in the 1 to 2.5 μm range, and since the comparison between PM<sub>1</sub> and PM<sub>2.5</sub> mass is reasonable, the authors could argue that it is not a large contribution. Also, I suggest the authors specifically note what RH range was used in the thermodynamic calculations, many of the assumptions, such as no separate organic/inorganic phases,

etc, may be less likely at lower RH. (say <40 to 50%). Line 231-232 notes that the observed RH was about 33 to 34% in the winter of 2017. This a very low RH to comfortably run ISORROPIA under the metastable assumption without some test on the reliability of the results.

Indeed, including nonvolatile cations in ISORROPIA calculations would influence the model results. But as the reviewer said, nonvolatile cations, i.e.,  $\text{Na}^+$ ,  $\text{K}^+$ ,  $\text{Ca}^{2+}$ ,  $\text{Mg}^{2+}$ , mainly exists in the size range of 1.0 to 2.5  $\mu\text{m}$  in particles and has a minor contribution to  $\text{PM}_{10}$ . Therefore, nonvolatile cations are not considered in pH calculation in this study. A previous study by Song et al. (2018) showed that including nonvolatile cations in ISORROPIA calculations did not significantly change the particle pH. Discussions about the effects of nonvolatile cations on pH calculations have been added in the manuscript “The effects of nonvolatile cations (i.e.,  $\text{Na}^+$ ,  $\text{K}^+$ ,  $\text{Ca}^{2+}$ ,  $\text{Mg}^{2+}$ ) are not considered in this study because the fraction of nonvolatile cations in  $\text{PM}_{10}$  in Beijing is generally negligible compared to  $\text{SO}_4^{2-}$ ,  $\text{NO}_3^-$ , and  $\text{NH}_4^+$  (Sun et al., 2014). Although nonvolatile nitrate may exist in ambient particles as  $\text{Ca}(\text{NO}_3)_2$  and  $\text{Mg}(\text{NO}_3)_2$ ,  $\text{Ca}^{2+}$  and  $\text{Mg}^{2+}$  are mainly abundant at sizes above 1  $\mu\text{m}$  (Zhao et al., 2017). In addition, the mixing state of  $\text{PM}_{10}$  nonvolatile cations with  $\text{SO}_4^{2-}$ ,  $\text{NO}_3^-$ , and  $\text{NH}_4^+$  remains to be investigated (Guo et al., 2016, 2017). Previous studies showed that including the nonvolatile cations in ISORROPIA-II does not significantly affect the pH calculations unless the cations become important relative to anions (Guo et al., 2016; Song et al., 2018). The sensitivity test for Beijing winter conditions suggested that with nonvolatile cations, the predicted pH values increase by about 0.1 units.”

We agree with the reviewer that RH ranges influence the liquid or solid phases of atmospheric aerosols. So far, there are no observational data showing whether aerosols are in a metastable or stable state in Beijing wintertime (Song et al., 2018). According to previous studies, at low RH, especially when  $\text{RH} < 20\%$  or  $30\%$ , aerosols are less likely to be in a completely liquid state (Fountoukis and Nenes, 2007; Guo et al., 2016, 2017). Therefore, we exclude periods when  $\text{RH} < 30\%$  in this study. After that, an average RH value of 50% is now used in the thermodynamic calculations assuming that aerosols were in metastable states. We also did a sensitivity study assuming that solid phases are present. For that case, over 88% of the data resulted in pH values approximating 7.6 with few variations, which is unrealistic. After the correction, the average pH values for year 2013, 2014, and 2017 are 4.5, 4.8, and 5.3, respectively. The results indicate a moderately acidic condition for aerosols in Beijing in winter, consistent with previous studies (Guo et al., 2017; Liu et al., 2017; Song et al., 2018). The correction did not change the trend of pH variation from 2013 to 2017 because the reduced sulfate concentration played a dominant role in pH variation. The corresponding explanations and corrections have been added and updated in the manuscript. “Up to now, there are no observational data showing whether aerosols are in a metastable or stable state in Beijing in winter (Song et al., 2018). According to previous studies, at low RH ( $\text{RH} < 20\%$  or  $30\%$ ), aerosols are less likely to be in a completely liquid state (Fountoukis and Nenes, 2007; Guo et al., 2016, 2017). Therefore, periods with  $\text{RH} < 30\%$  were excluded in this study.” “During 2013-2017, the average particle pH varied from 4.5 to 5.3, with a significant decrease in sulfate concentration, resulting in a more neutral atmospheric environment. The pH values here agree reasonably with previous ISORROPIA-II calculations, showing that fine particles are moderately acidic in northern China during wintertime (Guo et al., 2017; Liu et al., 2017; Song et al., 2018).”

Figures in the manuscript showing the results of thermodynamic analysis have also been updated:

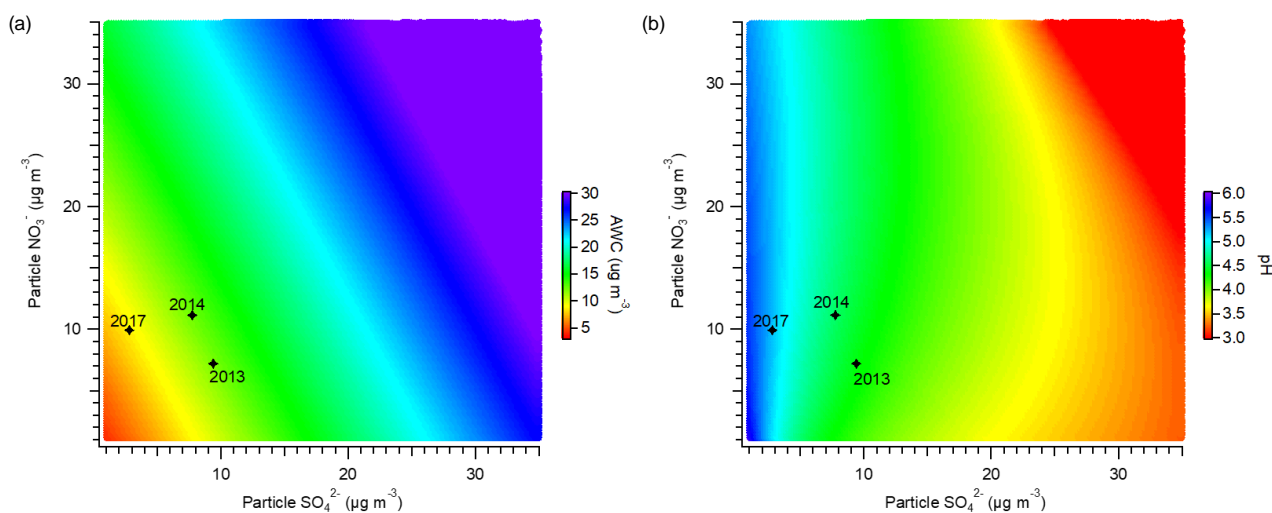


Figure 9. Sensitivity of (a) AWC and (b) particle pH to the mass concentrations of particulate sulfate and nitrate. The stars indicate the average winter conditions for the years 2013, 2014, and 2017.

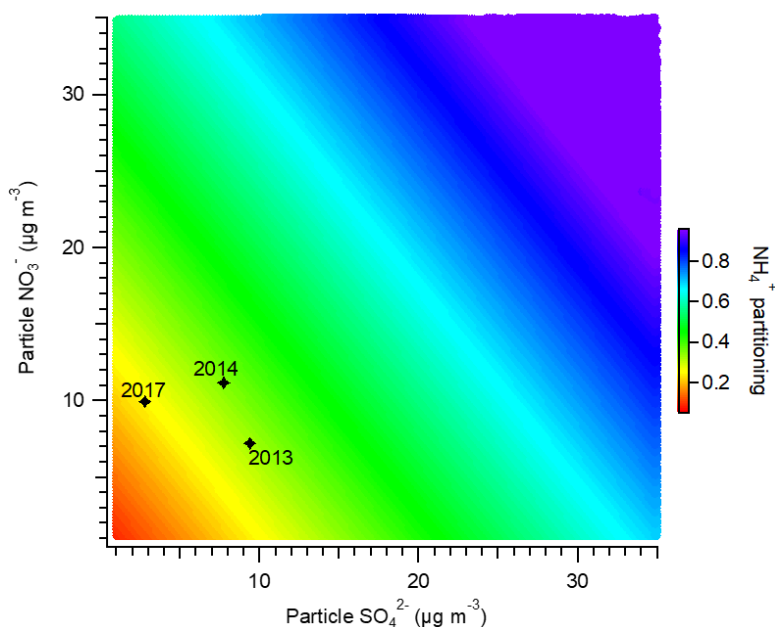


Figure 10. Sensitivity of the ammonium partitioning ratio to the mass concentrations of particulate sulfate and nitrate. The stars indicate the average winter conditions for the years 2013, 2014, and 2017.

In the experimental section, there was no discussion of measurement of  $\text{HNO}_3$  or  $\text{NH}_3$  (gas species), yet ISORROPIA was run such that these data are needed, ie, run in forward mode. More information is needed in the paper on how the model was run without these critical gas phase species.

To investigate how the variations in particulate nitrate and sulfate concentrations affect aerosol properties, this study used ISORROPIA-II to generate the contour plots in Fig. 9 and Fig. 10. ISORROPIA-II was run in the forward mode, which calculates the equilibrium partitioning with the total concentration of both gas and particle phase species. Previous study shows that the forward mode is less sensitive to measurement error than the reverse mode (Hennigan et al., 2015). To run the model, a selected sulfate concentration with the average temperature, RH, and total ammonia concentration ( $\text{NH}_3 + \text{NH}_4^+$ ) during the winters of 2014 and 2017 was input to ISORROPIA-II, where the total nitrate concentration ( $\text{HNO}_3 + \text{NO}_3^-$ ) was left as the free variable. The gaseous  $\text{HNO}_3$  and  $\text{NH}_3$  concentrations were not directly measured in this work. To estimate the  $\text{NH}_3$  concentration, an empirical equation derived based on long-term measurements in winter in Beijing was

applied,  $\text{NH}_3$  (ppb) =  $0.34 \times \text{NO}_x$  (ppb) + 0.63 (Meng et al., 2011). On average, the  $\text{NH}_3$  concentration was estimated to be around  $14.0 \mu\text{g m}^{-3}$  during the winters of 2014 and 2017 in Beijing, consistent with previous observations in the same season (Meng et al., 2011; Zhao et al., 2016; Zhang et al., 2018). For gaseous  $\text{HNO}_3$ , the total  $\text{NO}_3^-$  concentration ( $\text{HNO}_3 + \text{aerosol NO}_3^-$ ) varying from 0.2 to  $75 \mu\text{g m}^{-3}$  was used as the input.

More discussions about the consideration of gaseous  $\text{HNO}_3$  and  $\text{NH}_3$  concentrations have been added in the manuscript as follows: “The gaseous  $\text{HNO}_3$  and  $\text{NH}_3$  concentrations were not directly measured during our campaign. But long-term measurements in Beijing showed that gaseous  $\text{NH}_3$  concentration correlated well with  $\text{NO}_x$  concentration in winter (Meng et al., 2011). Therefore, the empirical equation derived from Meng et al. (2011),  $\text{NH}_3$  (ppb) =  $0.34 \times \text{NO}_x$  (ppb) + 0.63, was applied to estimate the gaseous  $\text{NH}_3$  concentration. On average, the  $\text{NH}_3$  concentration was approximated to be  $14.0 \mu\text{g m}^{-3}$  during the winters of 2014 and 2017, consistent with previous observations in the same season of Beijing (Meng et al., 2011; Zhao et al., 2016; Zhang et al., 2018). The total nitrate concentration, including both gaseous  $\text{HNO}_3$  and particulate nitrate, varied from 0.2 to  $75 \mu\text{g m}^{-3}$  for the sensitivity study.”

Line 175 or in Table 1 title state this is observational data (not model).

It has been clearly stated in the title of Table 1.

Line 258, what does Until 2017 mean? These changes were completed by 2017?

It means that these changes have been completed by the end of 2017. To make it more clearly, we changed “Until 2017” to “By the end of 2017”.

Line 311, does not tell the complete story. There are publications, see below, that show the predictions of Cheng et al. 2016 and Wang et al, 2016 are likely not correct due to their incorrect calculation of fine particle pH and that this proposed heterogeneous chemistry is highly sensitive to pH. This counter argument should also be noted here in this paper for completeness.

Liu, M., Y. Song, T. Zhoh, Z. Xu, C. Yan, M. Zheng, Z. Wu, M. Hu, Y. Wu, and T. Zhu (2017), Fine Particle pH during Severe Haze Episodes in Northern China, *Geophys. Res. Lett.*, 10.1002/2017GL073210.

Guo, H., R. J. Weber, and A. Nenes (2017), High levels of ammonia do not raise fine particle pH sufficiently to yield nitrogen oxide-dominated sulfate production, *Sci. Reports*, 7(12109), DOI:10.1038/s41598-41017-11704-41590.

Song, S., M. Gao, W. Xu, J. Shao, G. Shi, S. Wang, Y. Wang, Y. Sun, and M. B. McElroy (2018), Fine particle pH for Beijing winter haze as inferred from different thermodynamic equilibrium models, *Atm. Chem. Phys.*, 18, 7423-7438.

Agreed. The corresponding argument has been noted in the manuscript as follows: “Recently, studies have found that  $\text{SO}_2$  oxidation by  $\text{NO}_2$  in aerosol water with near neutral aerosol acidity, which is usually ignored in current model simulations, plays an important role in the persistent formation of sulfate during haze events in northern China (B. Zheng et al., 2015; Cheng et al., 2016; Wang et al., 2016). Others pointed out that regardless of the high  $\text{NH}_3$  levels, aerosols are always moderately acidic in northern China, and there are probably other alternative formation pathways contributing to fast sulfate production in haze pollution (Guo et al., 2017b; Liu et al., 2017; Song et al., 2018).”

Line 318-319, define SOR and NOR (ie, what does the acronym stand for?)

The SOR and NOR stand for sulfur oxidation ratio and nitrogen oxidation ratio, respectively. This has been clearly clarified in the manuscript as “The sulfur oxidation ratio (SOR) and nitrogen oxidation ratio (NOR) were further estimated as the molar ratio of sulfate to the sum of sulfate and  $\text{SO}_2$  and the molar ratio of nitrate to the sum of nitrate and  $\text{NO}_x$ , respectively, to quantify the degree of  $\text{SO}_2$  and  $\text{NO}_x$  oxidations (Zheng et al., 2015; Li et al., 2016).”

Lines 339 to 344. Although this discussion tends to follow the Seinfeld and Pandis discussion of sulfate/nitrate/ammonium interactions, it is largely based on weak intuitive arguments and not a rigorous thermodynamic discussion. It is suggested that these types of statements be avoided. Below are possible other ways to discuss the interplay between sulfate, nitrate and ammonium and gas species, nitric acid and ammonia:

Change: Particulate nitrate in PM<sub>2.5</sub> is mainly formed through the neutralization of HNO<sub>3</sub> with NH<sub>3</sub> to something like: Semivolatile PM<sub>2.5</sub> particulate nitrate is formed through the partitioning of HNO<sub>3</sub> to the particle phase, which is more favored at higher aerosol pH. pH is affected by gas phase NH<sub>3</sub> concentrations, where higher NH<sub>3</sub> generally leads to higher pH and so possibly more particulate nitrate.

Thanks for the suggestions. We have revised the text accordingly.

Change: Nitrate formation was also affected by the competition for available NH<sub>3</sub> between sulfate and nitrate. In the atmosphere, NH<sub>3</sub> prefers to react first with H<sub>2</sub>SO<sub>4</sub> to form ammonium sulfate due its stability. To: Because sulfate is nonvolatile, when it is a significant fraction of the aerosol mass it has a dominant influence on aerosol pH, making the aerosol acidic (low pH). In contrast ammonium and nitrate are semivolatile and so their particle-phase concentrations depend on the meteorological conditions (T, RH) their corresponding gas phase concentrations, (NH<sub>3</sub> and HNO<sub>3</sub> respectively) and aerosol pH. For example, at high sulfate and moderate NH<sub>3</sub> concentrations the aerosol can be too acidic for partitioning of HNO<sub>3</sub>, but at higher NH<sub>3</sub>, or if sulfate concentrations drop sufficiently (or RH increases), particle pH will increase and can reach a point at which HNO<sub>3</sub> partitioning can occur and nitrate aerosol formed. Lower T also favors partitioning to the particle phase through Henry's law constants.

Thanks for the suggestions. We have modified the text accordingly.

As for the last line, when RH>60% maybe an additional explanation for the trend in Fig8d is that as RH increases liquid water levels increase resulting in higher pH, which allows more nitrate to partition to the aerosol through a feedback loop, as is discussed later in the paper. That is, the increase in NOR may be due to more than just heterogeneous nitrate production.

Agreed. This additional explanation has been added as “In addition, as RH increases, the AWC increases accordingly, resulting in higher aerosol pH. This allows more semivolatile nitrate to partition to the particle phase through a feedback loop, thus favoring the formation of particulate nitrate.”

Line 366-369, In Fig S9a provide a reference for the calculation of epsilon(NO<sub>3</sub><sup>-</sup>). This pH of 3 at which the sensitivity of epsilon(NO<sub>3</sub><sup>-</sup>) changes, as found in this work, was discussed in detail by Guo et al., ACP 2018, which should be cited.

A reference for the calculation of  $\epsilon(\text{NO}_3^-)$  has been added. The reference of Guo et al., ACP 2018, has been cited.

Finally, there are a number of studies reporting pH in Beijing over different periods. Some of these did analysis to test the thermodynamic model predictions, which was not done here. A summary of these papers and comparison to pH reported in this paper is warranted to support this analysis.

According to the comments above regarding the thermodynamic analysis, summarization of previous studies reporting pH in Beijing and comparison with results in this study have been included in the manuscript. In addition, more information were added: “Previous studies showed that including the nonvolatile cations in ISORROPIA-II does not significantly affect the pH calculations unless the cations become important relative to anions (Guo et al., 2016; Song et al., 2018). The sensitivity test for Beijing winter conditions suggested that with nonvolatile cations, the predicted pH values increase by about 0.1 units.”

## References

- Fountoukis, C., and Nenes, A.: ISORROPIA II: a computationally efficient thermodynamic equilibrium model for  $K^+$ - $Ca^{2+}$ - $Mg^{2+}$ - $NH_4^+$ - $Na^+$ - $SO_4^{2-}$ - $NO_3^-$ - $Cl^-$ - $H_2O$  aerosols, *Atmos Chem Phys*, 7, 4639-4659, 2007.
- Guo, H., Sullivan, A. P., Campuzano-Jost, P., Schroder, J. C., Lopez-Hilfiker, F. D., Dibb, J. E., Jimenez, J. L., Thornton, J. A., Brown, S. S., Nenes, A., and Weber, R. J.: Fine particle pH and the partitioning of nitric acid during winter in the northeastern United States, *Journal of Geophysical Research: Atmospheres*, 121, 10,355-310,376, 10.1002/2016JD025311, 2016.
- Guo, H., Weber, R. J., and Nenes, A.: High levels of ammonia do not raise fine particle pH sufficiently to yield nitrogen oxide-dominated sulfate production, *Scientific Reports*, 7, 12109, 10.1038/s41598-017-11704-0, 2017.
- Hennigan, C. J., Izumi, J., Sullivan, A. P., Weber, R. J., and Nenes, A.: A critical evaluation of proxy methods used to estimate the acidity of atmospheric particles, *Atmos. Chem. Phys.*, 15, 2775-2790, <https://doi.org/10.5194/acp-15-2775-2015>, 2015.
- Liu, M., Song, Y., Zhou, T., Xu, Z., Yan, C., Zheng, M., Wu, Z., Hu, M., Wu, Y., and Zhu, T.: Fine particle pH during severe haze episodes in northern China, *Geophys Res Lett*, 44, 5213-5221, 10.1002/2017GL073210, 2017.
- Meng, Z. Y., Lin, W. L., Jiang, X. M., Yan, P., Wang, Y., Zhang, Y. M., Jia, X. F., and Yu, X. L.: Characteristics of atmospheric ammonia over Beijing, China, *Atmos. Chem. Phys.*, 11, 6139-6151, <https://doi.org/10.5194/acp-11-6139-2011>, 2011.
- Song, S., Gao, M., Xu, W., Shao, J., Shi, G., Wang, S., Wang, Y., Sun, Y., and McElroy, M. B.: Fine-particle pH for Beijing winter haze as inferred from different thermodynamic equilibrium models, *Atmos. Chem. Phys.*, 18, 7423-7438, <https://doi.org/10.5194/acp-18-7423-2018>, 2018.
- Zhao, M., Wang, S., Tan, J., Hua, Y., Wu, D., and Hao, J.: Variation of Urban Atmospheric Ammonia Pollution and its Relation with PM<sub>2.5</sub> Chemical Property in Winter of Beijing, China, *Aerosol Air Qual Res*, 16, 1378-1389, 10.4209/aaqr.2015.12.0699, 2016.
- Zhang, Y., Tang, A., Wang, D., Wang, Q., Benedict, K., Zhang, L., Liu, D., Li, Y., Collett Jr., J. L., Sun, Y., and Liu, X.: The vertical variability of ammonia in urban Beijing, China, *Atmos. Chem. Phys.*, 18, 16385-16398, <https://doi.org/10.5194/acp-18-16385-2018>, 2018.

## **Response to Referee Comment 2 (RC2) on “Rapid transition in winter aerosol composition in Beijing from 2014 to 2017: response to clean air actions” by H. Li et al.**

This study combines in-situ measurements of PM<sub>1</sub> composition in Beijing during the winters of 2014 and 2017 and the simulation results from a regional chemical transport model to investigate the impacts that the clean air actions in China have had on aerosol chemistry. The relative contributions of anthropogenic emissions, meteorological conditions, and regional transport to the changes in aerosol composition in Beijing are also investigated. This is an interesting work and provides a timely and relevant analysis of a current problem – how aerosol pollution in Beijing responded to the implementation of the Air Pollution Prevent and Control Policy. Overall, the manuscript is well written and fits well within ACP’s aims and scope. However, the current version may require substantial revision before publication can be considered. A major shortcoming in this manuscript is that the Methods section is very much lacking of important technical details, for example on aerosol source contribution analysis and CMT model performance, thereby raises doubts about the credibility of the results. Moreover, there are some inconsistencies in the results and discussions which could cause concerns about the quality of the data, representativeness of the findings, or validity of the conclusions. Additionally, the figure legends and captions are often too brief to make the figures understandable.

We thank the reviewer for the positive feedback and helpful comments. In the revised manuscript, more technical details in the Method section have been added. In the following, we will answer the comments point by point.

Detailed comments:

Line 44-46, how much did air pollutants reduce between 2013 – 2017 in the Beijing area?

Emission changes of different air pollutants in Beijing with the implementation of the clean air actions was analyzed in details in Section 3.2.2 and Figure 6.

Section 2.2. is cursory and provides very little information on the organic aerosol source apportionment analysis. Details must be provided on how the PMF/ME-2 analysis of the ACSM data was performed, what data treatments were implemented, and how the solution conditions (eg number of factors, a value, fpeak) were selected and evaluated.

For the ME-2 analysis of the ACSM organic data, the mass spectra and error matrices were prepared based on the procedures given by Ulbrich et al. (2009) and Zhang et al. (2011). Detailed evaluations of different solutions were provided in the Supplement (Figs. S2-11), including the factor time series, mass spectra, and diurnal patterns with different  $a$  values. Corresponding changes can be found in the revised manuscript and Supplement.

In Section 2.3. more information should be provided on the performance of the CMT model at simulating PM<sub>2.5</sub> composition and how the modeling results compare to observations for 2014 and 2017 winters separately.

As the reviewer suggested, we added more information about the evaluation of the CMT model performance in Section 2.3 and the Supplement (Table S1-2, Fig. S12).

Section 2.5 lists three assumptions about aerosol properties in the ISORROPIA modeling. Several references are cited and claimed to support these assumptions for this study. But upon reading the references more closely, they don’t seem so as the references either talked about aerosols from different locations or under different meteorological conditions, or simply did not provide direct evidence on aerosol physical states. In fact, given the wintry weather (very low RH and T) and intense local emissions in Beijing, it is hard to believe that internal mixing and single aqueous phase were the prevailing aerosol conditions relevant to this work.

When running the ISORROPIA model, it is assumed that aerosols are internally mixed and composed of a single aqueous phase. Previous study in Beijing during wintertime showed that ISORROPIA predictions with these assumptions were in good agreement with observations (Liu et al., 2017). Up to now, there are no observational data showing whether aerosols are in a metastable (only liquid) or stable (solid plus liquid) state in Beijing in winter (Song et al., 2018). At low RH (RH < 20% or 30%), aerosols are less likely to be in a completely liquid state (Fountoukis and Nenes, 2007; Guo et al., 2016, 2017). Therefore, periods with RH < 30% were excluded in this study and aerosol solutions were assumed to be metastable. Particle liquid-phase separations can occur between the inorganic and organic components. It remains unclear how the phase separations influence pH values. A recent laboratory study suggested that the pH value of the organic-rich fraction under phase separation is about 0.4 units higher than that for a fully mixed aqueous phase (Dallemagne et al., 2016; Song et al., 2018).

Line 168 – 171, there was no mentioning of NH<sub>3</sub> and HNO<sub>3</sub> measurements in 2.1., but it is mentioned here that the values of NH<sub>3</sub>+NH<sub>4</sub> and NO<sub>3</sub>+HNO<sub>3</sub> were input into the model. Where did the NH<sub>3</sub> and HNO<sub>3</sub> data come from?

In the revised manuscript, discussions were added about how the gas-phase NH<sub>3</sub> and HNO<sub>3</sub> were considered in this study. “The gaseous HNO<sub>3</sub> and NH<sub>3</sub> concentrations were not directly measured during our campaign. But long-term measurements in Beijing showed that gaseous NH<sub>3</sub> concentration correlated well with NO<sub>x</sub> concentration in winter (Meng et al., 2011). Therefore, the empirical equation derived from Meng et al. (2011), NH<sub>3</sub> (ppb) = 0.34 × NO<sub>x</sub> (ppb) + 0.63, was applied to estimate the gaseous NH<sub>3</sub> concentration. On average, the NH<sub>3</sub> concentration was approximated to be 14.0 μg m<sup>-3</sup> during the winters of 2014 and 2017, consistent with previous observations in the same season of Beijing (Meng et al., 2011; Zhao et al., 2016; Zhang et al., 2018). The total nitrate concentration, including both gaseous HNO<sub>3</sub> and particulate nitrate, varied from 0.2 to 75 μg m<sup>-3</sup> for the sensitivity study.”

Line 110, missing numbers after “0.” What “a” values were used?

For the ME-2 analysis, an optimal solution of four factors with the *a* value of 0 was accepted.

Line 167 -168, what does “the transition in aerosol composition” mean in this sentence?

The transition in aerosol composition refers to the variations in nitrate and sulfate concentrations. During the winters of 2014-2017, the mass concentrations of both sulfate and nitrate decreased due to the implementation of the clean air actions. The reduction in sulfate concentration was higher than that in nitrate concentration. In this study, we investigated how the variations in nitrate and sulfate concentrations influence particle properties.

Line 186 – 188, the Xu et al. study was also conducted in Beijing in the winters of similar years, but the nitrate to sulfate ratios reported there were much lower than in this study. Normal measurement uncertainty could not explain such large discrepancies (more than a factor of two in difference). Was it due to measurement artifacts or does it suggest some issues with the representativeness of the measurement data? What’s the implication for the validity of the conclusions presented in this paper?

The study by Xu et al. (2019b) performed aerosol measurements in Beijing from the mid of November to the mid of December in 2014 and 2016. In this work, field measurements were conducted in Beijing from 6 December to 27 February in the year of 2014 and from 11 December to 2 February in the year of 2017. For the same year of 2014, ambient observations were performed in different months in the study by Xu et al. (2019b) and in this work. Different emission intensities and different meteorological conditions influence the formation of particulate nitrate and sulfate in different months. In this work, one of the conclusions is that the ratio of nitrate/sulfate was higher in winter 2017 than in winter 2014 with the implementation of the clean air actions. The decrease in nitrate concentration was larger in the winter of 2017 than in the winter of 2014. This is consistent with the conclusions by Xu et al. (2019b).

Line 205 – 206, organics were higher than sulfate and nitrate and in both 2014 and 2017, so calling Beijing aerosol pollution being “sulfate-driven” or “nitrate-driven” does not seem logical.

The driving factors in this work refers to the species whose mass fractions increased with the increase of aerosol loadings, consistent with the discussions in previous studies (Wang et al., 2014, Li et al., 2017, 2018; Sun et al., 2018; Xu et al., 2019a). The driving factors favored the development of haze pollution and the increase of aerosol mass concentrations. While organics composed a high fraction of aerosols in both 2014 and 2017, the mass fraction of organics in aerosols decreased with the increase of aerosol loadings.

Line 259, for coal usage reduction in addition to quoting the absolute amount, it would be also interesting in knowing the relative amount of reduction.

The total coal usage for coal-fired boilers is around 20.4 million tons in Beijing in 2013. By the end of 2017, the coal use was reduced by more than 17 million tons in Beijing due to emission controls of coal-fired boilers. In other way, the coal usage in Beijing was reduced by ~83% for coal-fired boilers compared to 2013.

Figure 2, according to the diurnal profiles, HOA concentration in 2014 was 2-3 times lower than 2017. If HOA is representative of emissions from transportation, is this level of decrease consistent with the decrease in emissions according to emission inventory? Moreover, the decrease of BC concentration from 2014 to 2017 was between 30-40% but the reduction of total combustion POA (sum of CCOA, BBOA and HOA) was close to 70%. This would suggest some very large, probably unrealistic, changes in the combustion emission factors.

Compared with 2014, the HOA concentration in 2017 was reduced by around 50%. Consistently, emissions of primary organic carbon from transportation decreased by around 30% in Beijing from 2014 to 2017 according to the emission inventory. Compared to 2014, both BC concentration and POA concentration were reduced largely in 2017. This is not only caused by the changes in the combustion emission factors via the more advanced control technology but also contributed by the reduced usage of traditional fuels, i.e., coal and biomass, through the application of clean energy.

Line 289 – 292, the comparisons of PM1 concentrations between different air trajectory classes do not logically lead to a conclusion about how much Beijing aerosol was influenced by polluted air masses transported from surrounding areas. Beijing has local pollution sources which could cause high PM events as well. In fact, in the paragraph immediately beneath, the authors reported that CMT simulation indicates that regional transport contributes to only 30 -40% of PM2.5 in Beijing.

Back trajectory analysis shows the air masses paths as they move through time and space before they arrive at the receptor site. Different aerosol concentrations for different air masses indicate the influence of regional transport. For example, due to the high emissions of air pollutants and severe aerosol pollutions in the southern surrounding areas of Beijing, air masses transported from the south of Beijing usually showed higher PM<sub>1</sub> concentrations than the air masses from others regions. According to back trajectory analysis, Beijing was less influenced by polluted air masses from surrounding areas in 2017. This is consistent with the results of CMT model simulations, which showed that the lower PM<sub>2.5</sub> concentration from regional transport contributed around 40% to PM<sub>2.5</sub> reduction in Beijing in 2017. The results are not contradictory to the main conclusion that emission reductions in Beijing and its surrounding regions played a dominant role in air quality improvement during 2014-2017.

Section 3.2.4, 2nd paragraph, what are the rationales for using SO<sub>4</sub>/BC and NO<sub>3</sub>/BC ratios in the analysis? Sulfate is a secondary species with formation time scales usually much longer than the emission time scales of BC. So the physical meaning of SO<sub>4</sub>/BC ratio is unclear.

The absolute concentration of sulfate and nitrate in the atmosphere is not only controlled by atmospheric chemical reactions but also influenced by boundary layer developments. By using SO<sub>4</sub>/BC and NO<sub>3</sub>/BC in the analysis, we can see more clearly how the secondary formation of sulfate and nitrate varied compared to primary emissions.

Section 3.2.4, 2nd paragraph, nitrate/(nitrate+NO<sub>x</sub>) is not a proper index for the oxidation ratio of nitrogen. Discussions related to NOR should be either removed or revised.

According to the ISORROPIA calculations in this study, the fraction of particulate nitrate in total nitrate was higher than 0.99 for the average winter conditions in both 2014 and 2017. Therefore, it is meaningful to use  $\text{nitrate}/(\text{nitrate}+\text{NO}_x)$  to evaluate the oxidation ratio of nitrogen without the consideration of gas-phase  $\text{HNO}_3$ .

For the discussions of the relationship between SOR and RH, it is important to point out that RH was measured locally at the sampling site but sulfate was mostly formed on a regional scale, ie, in air masses upwind of Beijing. Is it valid to assume that in-situ RH measurement data are representative of the RH conditions in the air masses where sulfate was formed?

The locally measured RH was largely influenced by the RH of the air masses transported from the upwind direction. For example, the RH in Beijing is usually low when the dry northwesterly/northeasterly air masses arrive. When Beijing is influenced by the humid southerly air masses, the RH in Beijing is high (An et al., 2019). Therefore, in-situ RH measurements are representative of the RH conditions in the air masses where sulfate was formed. Relationship between sulfate and the locally measured RH has been discussed a lot by previous studies (Zheng et al., 2015; Li et al., 2017; Fang et al., 2019).

Line 330 -331, does the higher SOR in 2017 than 2014 necessarily demonstrate “a higher sulfate production rate in 2017”? A relatively larger contribution from background air masses could also lead to higher SOR.

With the implementation of the clean air actions,  $\text{SO}_2$  emissions were reduced in both Beijing and the surrounding regions. According to back trajectory analysis, Beijing was less influenced by polluted air masses from regional transport in 2017 and sulfate contributed a smaller fraction in the air masses transported from surrounding areas. Therefore, the higher SOR in 2017 than 2014 indicates the higher sulfate production rate in 2017.

Line 544- 545, this citation is incomplete

Updated.

Figures in the supplementary materials are fuzzy, need to use better resolution.

The fuzzy figures in the Supplement have been updated to better resolution.

Figure S6d, explain how to read the figure and the meanings of N-E, W-N, E-S, S-W?

The diurnal pattern in Figure S6d showed the diurnal variations in the contributions of different wind directions. The meanings of N-E, W-N, E-S, and S-W were already explained in the manuscript as “from north to east (N-E;  $0^\circ \leq \text{WD} < 90^\circ$ ), east to south (E-S;  $90^\circ \leq \text{WD} < 180^\circ$ ), south to west (S-W;  $180^\circ \leq \text{WD} < 270^\circ$ ), and west to north (W-N;  $270^\circ \leq \text{WD} \leq 360^\circ$ )”.

Figure S7, what do the color bars stand for?

The color bars indicate the variations of  $\text{PM}_{2.5}$  concentration, which was labelled in the figure.

## References

Fang, Y., Ye, C., Wang, J., Wu, Y., Hu, M., Lin, W., Xu, F., and Zhu, T.: RH and  $\text{O}_3$  concentration as two prerequisites for sulfate formation, *Atmos. Chem. Phys. Discuss.*, <https://doi.org/10.5194/acp-2019-284>, in review, 2019.

Li, H., Zhang, Q., Zhang, Q., Chen, C., Wang, L., Wei, Z., Zhou, S., Parworth, C., Zheng, B., Canonaco, F., Prévôt, A. S. H., Chen, P., Zhang, H., Wallington, T. J., and He, K.: Wintertime aerosol chemistry and haze evolution in an extremely polluted city of the North China Plain: significant contribution from coal and biomass combustion, *Atmos. Chem. Phys.*, 17, 4751-4768, <https://doi.org/10.5194/acp-17-4751-2017>, 2017.

Li, H., Zhang, Q., Zheng, B., Chen, C., Wu, N., Guo, H., Zhang, Y., Zheng, Y., Li, X., and He, K.: Nitrate-driven urban haze pollution during summertime over the North China Plain, *Atmos. Chem. Phys.*, 18, 5293-5306, <https://doi.org/10.5194/acp-18-5293-2018>, 2018.

Sun, P., Nie, W., Chi, X., Xie, Y., Huang, X., Xu, Z., Qi, X., Xu, Z., Wang, L., Wang, T., Zhang, Q., and Ding, A.: Two years of online measurement of fine particulate nitrate in the western Yangtze River Delta: influences of thermodynamics and N<sub>2</sub>O<sub>5</sub> hydrolysis, *Atmos. Chem. Phys.*, 18, 17177-17190, <https://doi.org/10.5194/acp-18-17177-2018>, 2018.

Wang, Y., Zhang, Q., Jiang, J., Zhou, W., Wang, B., He, K., Duan, F., Zhang, Q., Philip, S., and Xie, Y.: Enhanced sulfate formation during China's severe winter haze episode in January 2013 missing from current models, *Journal of Geophysical Research: Atmospheres*, 119, 425-440, [10.1002/2013JD021426](https://doi.org/10.1002/2013JD021426), 2014.

Xu, Q., Wang, S., Jiang, J., Bhattarai, N., Li, X., Chang, X., Qiu, X., Zheng, M., Hua, Y., and Hao, J.: Nitrate dominates the chemical composition of PM<sub>2.5</sub> during haze event in Beijing, China, *Sci Total Environ*, 689, 1293-1303, <https://doi.org/10.1016/j.scitotenv.2019.06.294>, 2019a.

Xu, W., Sun, Y., Wang, Q., Zhao, J., Wang, J., Ge, X., Xie, C., Zhou, W., Du, W., Li, J., Fu, P., Wang, Z., Worsnop, D. R., and Coe, H.: Changes in Aerosol Chemistry From 2014 to 2016 in Winter in Beijing: Insights From High-Resolution Aerosol Mass Spectrometry, *Journal of Geophysical Research: Atmospheres*, 124, 1132-1147, [10.1029/2018JD029245](https://doi.org/10.1029/2018JD029245), 2019b.

Zheng, G. J., Duan, F. K., Su, H., Ma, Y. L., Cheng, Y., Zheng, B., Zhang, Q., Huang, T., Kimoto, T., Chang, D., Pöschl, U., Cheng, Y. F., and He, K. B.: Exploring the severe winter haze in Beijing: the impact of synoptic weather, regional transport and heterogeneous reactions, *Atmos. Chem. Phys.*, 15, 2969-2983, <https://doi.org/10.5194/acp-15-2969-2015>, 2015.

## **Response to Short Comment 1 (SC1) on “Rapid transition in winter aerosol composition in Beijing from 2014 to 2017: response to clean air actions” by H. Li et al.**

(a) Overview The authors used fine particle data collected in Beijing during the winters of 2014 and 2017 to understand changes in the chemical composition of the PM over a period when particle mass decreased significantly. The results here are consistent with past data, showing a large decrease in PM mass, but also revealing that this is largely because of decreases in sulfate, organics, and unidentified components, as a result of decreasing local and regional emissions. The authors find that meteorology also contributed to lower PM concentrations in 2017 but that this was a smaller factor.

This is an interesting paper with a number of complementary components. On the other hand, there are a number of issues that need to be addressed, as described below. The thermodynamic modeling seems problematic and needs more clarification and information.

We would like to thank Cort Anastasio for giving the constructive and helpful comments and suggestions. In the following, we will answer the comments point by point.

(b) Major Points 1a. Figure 2 and lines 190 – 191: The text states that “All SIA species showed similar diel trends in the two winters: : :”. For some species this is true, but for many of the species, the diel variability is much lower in 2017 than in 2014, suggesting that while more local sources dominated in 2014, regional sources are more important in 2017. Take CCOA as an example: in 2014, the concentration varied by a factor of 3, while in 2017 the variation was probably only a factor of 1.5 or less. Can the change in diel variability be used as an indicator of local vs. regional pollution?

SIA species refer to sulfate, nitrate, and ammonium. For the SIA species, they showed similar diel trends in the winters of 2014 and 2017. For many of the other species, especially the primary species, their diel variability was much lower in 2017 than in 2014. However, the changes in the diel variability of these primary species can not be easily used as an indicator of local vs. regional pollution. For example, previous studies reported that coal combustion sources in Beijing were mainly attributed to regional transport from surrounding areas (Wang et al., 2011; Shang et al., 2018). Therefore, we could not rely on the diel variability of CCOA to provide information of local vs. regional pollution.

1b. Of course boundary layer height is a major influence on concentrations as well. I suggest you add a plot of CO as a tracer for BL height. Does plotting the ratio of PM component/CO help disentangle chemistry and BL height? These might be useful supplemental plots.

The ambient variations of PM components are not only controlled by atmospheric chemical reactions but are also influenced by boundary layer developments. According to the comment, we analyzed the CO-scaled concentrations for PM components to eliminate the influence of different dilution/mixing conditions. The corresponding diurnal plots are shown below. By plotting the ratio of PM component/CO, we can more clearly see the photochemical production of sulfate, nitrate, ammonium, and OOA during daytime. These diurnal plots are included in the supplementary information as Fig. S15.

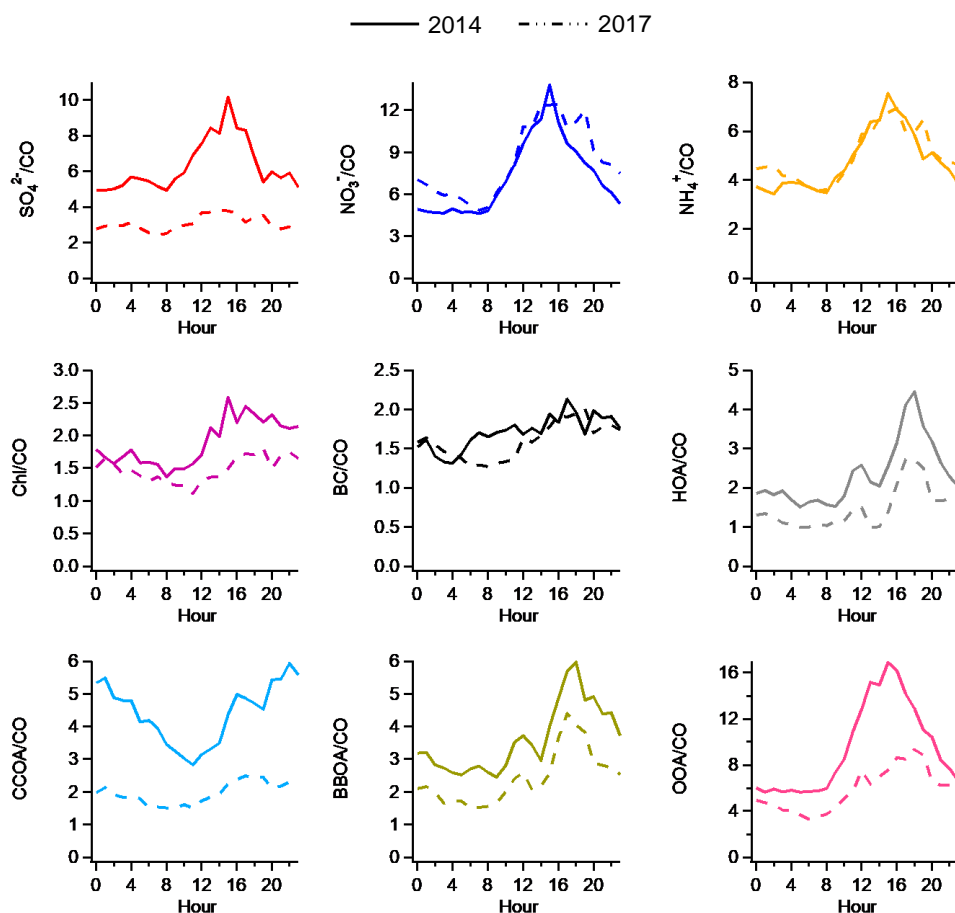
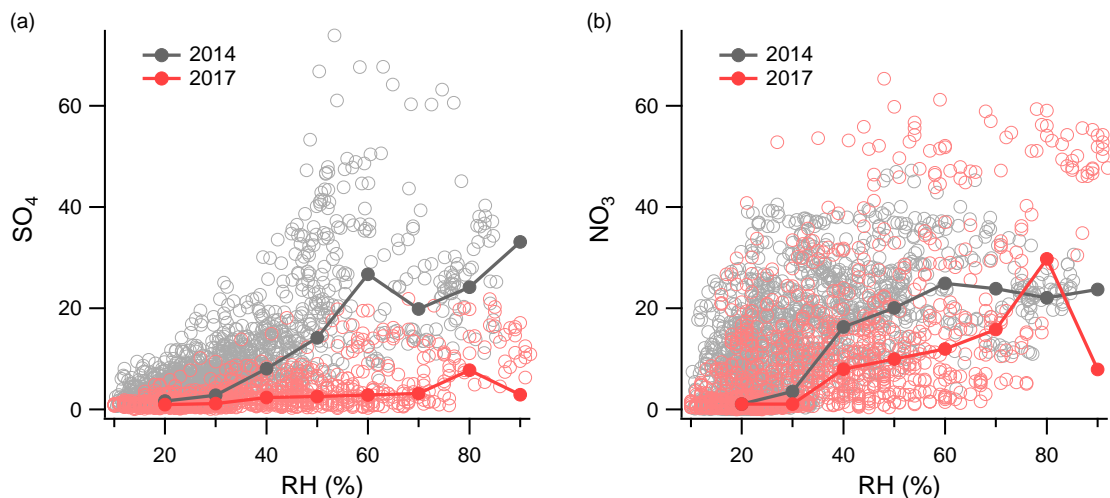


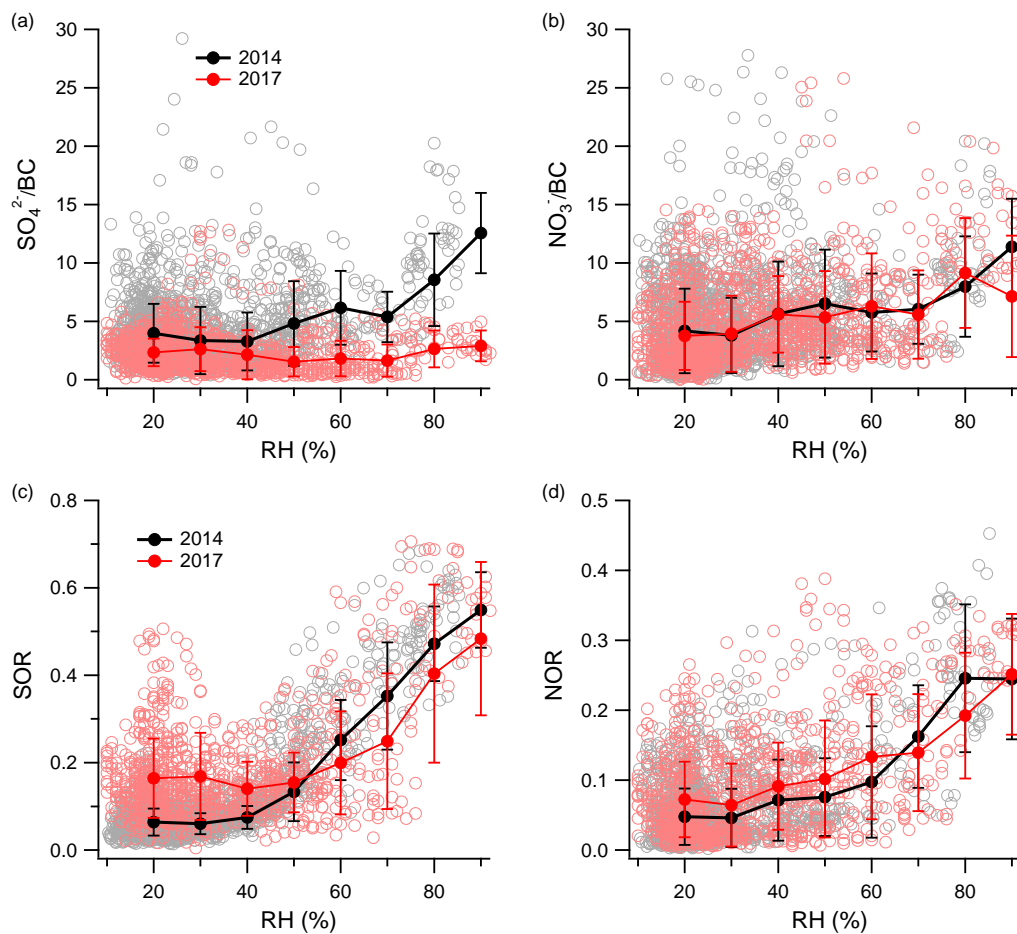
Figure S15. Average diurnal cycles of CO-scaled aerosol species in the winter of 2014 (solid line) and winter of 2017 (dashed line).

2. Figure 8 and its corresponding text. (i) Why normalize panels (a) and (b) to BC concentrations? Since both the numerator and denominator are changing between 2014 and 2017, the ratio seems less effective as a normalizing factor. What do the plots look like if sulfate and nitrate are not normalized by BC? (ii) The data are very noisy and so the authors have chosen to plot the median values (as the solid circles). But what does it look like if the mean and standard deviation are plotted instead? Are there any significant differences between RH values for a given year? If the authors want to stay with median, they should at least show some interquartile ranges or other measures of variability about the median. (iii) Line 323: “: :the starting point of SOR growth was clearly delayed in 2017: :”. Given the spread in the data, this is speculative since the median has no associated uncertainty or variability. Can this difference be tested statistically? (iv) Lines 330 – 335. The authors explain that the higher sulfate / (sulfate + SO<sub>2</sub>) ratio (i.e., SOR) in 2017 at low RH results from less of an oxidant limitation. But isn’t an alternative explanation that a higher fraction of the sulfur pollution in Beijing is from regional transport, which would have a higher SOR since it is more aged? (v) The nitrate / (nitrate + NO<sub>2</sub>) ratio (i.e., NOR) discussion in lines 339 – 344 seems to be missing a few points. First, NOR is a poor measure for the extent of NO<sub>x</sub> oxidation since it considers only particulate nitrate and not gas-phase HNO<sub>3</sub>. Under acidic particle conditions (as seems typical in 2014), most N(V) will be gas-phase HNO<sub>3</sub>, a result of sulfate acidity driving out the particle nitrate. But this is not accounted for if NOR is calculated only with particulate nitrate, as is done here. Running the e-AIM thermodynamic model on the average 2014 data shows that the gas-phase HNO<sub>3</sub> concentration is over an order of magnitude higher than particulate nitrate. Thus N(V) / NO<sub>x</sub> + N(V), with both phases considered for N(V), would be a better measure of NO<sub>x</sub> oxidation than NOR. ISOROPPIA could be run to examine HNO<sub>3</sub>(g) in the two years. (vi) As a consideration for future work, it would be enormously helpful to have gas-phase measurements of NH<sub>3</sub> and/or HNO<sub>3</sub> to constrain the modeled aerosol pH.

(i) BC is an aerosol species coming from only primary emissions and its variations well reflect the influence of atmospheric mixing conditions. The ratio of sulfate and nitrate to BC can better represent the contributions from chemical reactions. Plots not normalized by BC are shown below.



(ii) Figures with the mean and standard deviations are displayed below. They show no significant differences from the results with median values. The use of median values can to some extent avoid the bias by the odd values.



(iii) In this study, there were around 3-month and 2-month hourly data points for the winters of 2014 and 2017, respectively. To make the comparison between 2014 and 2017 more visible, we checked the mean and median

values. Both of them indicated that compared to the winter of 2014, the starting point of SOR growth with RH was delayed in the winter of 2017.

(iv) With the implementation of the clean air actions, SO<sub>2</sub> emissions were reduced in both Beijing and the surrounding regions. Compared to 2014, Beijing was less influenced by polluted air masses from regional transport, which has been analyzed in detail in Sect. 3.2.3. Therefore, the increase of SOR in 2017 at lower RH is more likely to be caused by the weakened oxidant limitation on SO<sub>2</sub> oxidations.

(v) According to the ISORROPIA calculations in this study, the fraction of particulate nitrate in total nitrate was higher than 0.99 for the average winter conditions in both 2014 and 2017. Therefore, the calculation of NOR without the consideration of gas-phase HNO<sub>3</sub> has no significant influence on the discussion of NO<sub>x</sub> oxidation.

(vi) We agree that the gas-phase measurements of NH<sub>3</sub> and HNO<sub>3</sub> are important for the calculation of aerosol pH. As we stated in the response to Rodney Weber, gas-phase NH<sub>3</sub> and HNO<sub>3</sub> were considered in the ISORROPIA calculations in this work.

3. Figure 9 and its corresponding text. (i) This figure indicates that the aerosol pH in 2014 was approximately 5, but this is inconsistent with the average composition indicated in Table 1. Using the averages for 2014 in Table 1, assuming protons make up the missing positive charge (which I assume was also done in ISORROPIA) and using a relative humidity of 60% in the e-AIM model results in a pH of -0.04 assuming a proton activity coefficient of 1; the pH is -0.7 if the e-AIM activity coefficient (4.22) is used. These results were done allowing solids to form, but it shouldn't change significantly if solids were not allowed to form. While the pH undoubtedly varies between samples, it is hard to believe the typical pH is near 5 given the ion imbalance in the data. (ii) Is the range of pH values given in line 361 (pH 5.0 to 6.2) from their work? Why is it for 2013 – 2017, rather than just the two winters of this study? It's not clear that the authors did much with the ISORROPIA data: why not report ALW and pH for every sample? This would be very useful information. (iii) The 2017 average data in Table 1 has a net positive charge, requiring a nonsensical negative concentration for protons that is of similar magnitude (though smaller) than the proton concentration from the 2014 data. This prevents use of a thermodynamic model and suggests that there are other charged species, likely organics, which are affecting the ion balance and the pH calculation. This should be discussed. Were the authors able to calculate ALW and pH values for the 2017 data? (iv) Under the acidic conditions I calculated for 2014, the value of NO<sub>3</sub><sup>-</sup> / (HNO<sub>3</sub> + NO<sub>3</sub><sup>-</sup>) is very small, in contrast to the values described in the manuscript. (v) Similarly, I calculate a NH<sub>4</sub><sup>+</sup>/NH<sub>x</sub> ratio near unity in 2014, in contrast to the small values reported in the text.

(i) According to ISORROPIA calculations, the average pH was around 4.8 in the winter of 2014, consistent with the results from previous studies. Many researches have shown that aerosols are moderately acidic in Beijing during wintertime (Guo et al., 2017; Liu et al., 2017; Song et al., 2018). In this study, the ISORROPIA was run in the forward mode. In addition to aerosol chemical compositions, gas-phase NH<sub>3</sub> and HNO<sub>3</sub> were also input into the model. Since only conditions with RH > 30% were considered, aerosols were assumed to be in a metastable state. Details about the ISORROPIA calculations were provided in the revised manuscript. A few studies have demonstrated that ion balance and equivalent ratios can not be used to predict the acidity of particles, especially under ammonia-rich conditions (Hennigan et al., 2015; Guo et al., 2016; Song et al., 2018). Song et al. (2018) showed that pH values calculated using the forward mode of thermodynamic models are not sensitive to the ion balance.

(ii) The pH values reported in the manuscript were calculated by this study. It has already been stated in the manuscript that "Data for the winter of 2013 were acquired from Sun et al. (2016)." While the ALW and pH were calculated for almost every sample, we did not report them in this study. The research focus of section 3.3 is to investigate how the clean air actions influence particle properties in different years.

(iii) As we stated above, the ion balance is not a good criteria to evaluate particle acidity, especially under ammonia-rich conditions. In addition to aerosol chemical compositions, gas-phase NH<sub>3</sub> and HNO<sub>3</sub> were also input into the thermodynamic model to calculate the pH values.

(iii) For the winter conditions of 2014, the fraction of particulate nitrate in total nitrate was higher than 0.99 according to ISORROPIA calculations. This is consistent with the results of Guo et al. (2018), which showed that the fraction of particulate nitrate in total nitrate was approaching 1 under Beijing winter conditions when aerosol pH was above 3.

(v) A  $\text{NH}_4^+/\text{NH}_x$  ratio near unity means that almost all  $\text{NH}_x$  remains in the particle phase, which is not possible in the winter of Beijing in 2014. Previous observations showed abundant existence of gas-phase  $\text{NH}_3$  in urban Beijing during wintertime (Meng et al., 2011; Zhao et al., 2016). The ISORROPIA predictions by Guo et al. (2018) demonstrated that with the gas-phase  $\text{NH}_3$  concentration above  $5 \mu\text{g m}^{-3}$ ,  $\text{NH}_4^+/\text{NH}_x$  ratio stays lower than 0.4.

(c) Minor Points 1. Throughout the manuscript, it would be much better (and more consistent with the other inorganic nomenclature in the paper) to use “Cl<sup>-</sup>” as the abbreviation for chloride rather than “Chl”.

Changed.

2. lines 183-184: This sentence is unclear. Clearer wording would be “The decreases in particulate nitrate and ammonium during this period were 1.3 and  $1.5 \text{ g m}^{-3}$ , respectively.”

Changed.

3. Figure 1. The second line of the figure caption is unclear. These are not “rates”, but rather decreases in concentrations, yes? Also, three significant figures in the decreases seems one too many.

The second sentence in the caption of Figure 1 were changed to “The decreases in the mass concentrations of different components from 2014 to 2017 are as follows”.

4. line 188: It is odd that the Xu nitrate/sulfate ratios are approximately half of the values in the current work. Why this discrepancy?

The measurements in winter 2014 in this study were conducted from the start of December to the end of February while those by Xu et al. (2019) were from the mid of November to the mid of December. Different emission intensities and different meteorological conditions influence the formation of particulate nitrate and sulfate in different months.

5. lines 203-204: Sulfate is a minor fraction of haze in 2014 as well as 2017, so this statement isn’t very useful. It would be better to indicate the sulfate contributions to each of the pollution classifications in 2017.

In the winter of 2014, the fraction of sulfate in total aerosol was more than 10% for all pollution levels. Therefore, it is not a minor fraction. Compared to 2014, sulfate comprised a smaller fraction of haze development in 2017. This has been stated in the revised manuscript.

6. lines 204–205: This description of nitrate contribution is for 2017?

Yes. This has been clearly stated in the revised manuscript.

7. line 208: State the 2014 and 2017 OA concentrations along with the overall decline.

The OA concentrations in the winters of 2014 and 2017 have been stated in the revised manuscript.

8. line 209: “The contribution from HOA was  $2.6 \text{ g m}^{-3}$  : :”. This is not as clear as it should be: better to state something like “HOA decreased by  $2.6 \text{ g m}^{-3}$  : :”.

The sentence has been changed to “The decrease in the mass concentration of HOA was  $2.6 \mu\text{g m}^{-3}$ ”.

9. lines 240 – 241: It is not clear what cases A, B, C, and D refer to. Are these panels of Fig. S7?

The explanations of cases A, B, C, and D was provided in the experimental method, section 2.3.

10. lines 258-259: This is unclear. Should “Until 2017: : :” be “By 2017: : :”?

Changed.

11. line 298: The 57.9% is not a “rate” and likely has one too many significant figure.

It has been changed to “a decrease of 57.9% in its mass concentration”.

(d) Recommendation I recommend that the paper be accepted after major revisions to address the points above.

## References

Guo, H., Sullivan, A. P., Campuzano-Jost, P., Schroder, J. C., Lopez-Hilfiker, F. D., Dibb, J. E., Jimenez, J. L., Thornton, J. A., Brown, S. S., Nenes, A., and Weber, R. J.: Fine particle pH and the partitioning of nitric acid during winter in the northeastern United States, *Journal of Geophysical Research: Atmospheres*, 121, 10,355-310,376, 10.1002/2016JD025311, 2016.

Guo, H., Weber, R. J., and Nenes, A.: High levels of ammonia do not raise fine particle pH sufficiently to yield nitrogen oxide-dominated sulfate production, *Scientific Reports*, 7, 12109, 10.1038/s41598-017-11704-0, 2017.

Guo, H. Y., Otjes, R., Schlag, P., Kiendler-Scharr, A., Nenes, A., and Weber, R. J.: Effectiveness of ammonia reduction on control of fine particle nitrate, *Atmos Chem Phys*, 18, 12241-12256, 2018.

Hennigan, C. J., Izumi, J., Sullivan, A. P., Weber, R. J., and Nenes, A.: A critical evaluation of proxy methods used to estimate the acidity of atmospheric particles, *Atmos. Chem. Phys.*, 15, 2775-2790, <https://doi.org/10.5194/acp-15-2775-2015>, 2015.

Liu, M., Song, Y., Zhou, T., Xu, Z., Yan, C., Zheng, M., Wu, Z., Hu, M., Wu, Y., and Zhu, T.: Fine particle pH during severe haze episodes in northern China, *Geophys Res Lett*, 44, 5213-5221, 10.1002/2017GL073210, 2017.

Meng, Z. Y., Lin, W. L., Jiang, X. M., Yan, P., Wang, Y., Zhang, Y. M., Jia, X. F., and Yu, X. L.: Characteristics of atmospheric ammonia over Beijing, China, *Atmos. Chem. Phys.*, 11, 6139-6151, <https://doi.org/10.5194/acp-11-6139-2011>, 2011.

Shang, X., Zhang, K., Meng, F., Wang, S., Lee, M., Suh, I., Kim, D., Jeon, K., Park, H., Wang, X., and Zhao, Y.: Characteristics and source apportionment of fine haze aerosol in Beijing during the winter of 2013, *Atmos. Chem. Phys.*, 18, 2573-2584, <https://doi.org/10.5194/acp-18-2573-2018>, 2018.

Song, S., Gao, M., Xu, W., Shao, J., Shi, G., Wang, S., Wang, Y., Sun, Y., and McElroy, M. B.: Fine-particle pH for Beijing winter haze as inferred from different thermodynamic equilibrium models, *Atmos. Chem. Phys.*, 18, 7423-7438, <https://doi.org/10.5194/acp-18-7423-2018>, 2018.

Wang, M., Zhu, T., Zhang, J. P., Zhang, Q. H., Lin, W. W., Li, Y., and Wang, Z. F.: Using a mobile laboratory to characterize the distribution and transport of sulfur dioxide in and around Beijing, *Atmos. Chem. Phys.*, 11, 11631-11645, <https://doi.org/10.5194/acp-11-11631-2011>, 2011.

Xu, W., Sun, Y., Wang, Q., Zhao, J., Wang, J., Ge, X., Xie, C., Zhou, W., Du, W., Li, J., Fu, P., Wang, Z., Worsnop, D. R., and Coe, H.: Changes in Aerosol Chemistry From 2014 to 2016 in Winter in Beijing: Insights From High-Resolution Aerosol Mass Spectrometry, *Journal of Geophysical Research: Atmospheres*, 124, 1132-1147, 10.1029/2018JD029245, 2019.

Zhao, M., Wang, S., Tan, J., Hua, Y., Wu, D., and Hao, J.: Variation of Urban Atmospheric Ammonia Pollution and its Relation with PM<sub>2.5</sub> Chemical Property in Winter of Beijing, China, *Aerosol Air Qual Res*, 16, 1378-1389, 10.4209/aaqr.2015.12.0699, 2016.

# 1 **Rapid transition in winter aerosol composition in Beijing from 2014 to** 2 **2017: response to clean air actions**

3 Haiyan Li<sup>1,a</sup>, Jing Cheng<sup>2</sup>, Qiang Zhang<sup>2</sup>, Bo Zheng<sup>1</sup>, Yuxuan Zhang<sup>2</sup>, Guangjie Zheng<sup>1</sup>, Kebin He<sup>1,3</sup>

4 <sup>1</sup> State Key Joint Laboratory of Environment Simulation and Pollution Control, School of Environment, Tsinghua University,  
5 Beijing 100084, China

6 <sup>2</sup> Ministry of Education Key Laboratory for Earth System Modeling, Department of Earth System Science, Tsinghua University,  
7 Beijing 100084, China

8 <sup>3</sup> State Environmental Protection Key Laboratory of Sources and Control of Air Pollution Complex, Tsinghua University, Beijing  
9 100084, China

10 <sup>a</sup>present address: Institute for Atmospheric and Earth System Research/Physics, Faculty of Science, University of Helsinki, 00014  
11 Helsinki, Finland

12 *Correspondence:* Qiang Zhang ([qiangzhang@tsinghua.edu.cn](mailto:qiangzhang@tsinghua.edu.cn))

13 **Abstract.** The clean air actions implemented by the Chinese government in 2013 have led to significantly improved air quality in  
14 Beijing. In this work, we combined the in-situ measurements of the chemical components of submicron particles (PM<sub>1</sub>) in Beijing  
15 during the winters of 2014 and 2017 and a regional chemical transport model to investigate the impact of clean air actions on  
16 aerosol chemistry and quantify the relative contributions of anthropogenic emissions, meteorological conditions, and regional  
17 transport to the changes in aerosol chemical composition from 2014 to 2017. We found that the average PM<sub>1</sub> concentration in  
18 winter in Beijing decreased by 49.5% from 2014 to 2017 (from 66.2 μg m<sup>-3</sup> to 33.4 μg m<sup>-3</sup>). Sulfate exhibited a much larger decline  
19 than nitrate and ammonium, which led to a rapid transition from sulfate-driven to nitrate-driven aerosol pollution during the  
20 wintertime. Organic aerosol (OA), especially coal combustion OA, and black carbon also showed large decreasing rates, indicating  
21 the effective emission control of coal combustion and biomass burning. The decreased sulfate contribution and increased nitrate  
22 fraction were highly consistent with the much faster emission reductions in sulfur dioxide (SO<sub>2</sub>) due to phasing out coal in Beijing  
23 compared to reduction in nitrogen oxides emissions estimated by bottom-up inventory. The chemical transport model simulations  
24 with these emission estimates reproduced the relative changes in aerosol composition and suggested that the reduced emissions in  
25 Beijing and its surrounding regions played a dominant role. The variations in meteorological conditions and regional transport  
26 contributed much less to the changes in aerosol concentration and its chemical composition during 2014-2017 compared to the  
27 decreasing emissions. Finally, we ~~observed-specified~~ that changes in precursor emissions ~~also-possibly~~ altered the aerosol  
28 formation mechanisms based on ambient observations. The observed explosive growth of sulfate at a relative humidity (RH) greater  
29 than 50% in 2014 was delayed to a higher RH of 70% in 2017, which was likely caused by the suppressed sulfate formation through  
30 heterogeneous reactions due to the decrease of SO<sub>2</sub> emissions. ~~The decreased SO<sub>2</sub> emissions suppressed the rapid formation of~~  
31 ~~secondary sulfate through heterogeneous reactions. The observed explosive growth of sulfate at a relative humidity (RH) greater~~  
32 ~~than 50% in 2014 was delayed to a higher RH of 70% in 2017.~~ Thermodynamic simulations showed that the decreased sulfate and  
33 nitrate concentrations have lowered the aerosol water content, particle acidity, and ammonium particle fraction. The results in this  
34 study demonstrated the response of aerosol chemistry to the stringent clean air actions and identified that the anthropogenic  
35 emission reductions are a major driver, which could help to further guide air pollution control strategies in China.

## 36 **1 Introduction**

37 Beijing, the capital of China, is one of the most heavily polluted cities in the world (Lelieveld et al., 2015), and it frequently  
38 experiences severe and persistent haze pollution episodes in winter (Guo et al., 2014). For example, in January 2013, the daily

39 concentration of ambient particles with an aerodynamic diameter less than 2.5  $\mu\text{m}$  ( $\text{PM}_{2.5}$ ) reached a record high of 569  $\mu\text{g m}^{-3}$  in  
40 Beijing (Ferreri et al., 2018), which was over 20 times higher than the World Health Organization standard (25  $\mu\text{g m}^{-3}$  for daily  
41 average  $\text{PM}_{2.5}$ ). As a complex mixture of many different components, ambient aerosols have a range of chemical compositions and  
42 originate from various emission sources and formation processes in the atmosphere (Seinfeld and Pandis, 2012). The adverse  
43 effects of aerosols on visibility (Pui et al., 2014), climate (IPCC, 2013), and human health (Pope et al., 2009) are intrinsically  
44 related to the chemical composition of particles.

45 To tackle severe aerosol pollution, the Chinese State Council implemented the Air Pollution Prevention and Control Action Plan  
46 (denoted as clean air actions) in September 2013, which is the most stringent pollution mitigation policy ever in China. As a  
47 consequence, China's anthropogenic emissions have declined by 59% for  $\text{SO}_2$ , 21% for  $\text{NO}_x$ , 32% for organic carbon (OC), and  
48 28% for black carbon (BC) during 2013-2017 (Zheng et al., 2018). The annual average  $\text{PM}_{2.5}$  concentration in Beijing decreased  
49 by 35.6% from 2013 to 2017, reaching 58  $\mu\text{g m}^{-3}$  in 2017. Combining the bottom-up emission inventory and chemical transport  
50 model simulations, our recent study (Cheng et al., 2019) quantified the relative contributions of meteorological conditions,  
51 emission reductions from surrounding regions, and emission reductions from local sources to the decrease in  $\text{PM}_{2.5}$  concentration  
52 in Beijing during 2013-2017. While changes in meteorological conditions partially explained air quality improvement in Beijing  
53 in 2017, local and regional emission controls played major roles. In addition, the aerosol chemical composition is expected to  
54 change correspondingly due to the rapid reductions in precursor emissions, which is not well understood yet because the chemical  
55 components of  $\text{PM}_{2.5}$  are not measured by China's monitoring network. A few studies have examined the change in aerosol  
56 composition in Beijing after 2013, including a semicontinuous measurement of carbonaceous aerosols during 2013-2018 (Ji et al.,  
57 2019) and an aerosol mass spectrometry study comparing aerosol composition and size distribution between 2014 and 2016 (Xu  
58 et al., 2019). However, neither performed a comprehensive assessment of all the main factors affecting aerosol concentration and  
59 its composition. A deep understanding of how the aerosol composition has changed since the clean air actions were activated and  
60 the possible linkage between them is urgently needed.

61 The chemical composition of  $\text{PM}_{2.5}$  is mainly affected by ~~three~~ the following factors: precursor emissions, meteorological  
62 conditions, atmospheric chemical reactions, and regional transport and deposition patterns. Emissions are typically the main driver  
63 of aerosol composition changes. During 2005-2012, the sulfate concentration in China decreased, while the nitrate concentration  
64 increased, which was caused by the considerable reduction in  $\text{SO}_2$  emissions but limited control of  $\text{NO}_x$  (Geng et al., 2017). Based  
65 on the measurements of organic aerosol (OA) composition in Beijing, a larger decrease in secondary OA than primary OA was  
66 found during the 2014 Asia-Pacific Economic Cooperation summit due to the strict emission controls (Sun et al., 2016).  
67 Meteorological conditions affect aerosol composition by changing emissions, chemical reactions, and transport and deposition  
68 processes (Mu and Liao, 2014). For example, increases in relative humidity (RH) enhance the secondary formation of sulfate  
69 through heterogeneous reactions (Zheng et al., 2015; Cheng et al., 2016), and decreases in temperature favor particulate nitrate  
70 formation by facilitating gas-to-particle partitioning (Pye et al., 2009; Li et al., 2018). With chemical transport model simulations  
71 in China for the years 2004-2012, Mu and Liao (2014) demonstrated that due to the large variations in meteorological parameters  
72 in North China, all aerosol species showed large corresponding interannual variations. Furthermore, aerosol characteristics in  
73 Beijing are influenced by regional transport from adjacent polluted regions. Polluted air masses from the southern regions  
74 contributed more secondary inorganic aerosols (SIAs) than primary aerosols in Beijing (Zhang et al., 2014; Du et al., 2018).  
75 Following our previous work (Cheng et al., 2019), the main objective of this study is to investigate the impact of clean air actions  
76 on changes in aerosol chemical composition from 2014 to 2017. With both the in-situ observations of aerosol species in Beijing  
77 during the winters of 2014 and 2017 and model simulations for the corresponding periods, this work provides the opportunity for  
78 a detailed evaluation of the underlying drivers. First, changes in aerosol characteristics are illustrated for inorganics and organics

79 by comparing aerosol measurements in 2014 and 2017. Then, the relative importance of different factors in varying aerosol  
80 composition is assessed by combining direct observations and model simulations, including synoptic conditions, emission changes,  
81 regional transport and formation mechanisms. Last, we show that the transition in aerosol characteristics influenced particle  
82 properties, such as aerosol water content (AWC) and particle acidity, which in turn affects secondary aerosol formation.

## 83 **2 Experimental methods**

### 84 **2.1 Ambient sampling and instrumentation**

85 Online aerosol measurements were performed in urban Beijing during the winters of 2014 (from 6 December 2014 to 27 February  
86 2015) and 2017 (from 11 December 2017 to 2 February 2018). The sampling site is located on the roof of a three-story building  
87 on the campus of Tsinghua University (40.0° N, 116.3° E), which is surrounded by school and residential areas. No major industrial  
88 sources are situated nearby. An Aerodyne Aerosol Chemical Speciation Monitor (ACSM) was deployed for the real-time chemical  
89 observations of nonrefractory PM<sub>1</sub> (NR-PM<sub>1</sub>), including organics, sulfate, nitrate, ammonium, and chloride. A detailed description  
90 of the instrument can be found in Ng et al. (2011a). The mass concentration of BC in PM<sub>1</sub> was measured using a multiangle  
91 absorption photometer (MAAP, model 5012; Petzold and Schönlinner, 2004). In addition, the total PM<sub>2.5</sub> mass was simultaneously  
92 recorded with a PM-712 monitor based on the  $\beta$ -ray absorption method (Kimoto Electric Co., Ltd., Japan). For gaseous species,  
93 the mixing ratios of SO<sub>2</sub>, NO<sub>x</sub>, CO, and O<sub>3</sub> were monitored by a suite of commercial gas analyzers (Thermo Scientific). The  
94 meteorological parameters, including temperature, RH, wind speed (WS), and wind direction (WD), were obtained from an  
95 automatic meteorological observation instrument (MILOS520, VAISALA Inc., Finland).

### 96 **2.2 ACSM data analysis**

97 The ACSM data were analyzed using the standard analysis software within Igor Pro (WaveMetrics, Inc., Oregon USA). Default  
98 relative ionization efficiencies (RIEs) were applied to organics (1.4), nitrate (1.1), and chloride (1.3), while the RIEs of ammonium  
99 and sulfate were experimentally determined through calibrations with pure ammonium nitrate and ammonium sulfate, respectively.  
100 A composition-dependent collection efficiency (CE) algorithm was used to account for the incomplete detection of aerosol particles  
101 (Middlebrook et al., 2012). As shown in Fig. S1, the total measured PM<sub>1</sub> mass (NR-PM<sub>1</sub> plus BC) correlated well with the PM<sub>2.5</sub>  
102 obtained from PM-712 ( $r^2 = 0.80$  and  $0.87$  for 2014 and 2017, respectively). On average, PM<sub>1</sub> accounted for 68% and 80% of the  
103 total PM<sub>2.5</sub> in Beijing during the winters of 2014 and 2017.

104 The ACSM provides unit-mass-resolution mass spectra of submicron particles, facilitating source apportionment via factor analysis.  
105 In this study, positive matrix factorization (PMF) was implemented to resolve OA into various sources using a multilinear engine  
106 (ME-2; Paatero, 1999) via the SoFi toolkit (Source Finder; Canonaco et al., 2013). The so-called  $a$  value approach allows for the  
107 introduction of a priori factor profile or time series to reduce the rotational ambiguity and obtain a unique solution. The spectra  
108 and error matrices of organics were pretreated based on the procedures given by Ulbrich et al. (2009) and Zhang et al. (2011). Ions  
109 ~~up to larger than~~  $m/z$  120 were not considered in this study given the interferences of the internal standard of naphthalene at  $m/z$   
110 127-129, ~~and~~ the low signal-to-noise ratio of larger ions, and their low contributions to OA loading. For the winter of 2014, a  
111 reference hydrocarbon-like OA (HOA) profile from Ng et al. (2011b) was introduced into the ME-2 analysis to constrain the model  
112 performance, varying  $a$  values from 0 to 1. Following the guidelines by Canonaco et al. (2013) and Crippa et al. (2014), After a  
113 detailed evaluation of the factor profiles, time series, diurnal variations, and correlations with external tracers, an optimal solution  
114 with four factors was finally accepted, with an  $a$  value of 0. Detailed evaluation of the factor time series, mass spectra, and diurnal  
115 patterns with different  $a$  values can be found in the Supplement (Figs. S2-10). Figure S11~~2~~ shows the source apportionment results

116 with three primary factors, i.e., HOA, coal combustion OA (CCOA), and biomass burning OA (BBOA), and one secondary factor,  
117 oxygenated OA (OOA). For the 2017 dataset, the mass spectral profiles of HOA, CCOA, and BBOA from the ME-2 analysis of  
118 2014 were adopted to constrain the model performance. Similarly, a four-factor solution with HOA, BBOA, CCOA, and OOA was  
119 selected for the winter of 2017, which allowed a better comparison of the OA sources between 2014 and 2017.

### 120 2.3 WRF-CMAQ model

121 The Weather Research and Forecasting (WRF) model, version 3.8, and the Community Multiscale Air Quality (CMAQ) model,  
122 version 5.1, were applied to evaluate the impact of meteorological changes, regional transport and emission variations on the  $PM_{2.5}$   
123 concentration in Beijing in winter. The simulated area was designed as three nested domains, and the innermost area covered  
124 Beijing and its surrounding regions (including Tianjin, Hebei, Shanxi, Henan, Shandong and Inner Mongolia), with a horizontal  
125 resolution of  $4\text{ km} \times 4\text{ km}$ . The simulated period basically followed the observation time, which covered December 2014 – February  
126 2015 and December 2017 – February 2018. A one-month spin-up was applied in each simulation.

127 The WRF model is driven by the National Centers for Environmental Prediction Final Analysis (NCEP-FNL) reanalysis data,  
128 which then provided the meteorological fields for the CMAQ model. We used CB05 and AERO6 as the gas and particulate matter  
129 chemical mechanisms, respectively. The in-line windblown dust and photolytic rate calculation modules were also adopted to  
130 improve the simulation. The chemical initial and boundary conditions originated from the interpolated outputs of the Goddard  
131 Earth Observing System with chemistry (GEOS-Chem) model (Bay et al., 2001).

132 The anthropogenic emission inventory for Beijing was taken from the Beijing Municipal Environmental Monitoring Center  
133 (BMEMC), which was documented and analyzed in Cheng et al. (2019), while the emission inventory outside Beijing was provided  
134 by the Multi-resolution Emission Inventory for China (MEIC) (<http://www.meicmodel.org>; Zheng et al., 2018) and the MIX  
135 emission inventory for the other Asian countries (M. Li et al., 2017). The biogenic emissions were obtained by the Model of  
136 Emission of Gases and Aerosols from Nature (MEGAN v2.1); however, open biomass burning was not considered in this work.

137 Detailed model configurations and validations can be found in Cheng et al. (2019), and the simulated results well reproduced the  
138 temporal and spatial distributions and variations in  $PM_{2.5}$  in Beijing and its surrounding areas. In this study, we evaluated the model  
139 performance by comparing the simulated  $PM_{2.5}$  concentrations and compositions in Beijing with observation data. The hourly  
140 observed  $PM_{2.5}$  concentrations were collected from the Beijing Municipal Environmental Protection Bureau; and the observed  
141  $PM_{2.5}$  compositions came from the Surface PARTICulate mAtter Network (SPARTAN, [www.spartan-network.org](http://www.spartan-network.org)). We also  
142 compared the simulated  $PM_{2.5}$  compositions with the observed  $PM_1$  species from this work. The average simulated  $PM_{2.5}$  in Beijing  
143 decreased from  $91.5$  (winter of 2014) to  $52.5$  (winter of 2017)  $\mu\text{g m}^{-3}$ , with a total decrease of  $39\text{ }\mu\text{g m}^{-3}$ , while the observed  $PM_{2.5}$   
144 varied from  $81.9$  to  $40.6\text{ }\mu\text{g m}^{-3}$ , decreasing by  $41.3\text{ }\mu\text{g m}^{-3}$ . Generally, ~~The Pearson correlation coefficients between~~ the simulated  
145 and observed  $PM_{2.5}$  (24-hour averages) in Beijing were  $0.81$  (winter of 2014) and  $0.78$  (winter of 2017) ~~agreed well~~. The time series  
146 comparison and detailed monthly descriptive statistic of the observed and CMAQ-simulated  $PM_{2.5}$  concentrations can be found in  
147 Fig. S12 and Table S1. For  $PM_{2.5}$  compositions, the Pearson correlation coefficients between simulated  $PM_{2.5}$  and observed  $PM_1$   
148 components were all above  $0.7$  (Table S2a), indicating that the model simulations could well reproduce the species variations.  
149 Detailed comparisons of the simulated and observed  $PM_{2.5}$  components were listed in Table S2b.

150 We designed six simulation cases to investigate the impact of meteorological and emission variations. Two base cases were driven  
151 by the actual emission inventory and meteorological conditions in the winter of 2014 (case A) and winter of 2017 (case B). Cases  
152 C and D were designed to quantify the impact of meteorological changes; case C was simulated with the emissions in 2014 and  
153 meteorological conditions of 2017, while case D used the 2017 emissions and 2014 meteorological conditions. Therefore, the  
154 differences between A and C or between B and D show the influence of meteorological conditions, and the differences between A

155 and *D* or between *B* and *C* correspond to the contributions of emission variations. We used the averaged differences as the final  
156 impacts. Cases *E* and *F* were developed to evaluate the effect of regional transport on PM<sub>2.5</sub> variations in Beijing in the winter of  
157 2014 (*E*) and winter of 2017 (*F*). In these two cases, the emissions in Beijing were set to zero, while the regional emissions  
158 remained at the actual level. The balances between *A* and *E* or between *B* and *F* represent the contributions of regional transport to  
159 the PM<sub>2.5</sub> concentration in Beijing during the corresponding periods.

## 160 2.4 Clustering analysis of back trajectories

161 The Hybrid Single Particle Lagrangian Integrated Trajectory (HYSPLIT) model was conducted to calculate the back trajectories  
162 of air masses arriving in Beijing during the observation periods in 2014 and 2017. The meteorological input was downloaded from  
163 the National Oceanographic and Atmospheric Administration (NOAA) Air Resource Laboratory Archived Global Data  
164 Assimilation System (GDAS) (<ftp://arlftp.arlhq.noaa.gov/pub/archives/>). Each trajectory was run for three days, with a time  
165 resolution of 1 hour, and the initialized height was 100 m above ground level. In total, 2108 and 1292 trajectories were obtained  
166 for the winters of 2014 and 2017, respectively. Based on the built-in clustering calculation, the trajectories were then classified  
167 into different groups to represent the main airflows influencing the receptor site. Finally, the optimal 5-cluster and 7-cluster  
168 solutions were adopted for the winters of 2014 and 2017, respectively. Details are shown in Fig. S13.

## 169 2.5 ISORROPIA-II equilibrium calculation

170 The ISORROPIA-II thermodynamic model was used to investigate the effects of particle chemical composition on aerosol  
171 properties, i.e., particle pH, AWC, and the partitioning of semivolatile species (Fountoukis and Nenes, 2007). The model computes  
172 the equilibrium state of an NH<sub>4</sub><sup>+</sup>-SO<sub>4</sub><sup>2-</sup>-NO<sub>3</sub><sup>-</sup>-Cl<sup>-</sup>-Na<sup>+</sup>-Ca<sup>2+</sup>-K<sup>+</sup>-Mg<sup>2+</sup>-H<sub>2</sub>O inorganic aerosol system with its corresponding gases  
173 (Fountoukis and Nenes, 2007). When running the ISORROPIA-II model, it is assumed that ~~the bulk PM<sub>1</sub> or PM<sub>2.5</sub> properties have~~  
174 ~~no compositional dependence on particle size, and~~ aerosols are internally mixed and composed of a single aqueous phase. The  
175 validity of these assumptions has been evaluated by a number of studies in various locations (Guo et al., 2015; Weber et al., 2016;  
176 M.X. Liu et al., 2017; Li et al., 2018).

177 The model was run in the forward mode by assuming that aerosol solutions were metastable. The forward mode calculates the gas-  
178 particle equilibrium partitioning with the total concentrations of both gas and particle phase species. Compared to the reverse mode  
179 using only aerosol phase compositions, calculations with the forward mode are affected much less by the measurement errors  
180 (Hennigan et al., 2015; Guo et al., 2017a; Song et al., 2018). Particle water associated with OA was not considered in this study  
181 given its minor effects. M. X. Liu et al. (2017) showed that organic matter (OM)-induced particle water accounted for only 5% of  
182 the total AWC in Beijing. Up to now, there are no observational data showing whether aerosols are in a metastable (only liquid)  
183 or stable (solid plus liquid) state in Beijing in winter (Song et al., 2018). According to previous studies, at low RH (RH < 20% or  
184 30%), aerosols are less likely to be in a completely liquid state (Fountoukis and Nenes, 2007; Guo et al., 2016, 2017). Therefore,  
185 periods with RH < 30% were excluded in this study. The effects of nonvolatile cations (i.e., Na<sup>+</sup>, K<sup>+</sup>, Ca<sup>2+</sup>, Mg<sup>2+</sup>) are not considered  
186 in this study because the fraction of nonvolatile cations in PM<sub>1</sub> in Beijing is generally negligible compared to SO<sub>4</sub><sup>2-</sup>, NO<sub>3</sub><sup>-</sup>, and  
187 NH<sub>4</sub><sup>+</sup> (Sun et al., 2014). Although nonvolatile nitrate may exist in ambient particles as Ca(NO<sub>3</sub>)<sub>2</sub> and Mg(NO<sub>3</sub>)<sub>2</sub>, Ca<sup>2+</sup> and Mg<sup>2+</sup>  
188 are mainly abundant at sizes above 1 μm (Zhao et al., 2017). In addition, the mixing state of PM<sub>1</sub> nonvolatile cations with SO<sub>4</sub><sup>2-</sup>,  
189 NO<sub>3</sub><sup>-</sup>, and NH<sub>4</sub><sup>+</sup> remains to be investigated (Guo et al., 2016, 2017). Previous studies showed that including the nonvolatile cations  
190 in ISORROPIA-II does not significantly affect the pH calculations unless the cations become important relative to anions (Guo et  
191 al., 2016; Song et al., 2018). The sensitivity test for Beijing winter conditions suggested that with nonvolatile cations, the predicted  
192 pH values increase by about 0.1 units.

193 In this study, the transition in aerosol composition was mainly reflected in the variations in nitrate and sulfate concentrations. For  
194 the analysis of the sensitivity of aerosol properties to particle composition, a selected sulfate concentration combined with the  
195 average temperature, RH, and total ammonia concentration ( $\text{NH}_3 + \text{NH}_4^+$ ) during the winters of 2014 and 2017 was input into the  
196 ISORROPIA-II model, where the total nitrate concentration ( $\text{HNO}_3 + \text{NO}_3^-$ ) was left as the free variable. The gaseous  $\text{HNO}_3$  and  
197  $\text{NH}_3$  concentrations were not directly measured during our campaign. But long-term measurements in Beijing showed that gaseous  
198  $\text{NH}_3$  concentration correlated well with  $\text{NO}_x$  concentration in winter (Meng et al., 2011). Therefore, the empirical equation derived  
199 from Meng et al. (2011),  $\text{NH}_3$  (ppb) =  $0.34 \times \text{NO}_x$  (ppb) + 0.63, was applied to estimate the gaseous  $\text{NH}_3$  concentration. On average,  
200 the  $\text{NH}_3$  concentration was approximated to be  $14.0 \mu\text{g m}^{-3}$  during the winters of 2014 and 2017, consistent with previous  
201 observations in the same season of Beijing (Meng et al., 2011; Zhao et al., 2016; Zhang et al., 2018). The total nitrate concentration,  
202 including both gaseous  $\text{HNO}_3$  and particulate nitrate, varied from 0.2 to  $75 \mu\text{g m}^{-3}$  for the sensitivity study.

## 203 3 Results and discussions

### 204 3.1 Overall variations in aerosol characteristics from 2014 to 2017

205 Figures S14 and S15 display the temporal variations in meteorological parameters, trace gases, and aerosol species during the two  
206 winter campaigns, with the average values shown in Table 1. Compared to the frequently occurring haze episodes in the winter of  
207 2014, more clean days with lower  $\text{PM}_{10}$  concentrations were observed in the winter of 2017. On average, the  $\text{PM}_{10}$  concentrations  
208 were  $66.2 \mu\text{g m}^{-3}$  and  $33.4 \mu\text{g m}^{-3}$  during the winters of 2014 and 2017, respectively. The large reduction in  $\text{PM}_{10}$  concentration  
209 reflects the effectiveness of pollution abatement strategies. Satellite-derived estimates also showed an evident decrease in  $\text{PM}_{2.5}$   
210 concentration in North China in recent years (Gui et al., 2019).

#### 211 3.1.1 Changes in SIA characteristics

212 Sulfate, nitrate, and ammonium are the dominant components in SIAs and are generally recognized as ammonium sulfate and  
213 ammonium nitrate in  $\text{PM}_{2.5}$ . With the implementation of clean air actions, sulfate underwent the largest decline in the mass  
214 concentration among all SIA species (from  $7.7 \mu\text{g m}^{-3}$  to  $2.8 \mu\text{g m}^{-3}$  during 2014-2017). The decreases in particulate contributions  
215 of nitrate and ammonium to  $\text{PM}_{10}$  mass reduction during this period were  $1.3 \mu\text{g m}^{-3}$  and  $1.5 \mu\text{g m}^{-3}$ , respectively. Different changes  
216 in the mass concentration of SIA species led to variations in the  $\text{PM}_{10}$  chemical composition. As illustrated in Fig. 1, nitrate exhibited  
217 an increasing mass fraction in  $\text{PM}_{10}$  from 18% to 30%, whereas the mass contribution of sulfate decreased from 12% to 8%.  
218 Correspondingly, the mass ratio of nitrate/sulfate increased from 1.4 in 2014 to 3.5 in 2017. Based on the measurements in Beijing  
219 from November to December, Xu et al. (2019) also observed a higher nitrate/sulfate ratio in 2016 (1.36) than in 2014 (0.72).  
220 Similar annual variations in aerosol chemical composition were found in North America over 2000-2016, with an increased  
221 proportion of nitrate and a decreased contribution of sulfate (van Donkelaar et al., 2019). The diurnal cycles of SIAs are displayed  
222 in Fig. 2. All SIA species showed similar diel trends in the two winters, with increasing concentrations after noon due to enhanced  
223 photochemical processes and peak concentrations at night caused by a lower boundary layer height. The CO-scaled diurnal plots  
224 for SIA species are shown in Fig. S16 to eliminate the influence of different dilution/mixing conditions. However, the absolute  
225 variations in the SIA mass concentration differed greatly between 2014 and 2017. While the mass concentration of sulfate  
226 decreased by a factor of 2-3 in 2017, nitrate and ammonium showed much smaller reductions of 15-40% in their mass  
227 concentrations throughout the day.

228 Previous studies have concluded that the dramatically enhanced contribution of sulfate was a main driving factor of winter haze  
229 pollution in China (Wang et al., 2014; Wang et al., 2016; H. Y. Li et al., 2017). However, with the emission mitigation efforts, the

230 role of SIA species in aerosol pollution changed significantly. Aerosol pollution was classified into three categories in this study:  
231 clean ( $PM_1 \leq 35 \mu g m^{-3}$ ), slightly polluted ( $35 < PM_1 \leq 115 \mu g m^{-3}$ ), and polluted ( $PM_1 > 115 \mu g m^{-3}$ ). The contributions of different  
232 pollution levels and the  $PM_1$  chemical compositions at each pollution level are shown in Fig. 3 for the winters of 2014 and 2017.  
233 While the polluted level accounted for 38% of the observation period in the winter of 2014, only 14% of the observation period  
234 was recognized as being polluted in the winter of 2017. In 2014, the mass fraction of sulfate in  $PM_1$  was 16.1% during clean  
235 periods. With the increase in pollution level, the contribution of sulfate increased from 10.6% in slightly polluted periods to 13.6%  
236 in polluted periods, while the mass fraction of nitrate decreased. In contrast, sulfate comprised a ~~minor~~smaller fraction of haze  
237 development in 2017 compared to 2014. It was nitrate that exhibited a substantially increased mass fraction at higher  $PM_1$  loadings  
238 in the winter of 2017. From clean to polluted periods, the nitrate contribution to  $PM_1$  increased from 22.6% to 34.9%. These results  
239 demonstrated that aerosol pollution in Beijing has gradually changed from sulfate-driven to nitrate-driven in recent years.

### 240 3.1.2 Changes in OA characteristics

241 In response to the strict emission controls, the mass concentration of organics declined by  $\sim 18.5 \mu g m^{-3}$  from 2014 ( $30.4 \mu g m^{-3}$ )  
242 to 2017 ( $11.9 \mu g m^{-3}$ ), which was mainly caused by OOA ( $\sim 6.8 \mu g m^{-3}$ ) and CCOA ( $\sim 6.0 \mu g m^{-3}$ ). The ~~contribution from decrease~~  
243 in the mass concentration of HOA was  $2.6 \mu g m^{-3}$ , which was associated with the strengthened controls on vehicle emissions.  
244 BBOA decreased by  $3.2 \mu g m^{-3}$  because the use of traditional biofuels, such as wood and crop residuals, was forbidden in Beijing  
245 by the end of 2016. Generally, the concentrations of all OA factors declined substantially throughout the day in 2017. For primary  
246 factors, the reductions in their mass concentrations were much higher at night than during the day (Fig. 2). Compared to 2014,  
247 CCOA decreased by a factor of 4-5 at night in 2017 and a factor of 1.5 during the day.

248 Overall, the mass fraction of organics in  $PM_1$  declined from 49% to 36% over the period (Fig. 1). The source apportionment results  
249 demonstrated that coal combustion was largely accountable for the reduced contribution of organics. During 2014-2017, the mass  
250 fraction of CCOA in the total OA decreased from 27% to 18%. Reports from the Beijing Municipal Environmental Protection  
251 Bureau (MEPB) also revealed that the contribution of coal combustion to aerosol pollution showed a large decrease during 2013-  
252 2017. The decline in CCOA was largely driven by the reduced emissions of organics from coal combustion with the implementation  
253 of clean air actions. In contrast, the mass contribution of OOA in the total OA increased from 41% to 49% during 2014-2017.  
254 OOA is formed in the atmosphere through various oxidation reactions of volatile organic compounds (VOCs). From 2013 to 2017,  
255 VOCs emissions decreased by approximately half in Beijing but remained constant in the surrounding regions. Large amounts of  
256 OOA brought to Beijing via regional transport weakened the efforts of local emission cuts. Therefore, stronger emission controls  
257 of VOCs need to be placed in both local Beijing and adjacent areas in the future.

### 258 3.2 Factors affecting aerosol characteristics from 2014 to 2017

#### 259 3.2.1 Meteorological conditions

260 To evaluate the influence of weather conditions on air quality improvement, we compared the daily changes in meteorological  
261 parameters during the winters of 2014 and 2017 (Fig. S176). Compared to 2014, the temperature in 2017 was slightly lower  
262 throughout the whole day, which may have facilitated gas-particle conversion for semivolatile species, such as ammonium nitrate.  
263 Although the RH was similar between 2014 and 2017 during the daytime, the nighttime RH in 2017 was slightly higher than that  
264 in 2014, which was favorable for the heterogeneous reactions of secondary species. On average, the observed RH was 29.6% in  
265 the winter of 2014 and 33.9% in the winter of 2017. Diurnal cycles of WS showed that the WS in winter of 2017 was somewhat  
266 higher, implying beneficial conditions for the dispersal of air pollutants. To illustrate the variations in WD, the observed data were  
267 classified into four groups: from north to east (N-E;  $0^\circ \leq WD < 90^\circ$ ), east to south (E-S;  $90^\circ \leq WD < 180^\circ$ ), south to west (S-W;

268  $180^\circ \leq WD < 270^\circ$ ), and west to north (W-N;  $270^\circ \leq WD \leq 360^\circ$ ). As displayed in Fig. S176d, the winters of 2014 and 2017 were  
269 both dominated by W-N and N-E, which usually bring clean air masses. After noon, the contribution of winds from S-W started  
270 to increase. According to previous studies, southerly winds arriving in Beijing generally carry higher levels of air pollutants from  
271 the southern regions (Sun et al., 2006; Zhao et al., 2009).

272 Simulations with the WRF-CMAQ model helped to assess the relative importance of meteorology for changes in aerosol  
273 concentration and chemical composition. The effects of meteorology were quantified by comparing cases A and C or cases B and  
274 D. The differences between A and D or B and C reflected the effectiveness of emission control. For the total  $PM_{2.5}$  concentration,  
275 the simulation results clearly demonstrated that variations in meteorology from 2014 to 2017 had a much lower influence on the  
276  $PM_{2.5}$  reduction than the changes in air pollutant emissions (Fig. S187). On average, changes in weather conditions resulted in a  
277  $PM_{2.5}$  decrease of  $9.6 \mu\text{g m}^{-3}$ , which explained 24.8% of the total  $PM_{2.5}$  reduction. These results suggest that meteorological  
278 variations are far from sufficient to explain  $PM_{2.5}$  abatement during 2014-2017. In terms of aerosol composition, we compared the  
279 simulated results of cases B and D and found that meteorological changes from 2014 to 2017 had a negligible influence on the  
280 chemical composition of  $PM_{2.5}$  (Fig. 4). Therefore, we conclude that weather conditions in 2017 marginally favored air quality  
281 improvement in Beijing, and emission reductions in air pollutants played a dominant role in the variations in aerosol concentration  
282 and composition.

### 283 3.2.2 Emission changes

284 According to both the observations (Fig. 1) and simulation results (Fig. 5a), sulfate and organics experienced the largest decreases  
285 among different components in Beijing from 2014 to 2017, which is consistent with the considerable emission reductions in  $SO_2$   
286 and primary OC in local Beijing and its surrounding regions (Fig. 6; i.e., Tianjin, Hebei, Shandong, Henan, Shanxi, and Inner  
287 Mongolia). Comparatively, the wintertime nitrate concentration showed the lowest reduction during 2014-2017, which was  
288 expected from the smaller emission cut of  $NO_x$  in Beijing and its surrounding areas.

289 Based on the bottom-up emission inventories (Zheng et al., 2018; Cheng et al., 2019),  $SO_2$  emissions decreased by 79.9% in Beijing  
290 during 2014-2017, mainly due to the effective control of coal combustion sources and the optimization of the energy structure.  
291 Until By the end of 2017, all coal-fired power units were shut down, and small coal-fired boilers with capacities of  $<7$  MW were  
292 eliminated in Beijing, which reduced coal use by more than 17 million tons. In addition, most of the clustered and highly polluted  
293 enterprises and factories were phased out during this period. These control measures remarkably reduced  $SO_2$  emissions from  
294 power and industry sectors. Enhanced energy restructuring was also implemented in the residential sector. During 2013-2017,  
295 more than 2 million tons of residential coal was replaced by cleaner natural gas and electricity, involving 900,000 households in  
296 Beijing. Apart from coal burning, the use of traditional biomass, such as wood and crops, was thoroughly forbidden in Beijing by  
297 the end of 2016. The strict governance of residential fuel also made substantial contributions to the BC and OC emission reductions  
298 in Beijing, which decreased by 71.2% and 59.9%, respectively, during 2014-2017. In comparison,  $NO_x$  showed a lower emission  
299 reduction of 38.1% from 2014 to 2017 in Beijing. The decline in  $NO_x$  emissions was mainly caused by the strengthened emission  
300 control of on-road and off-road transportation, the shutdown of all coal-fired power plants, and the application of low-nitrogen-  
301 burning (LNB) technologies in industrial boilers. However, due to the insufficient end-of-pipe control of widespread gas-fired  
302 facilities and the rapid increase in the vehicle population (the number of vehicles in Beijing increased by nearly 10% during 2013-  
303 2017), the  $NO_x$  emission reduction in Beijing was not as significant as the  $SO_2$  emission reduction.

304 In adjacent regions,  $SO_2$  emissions decreased by 50.6% from 2014 to 2017, while  $NO_x$  emissions showed a much smaller reduction  
305 of 15.2%. Comparatively, the energy structure adjustments in surrounding areas were less intense than those in Beijing. Emission  
306 reductions in  $SO_2$  and  $NO_x$  in surrounding regions were mainly attributed to ultralow power plant emissions and the reinforced

307 end-of-pipe control of key industries. Because of the looser emission standards for vehicles and the lack of vehicle management,  
308 control measures on transportation in adjacent regions were highly insufficient for  $\text{NO}_x$  emission reduction compared with those  
309 in Beijing. Overall, the observed transition in  $\text{PM}_{10}$  chemical composition with increasing nitrate contribution and decreasing sulfate  
310 fraction was in agreement with the emission changes in their precursors.

### 311 3.2.3 Regional transport

312 Variations in regional weather patterns and emission changes in air pollutants in surrounding regions influenced the effect of  
313 regional transport on aerosol characteristics in Beijing. Statistical analysis of air mass trajectories was performed using the  
314 HYSPLIT model. Based on the clustering technique, back trajectories were classified into groups of similar length and curvature  
315 to identify the main airflows affecting the site. The five-cluster solution and seven-cluster solution were adopted for the winters of  
316 2014 and 2017, respectively. The  $\text{PM}_{10}$  mass concentration and mass composition for each cluster are shown in Fig. S198. For a  
317 better comparison between 2014 and 2017, clusters were further grouped into two categories according to  $\text{PM}_{10}$  loadings. Clusters  
318 arriving in Beijing when the local  $\text{PM}_{10}$  concentration was less than  $35 \mu\text{g m}^{-3}$  were recognized as clean clusters, while clusters with  
319  $\text{PM}_{10}$  concentrations greater than  $35 \mu\text{g m}^{-3}$  were defined as polluted clusters. As displayed in Fig. 7, the average  $\text{PM}_{10}$  concentration  
320 in local Beijing was  $114 \mu\text{g m}^{-3}$  in 2014 when the polluted clusters arrived, which was much higher than that in 2017 ( $74 \mu\text{g m}^{-3}$ ).  
321 While the contribution of polluted clusters in 2014 was 47%, polluted air masses transported from surrounding regions influenced  
322 Beijing approximately 20% of the time in 2017. The results here indicate that compared to 2014, Beijing was less influenced by  
323 polluted air masses transported from surrounding areas in 2017 during the wintertime, which benefited air quality improvement.  
324 In addition, air masses in 2017 brought more nitrate and less sulfate to Beijing than those in 2014.

325 The WRF-CMAQ model simulations showed that the contributions of regional transport to the  $\text{PM}_{2.5}$  concentration in Beijing were  
326  $31.4 \mu\text{g m}^{-3}$  and  $19.0 \mu\text{g m}^{-3}$  in the winters of 2014 and 2017, respectively (Fig. 5b). Although the proportion of regional transport  
327 (relative to the total  $\text{PM}_{2.5}$  concentration in Beijing) remained at approximately 35% in the two winters (34.4% in the winter of  
328 2014 and 36.4% in the winter of 2017), the absolute amount decreased by 39.6%. This result further supported that less  $\text{PM}_{2.5}$   
329 transported from surrounding regions indeed helped with  $\text{PM}_{2.5}$  abatement in Beijing. Compared with 2014, the variations in  $\text{PM}_{2.5}$   
330 components due to regional transport (Fig. 5b) in 2017 were basically consistent with the total aerosol composition changes that  
331 were observed (Fig. 1) and simulated (Fig. 5a) in Beijing. Sulfate had the most notable decrease, with a ~~decreasing rate~~ decrease of  
332 57.9% in its mass concentration, and the regional transport of OM and BC decreased by over 38%. The significant reduction in  
333 sulfate was mainly attributed to the effective  $\text{SO}_2$  emission controls in the surrounding regions, such as the special emission limits  
334 for power plants and the innovation of industrial boilers. The decreasing rate of regional transport OM was obviously lower than  
335 the total change, suggesting that the local emission controls of VOCs and primary OM in Beijing had a dominant contribution to  
336 the decrease in OM. The reduction in nitrate from regional transport was much smaller than that in other components. This was  
337 not only due to the insufficient  $\text{NO}_x$  emission controls in the surrounding areas but also the relatively rich ammonium environment  
338 in North China, which might have weakened the effects of  $\text{NO}_x$  reductions. Therefore, the collaborative reductions in  $\text{NO}_x$  and  
339  $\text{NH}_3$  are important for future air pollution control strategies (Liu et al., 2019).

### 340 3.2.4 Formation mechanisms

341 From a traditional viewpoint, sulfate formation mainly includes  $\text{SO}_2$  oxidation by OH in the gas phase and  $\text{SO}_2$  oxidation in cloud  
342 droplets by  $\text{H}_2\text{O}_2$  and  $\text{O}_3$  in the aqueous phase (Seinfeld and Pandis, 2012). This is actually the case for global sulfate production  
343 (Roelofs et al., 1998). The formation rate of sulfate through aqueous reactions is typically much faster than that through gas-phase  
344 oxidations. Recently, studies have found that ~~the heterogeneous oxidation of~~  $\text{SO}_2$  oxidation by  $\text{NO}_2$  in aerosol water with near

345 neutral aerosol acidity, which is usually ignored in current model simulations, plays an important role in the persistent formation  
346 of sulfate during haze events in northern China (B. Zheng et al., 2015; Cheng et al., 2016; Wang et al., 2016). ~~However, Others~~  
347 pointed out that regardless of the high NH<sub>3</sub> levels, aerosols are always moderately acidic in northern China, and there are probably  
348 other alternative formation pathways contributing to fast sulfate production in haze pollution (Guo et al., 2017b; Liu et al., 2017;  
349 Song et al., 2018). As the SO<sub>2</sub> emissions decreased substantially with the clean air actions, with the substantial decrease in SO<sub>2</sub>  
350 ~~emissions currently,~~ the importance of heterogeneous chemistry in sulfate formation is highly uncertain.

351 To shed light on this query, the formation of sulfate and nitrate with increasing RH was compared between 2014 and 2017. As  
352 displayed in Fig. 8, the SO<sub>4</sub>/BC ratio was much lower in 2017 than in 2014, especially at a higher RH, indicating greatly weakened  
353 sulfate formation in 2017 compared to primary BC emissions. NO<sub>3</sub>/BC showed little difference between 2014 and 2017. The sulfur  
354 oxidation ratio (SOR)~~s~~ and nitrogen oxidation ratio (NOR) of sulfur and nitrogen were further estimated as SOR (the molar ratio  
355 of sulfate to the sum of sulfate and SO<sub>2</sub>) and NOR (the molar ratio of nitrate to the sum of nitrate and NO<sub>x</sub>), respectively, to quantify  
356 the degree of SO<sub>2</sub> and NO<sub>x</sub> oxidations (Zheng et al., 2015; Li et al., 2016). Median values were used for comparison between 2014  
357 and 2017 to avoid bias caused by outliers. When the RH>50%, SOR started to increase significantly with the enhancement in RH  
358 in 2014, which was consistent with previous observations in Beijing in 2013 (G. J. Zheng et al., 2015). A year-long study in Beijing  
359 from 2012 to 2013 also revealed that a rapid increase in SOR was found at a RH threshold of ~45% (Fang et al., 2019). However,  
360 the starting point of SOR growth was clearly delayed in 2017, with a higher RH of 70%. Considering the decrease in the SO<sub>2</sub>  
361 mixing ratio from 15.5 ppb in the winter of 2014 to 2.8 ppb in the winter of 2017 (Table 1), ~~the results here imply we speculated~~  
362 that with the large reduction in gaseous precursors, the rapid formation of sulfate through heterogeneous reaction is more difficult  
363 to occur. In addition to emission reduction, reduced regional transport from southern polluted regions in 2017 helped to lower SO<sub>2</sub>  
364 concentrations in Beijing. Previous studies have revealed the positive feedback between aerosols and boundary layers, as high  
365 aerosol loadings could decrease the boundary layer height and further increase aerosol concentrations (Petäjä et al., 2016; Z. Li et  
366 al., 2017). With a lower PM<sub>2.5</sub> concentration in 2017, the interactions between aerosols and the boundary layer were weakened,  
367 which in turn also favored a decrease in the SO<sub>2</sub> concentration. At a lower RH, the SOR in 2017 (~0.14) was unexpectedly higher  
368 than that in 2014 (~0.06), demonstrating a higher sulfate production rate in 2017. Similar results have been observed over the  
369 eastern United States, where a considerable decrease in SO<sub>2</sub> resulted in the more efficient formation of particulate sulfate during  
370 wintertime (Shah et al., 2018). Combining airborne measurements, ground-based observations, and GEOS-Chem simulations, Shah  
371 et al. (2018) explained that sulfate production in winter is limited by the availability of oxidants and particle acidity. At lower  
372 concentrations of precursor gases, the oxidant limitation on SO<sub>2</sub> oxidation weakened, leading to a higher formation rate of sulfate.

373 Semivolatile PM<sub>2.5</sub> nitrate is formed through the partitioning of HNO<sub>3</sub> to the particle phase, which is more favored at higher aerosol  
374 pH. Aerosol pH is affected by gas phase NH<sub>3</sub> concentrations, where higher NH<sub>3</sub> generally leads to higher pH and therefore possibly  
375 more particulate nitrate. Aerosol pH is also influenced by the abundance of particulate sulfate (Seinfeld and Pandis, 2012). Sulfate  
376 is nonvolatile in the atmosphere. When sulfate is a significant fraction of aerosol mass, it has a dominant influence on aerosol pH,  
377 making aerosol acidic (low pH). In contrast, ammonium and nitrate are mainly semivolatile in the atmosphere. The particle-phase  
378 concentrations of ammonium and nitrate depend on the meteorological conditions (i.e., temperature and RH), their corresponding  
379 gas phase concentrations (NH<sub>3</sub> and HNO<sub>3</sub> respectively), and aerosol pH. For example, at high sulfate and moderate NH<sub>3</sub>  
380 concentrations, aerosols can be too acidic for the partitioning of HNO<sub>3</sub> to particle phase. However, at higher RH, or higher NH<sub>3</sub>  
381 concentrations, or if sulfate concentrations drop sufficiently, particle pH will increase and can reach a point at which HNO<sub>3</sub>  
382 partitioning to the particle phase occurs and particulate nitrate is formed. Lower temperature also favors HNO<sub>3</sub> partitioning to the  
383 particle phase through Henry's law constants. Particulate nitrate in PM<sub>2.5</sub> is mainly formed through the neutralization of HNO<sub>3</sub>  
384 with NH<sub>3</sub>. HNO<sub>3</sub> is produced by NO<sub>2</sub> oxidation via OH during the day and the hydrolysis reaction of dinitrogen pentoxide (N<sub>2</sub>O<sub>5</sub>)

385 ~~at night, with the former being the dominant pathway (Alexander et al., 2009). In this study, a~~At a lower RH, NOR was slightly  
386 higher in 2017 than in 2014 (Fig. 8), which may ~~have been~~ caused by the higher aerosol pH associated with the decrease in  
387 sulfate concentration reduced limitation of oxidants with lower NO<sub>x</sub> emissions in 2017 (details in Sect. 3.3). Nitrate formation was  
388 also affected by the competition for available NH<sub>3</sub> between sulfate and nitrate. In the atmosphere, NH<sub>3</sub> prefers to react first with  
389 H<sub>2</sub>SO<sub>4</sub> to form ammonium sulfate due to its stability. When excess NH<sub>3</sub> is available, ammonium nitrate is formed (Seinfeld and  
390 Pandis, 2012). With the decrease in sulfate concentration in 2017, some NH<sub>3</sub> was freed up to react with HNO<sub>3</sub>. This may have also  
391 facilitated the formation rate of nitrate. When RH>60%, NOR increased substantially in 2014 and 2017, indicating the importance  
392 of heterogeneous reactions in nitrate production. In addition, as RH increases, the AWC increases accordingly, resulting in higher  
393 aerosol pH. This allows more semivolatile nitrate to partition to the particle phase through a feedback loop, thus favoring the  
394 formation of particulate nitrate.

### 395 3.3 Influence of the transition in aerosol characteristics on particle properties

396 According to thermodynamic calculations, various aerosol properties were affected by changes in aerosol characteristics associated  
397 with clean air actions. As shown in Fig. 9a, nitrate and sulfate play key roles in determining the AWC in PM<sub>2.5</sub>. The decreasing  
398 mass concentrations of nitrate and sulfate result in a lower AWC. Similar observations have been reported previously across  
399 northern China, revealing that nitrate and sulfate are dominant anthropogenic inorganic salts driving AWC (Wu et al., 2018). With  
400 the clean air actions enacted, the mass concentrations of nitrate and sulfate decreased during 2013-2017, leading to an average  
401 decline in AWC from 12.04.8 to 8.2.5 μg m<sup>-3</sup>. Data for the winter of 2013 were acquired from Sun et al. (2016). The reduced AWC  
402 further helped air quality improvement by lowering the ambient aerosol mass and enhancing visibility. Because aqueous-phase  
403 reactions contribute largely to sulfate formation in winter, the decrease in AWC decelerated the formation of sulfate. In addition,  
404 the lower AWC slowed down the uptake coefficient of N<sub>2</sub>O<sub>5</sub> for heterogeneous processing, thereby suppressing the formation of  
405 particulate nitrate.

406 Figure 9b displays the effects of nitrate and sulfate concentrations on particle acidity. Particle acidity is largely driven by the mass  
407 concentration of sulfate and is less sensitive to the variation in nitrate. Particle pH substantially decreases with increasing sulfate  
408 concentration. Ding et al. (2019) suggested that sulfate is one of the common driving factors influencing particle acidity in Beijing  
409 across all four seasons. In contrast, more particulate nitrate leads to a slightly higher pH by increasing the particle liquid water and  
410 diluting aqueous H<sup>+</sup> concentrations. Through the comparison of pH predictions among various locations worldwide, Guo et al.  
411 (2018) also found that a higher particle pH was generally associated with higher concentrations of nitrate. During 2013-2017, the  
412 average particle pH varied from 4.55.0 to 5.36.2, with a significant decrease in sulfate concentration, ~~resulting in a more neutral~~  
413 ~~atmospheric environment.~~ The pH values here agree reasonably with previous ISORROPIA-II calculations, showing that fine  
414 particles are moderately acidic in northern China during wintertime (Guo et al., 2017a; Liu et al., 2017; Song et al., 2018; Ding et  
415 al., 2019). When pH > 5.0, aqueous-phase productions of sulfate are dominated by SO<sub>2</sub> oxidation with H<sub>2</sub>O<sub>2</sub>, O<sub>3</sub>, and NO<sub>2</sub> under  
416 haze conditions in Beijing (Cheng et al., 2016). The sulfate oxidation rates by O<sub>3</sub> and NO<sub>2</sub> increase with increasing particle pH.  
417 Therefore, a more neutral atmosphere would favor aqueous-phase sulfate formation in Beijing. Particle acidity also influences the  
418 gas-particle partitioning of nitrate. The rising particle pH would result in a higher fraction of particulate nitrate ( $\epsilon(NO_3^-) =$   
419  $\frac{[NO_3^-]}{[HNO_3] + [NO_3^-]}$ ) (Guo et al., 2016). Figure S209a displays the variation in  $\epsilon(NO_3^-)$  as a function of particle pH under typical Beijing  
420 winter conditions (temperature of approximately 0°C). With a particle pH below 3,  $\epsilon(NO_3^-)$  increases sufficiently with the  
421 enhancement in particle pH. However, when the particle pH is larger than 3,  $\epsilon(NO_3^-)$  remains relatively stable (approaching 1),  
422 consistent with previous findings by Guo et al. (2018). From 2013 to 2017, with the particle pH remaining above 3 in Beijing, no  
423 clear change in  $\epsilon(NO_3^-)$  was observed (Fig. S209b).

424 The variations in nitrate and sulfate concentrations also affected the gas-particle partitioning of total ammonium ( $\text{NH}_x = \text{NH}_3 +$   
425  $\text{NH}_4^+$ ). As expected, the decreased concentrations of nitrate and sulfate led to a reduction in the ammonium particle fraction ( $\epsilon$   
426  $(\text{NH}_4^+) = \text{NH}_4^+/\text{NH}_x$ ; Fig. 10). From 2013 to 2017,  $\epsilon$  ( $\text{NH}_4^+$ ) in Beijing always stayed below 0.43, indicating that most  
427 ammonium existed in the gas phase. Therefore, a minor reduction in  $\text{NH}_x$  would not be sufficient for air quality improvement. Guo  
428 et al. (2018) revealed that for winter haze conditions in Beijing, an approximate 60% decrease in  $\text{NH}_x$  was required to achieve an  
429 effective reduction in  $\text{PM}_{2.5}$ . Due to the close linkage between ammonia emissions and agricultural activities, it may be difficult to  
430 attain substantial ammonia reduction in China.

#### 431 4 Conclusions

432 This study investigated the variations in aerosol characteristics in Beijing during the winters of 2014 and 2017 by combining the  
433 online measurements of aerosol chemical composition with a comprehensive model analysis of meteorological conditions,  
434 anthropogenic emissions, and regional transport. The average  $\text{PM}_{10}$  concentration decreased from  $66.2 \mu\text{g m}^{-3}$  in the winter of 2014  
435 to  $33.4 \mu\text{g m}^{-3}$  in the winter of 2017, with decreasing concentrations of organics, sulfate, nitrate, and ammonium by  $18.5 \mu\text{g m}^{-3}$ ,  
436  $4.9 \mu\text{g m}^{-3}$ ,  $1.3 \mu\text{g m}^{-3}$ , and  $1.5 \mu\text{g m}^{-3}$ , respectively. These changes reduced the mass fractions of organics and sulfate from 59%  
437 to 36% and from 13% to 9%, respectively, whereas increased the nitrate contribution from 19% to 32%. Consequently, the winter  
438 haze pollution changed from sulfate-driven to nitrate-driven in Beijing from 2014 to 2017, implicating the increasing role of nitrate  
439 in aerosol pollution.

440 The chemical transport model simulations suggest that the rapidly declining emissions in Beijing and its adjacent regions account  
441 for ~75% of  $\text{PM}_{2.5}$  abatement in Beijing, and the remaining portion can be explained by the favorable weather conditions in 2017.  
442 The faster reductions in  $\text{SO}_2$  emissions compared to  $\text{NO}_x$  emissions are in line with the decreased sulfate contribution and increased  
443 nitrate fraction in observed aerosols, and the model simulations with these emission estimates can reproduce the relative changes  
444 in aerosol composition. Regional transport contributed moderately to the variations in aerosol concentration and its chemical  
445 composition, with less polluted air masses transported from surrounding regions to Beijing in the winter of 2017. The air masses  
446 were observed to have brought more nitrate and less sulfate to Beijing. Furthermore, The fast  $\text{SO}_2$ -to-sulfate conversion through  
447 heterogeneous reactions was observed to increase promptly at a RH threshold of ~50% in 2014, while a higher RH of 70% was  
448 observed in 2017. Based on these ambient observations, the suppressed sulfate formation during wintertime was possibly caused  
449 by the considerable decrease in  $\text{SO}_2$  emissions-suppressed the rapid formation of sulfate during wintertime. The fast  $\text{SO}_2$ -to-sulfate  
450 conversion through heterogeneous reactions was observed to increase promptly at a RH threshold of ~50% in 2014, while a higher  
451 RH of 70% was observed in 2017.

452 Thermodynamic calculations showed that the decreased sulfate and nitrate concentrations in 2017 caused a lower AWC in  $\text{PM}_{2.5}$ ,  
453 which further decreased the ambient aerosol mass and weakened the formation rates of sulfate and nitrate through aqueous-phase  
454 reactions. Particle acidity displayed a decline during 2014-2017, mostly driven by the declining sulfate concentration. In turn, the  
455 more neutral ambient environment would favor the aqueous oxidation of sulfate in Beijing. Analysis of the ammonium particle  
456 fraction indicated that most ammonium in Beijing existed in the gas phase. Therefore, increased efforts are needed to achieve an  
457 effective reduction in particle ammonium in the future.

458 **Author contributions**

459 QZ and KH conceived the study. HL conducted the field measurements and carried out the data analysis. JC provided the emission  
460 data and performed the model simulations. BZ participated the data analysis. HL, JC and QZ wrote the paper with inputs from all  
461 coauthors.

462 **Acknowledgements**

463 This work was funded by the National Natural Science Foundation of China (41571130035, 41571130032 and 41625020).

464 **References**

- 465 Bey, I., Jacob, D. J., Yantosca, R. M., Logan, J. A., Field, B. D., Fiore, A. M., Li, Q., Liu, H., Mickley, L. J., and Schultz, M. G.:  
466 Global modeling of tropospheric chemistry with assimilated meteorology: Model description and evaluation, *J. Geophys. Res.*,  
467 106, D19, 23073–23095, <https://doi.org/10.1029/2001JD000807>, 2001.
- 468 Canonaco, F., Crippa, M., Slowik, J. G., Baltensperger, U., and Prevot, A. S. H.: SoFi, an IGOR-based interface for the efficient  
469 use of the generalized multilinear engine (ME-2) for the source apportionment: ME-2 application to aerosol mass spectrometer  
470 data, *Atmos Meas Tech*, 6, 3649-3661, 2013.
- 471 Cheng, J., Su, J., Cui, T., Li, X., Dong, X., Sun, F., Yang, Y., Tong, D., Zheng, Y., Li, Y., Li, J., Zhang, Q., and He, K.: Dominant  
472 role of emission reduction in PM<sub>2.5</sub> air quality improvement in Beijing during 2013–2017: a model-based decomposition  
473 analysis, *Atmos. Chem. Phys.*, 19, 6125-6146, <https://doi.org/10.5194/acp-19-6125-2019>, 2019.
- 474 Cheng, Y. F., Zheng, G. J., Wei, C., Mu, Q., Zheng, B., Wang, Z. B., Gao, M., Zhang, Q., He, K. B., Carmichael, G., Poschl, U.,  
475 and Su, H.: Reactive nitrogen chemistry in aerosol water as a source of sulfate during haze events in China, *Sci Adv*, 2, 2016.
- 476 Cohen, A. J., Brauer, M., Burnett, R., Anderson, H. R., Frostad, J., Estep, K., Balakrishnan, K., Brunekreef, B., Dandona, L.,  
477 Dandona, R., Feigin, V., Freedman, G., Hubbell, B., Jobling, A., Kan, H., Knibbs, L., Liu, Y., Martin, R., Morawska, L., Pope,  
478 C. A., Shin, H., Straif, K., Shaddick, G., Thomas, M., van Dingenen, R., van Donkelaar, A., Vos, T., Murray, C. J. L., and  
479 Forouzanfar, M. H.: Estimates and 25-year trends of the global burden of disease attributable to ambient air pollution: an  
480 analysis of data from the Global Burden of Diseases Study 2015, *Lancet*, 389, 1907-1918, 2017.
- 481 Fang, Y., Ye, C., Wang, J., Wu, Y., Hu, M., Lin, W., Xu, F., and Zhu, T.: RH and O<sub>3</sub> concentration as two prerequisites for sulfate  
482 formation, *Atmos. Chem. Phys. Discuss.*, 2019, 1-25, [10.5194/acp-2019-284](https://doi.org/10.5194/acp-2019-284), 2019.
- 483 Fountoukis, C., and Nenes, A.: ISORROPIA II: a computationally efficient thermodynamic equilibrium model for K<sup>+</sup>-Ca<sup>2+</sup>-Mg<sup>2+</sup>-  
484 NH<sub>4</sub><sup>+</sup>-Na<sup>+</sup>-SO<sub>4</sub><sup>2-</sup>-NO<sub>3</sub><sup>-</sup>-Cl<sup>-</sup>-H<sub>2</sub>O aerosols, *Atmos Chem Phys*, 7, 4639-4659, 2007.
- 485 Gao, M., Carmichael, G. R., Saide, P. E., Lu, Z., Yu, M., Streets, D. G., and Wang, Z.: Response of winter fine particulate matter  
486 concentrations to emission and meteorology changes in North China, *Atmos. Chem. Phys.*, 16, 11837-11851, [10.5194/acp-](https://doi.org/10.5194/acp-16-11837-2016)  
487 16-11837-2016, 2016.
- 488 Geng, G., Zhang, Q., Tong, D., Li, M., Zheng, Y., Wang, S., and He, K.: Chemical composition of ambient PM<sub>2.5</sub> over China  
489 and relationship to precursor emissions during 2005–2012, *Atmos. Chem. Phys.*, 17, 9187-9203, [10.5194/acp-17-9187-2017](https://doi.org/10.5194/acp-17-9187-2017),  
490 2017.
- 491 Gui, K., Che, H., Wang, Y., Wang, H., Zhang, L., Zhao, H., Zheng, Y., Sun, T., and Zhang, X.: Satellite-derived PM<sub>2.5</sub>  
492 concentration trends over Eastern China from 1998 to 2016: Relationships to emissions and meteorological parameters,  
493 *Environ Pollut*, 247, 1125-1133, <https://doi.org/10.1016/j.envpol.2019.01.056>, 2019.
- 494 Guo, H., Xu, L., Bougiatioti, A., Cerully, K. M., Capps, S. L., Hite, J. R., Carlton, A. G., Lee, S. H., Bergin, M. H., Ng, N. L.,  
495 Nenes, A., and Weber, R. J.: Fine-particle water and pH in the southeastern United States, *Atmos Chem Phys*, 15, 5211-5228,  
496 2015.
- 497 [Guo, H., Sullivan, A. P., Campuzano-Jost, P., Schroder, J. C., Lopez-Hilfiker, F. D., Dibb, J. E., Jimenez, J. L., Thornton, J. A.,](#)  
498 [Brown, S. S., Nenes, A., and Weber, R. J.: Fine particle pH and the partitioning of nitric acid during winter in the northeastern](#)  
499 [United States, \*Journal of Geophysical Research: Atmospheres\*, 121, 10,355-310,376, \[10.1002/2016JD025311\]\(https://doi.org/10.1002/2016JD025311\), 2016.](#)

- 500 [Guo, H., Liu, J., Froyd, K. D., Roberts, J. M., Veres, P. R., Hayes, P. L., Jimenez, J. L., Nenes, A., and Weber, R. J.: Fine particle](#)  
501 [pH and gas-particle phase partitioning of inorganic species in Pasadena, California, during the 2010 CalNex campaign, \*Atmos.\*](#)  
502 [\*Chem. Phys.\*, 17, 5703-5719, 10.5194/acp-17-5703-2017, 2017a.](#)
- 503 [Guo, H., Weber, R. J., and Nenes, A.: High levels of ammonia do not raise fine particle pH sufficiently to yield nitrogen oxide-](#)  
504 [dominated sulfate production, \*Scientific Reports\*, 7, 12109, 10.1038/s41598-017-11704-0, 2017a.](#)
- 505 Guo, H. Y., Otjes, R., Schlag, P., Kiendler-Scharr, A., Nenes, A., and Weber, R. J.: Effectiveness of ammonia reduction on control  
506 of fine particle nitrate, *Atmos Chem Phys*, 18, 12241-12256, 2018.
- 507 [Hennigan, C. J., Izumi, J., Sullivan, A. P., Weber, R. J., and Nenes, A.: A critical evaluation of proxy methods used to estimate the](#)  
508 [acidity of atmospheric particles, \*Atmos. Chem. Phys.\*, 15, 2775-2790, <https://doi.org/10.5194/acp-15-2775-2015>, 2015.](#)
- 509 Huang, X. F., He, L. Y., Hu, M., Canagaratna, M. R., Sun, Y., Zhang, Q., Zhu, T., Xue, L., Zeng, L. W., Liu, X. G., Zhang, Y. H.,  
510 Jayne, J. T., Ng, N. L., and Worsnop, D. R.: Highly time-resolved chemical characterization of atmospheric submicron  
511 particles during 2008 Beijing Olympic Games using an Aerodyne High-Resolution Aerosol Mass Spectrometer, *Atmos Chem*  
512 *Phys*, 10, 8933-8945, 2010.
- 513 Intergovernmental Panel on Climate Change (IPCC) (2013), *Climate Change 2013: The Physical Science Basis. Contribution of*  
514 *Working Group I to the Fifth Assessment Report of the Intergovernmental Panel on Climate Change*, 1535 pp., Cambridge  
515 Univ. Press, Cambridge, U. K., and New York.
- 516 Li, H. Y., Zhang, Q., Zhang, Q., Chen, C. R., Wang, L. T., Wei, Z., Zhou, S., Parworth, C., Zheng, B., Canonaco, F., Prevot, A. S.  
517 H., Chen, P., Zhang, H. L., Wallington, T. J., and He, K. B.: Wintertime aerosol chemistry and haze evolution in an extremely  
518 polluted city of the North China Plain: significant contribution from coal and biomass combustion, *Atmos Chem Phys*, 17,  
519 4751-4768, 2017.
- 520 Li, H. Y., Zhang, Q., Zheng, B., Chen, C. R., Wu, N. N., Guo, H. Y., Zhang, Y. X., Zheng, Y. X., Li, X., and He, K. B.: Nitrate-  
521 driven urban haze pollution during summertime over the North China Plain, *Atmos Chem Phys*, 18, 5293-5306, 2018.
- 522 Li, M., Zhang, Q., Kurokawa, J. I., Woo, J. H., He, K., Lu, Z., Ohara, T., Song, Y., Streets, D. G., Carmichael, G. R., Cheng, Y.,  
523 Hong, C., Huo, H., Jiang, X., Kang, S., Liu, F., Su, H., and Zheng, B.: MIX: a mosaic Asian anthropogenic emission inventory  
524 under the international collaboration framework of the MICS-Asia and HTAP, *Atmos. Chem. Phys.*, 17, 935-963,  
525 <https://doi.org/10.5194/acp-17-935-2017>, 2017.
- 526 [Li, T.-C., Yuan, C.-S., Huang, H.-C., Lee, C.-L., Wu, S.-P., and Tong, C.: Inter-comparison of Seasonal Variation, Chemical](#)  
527 [Characteristics, and Source Identification of Atmospheric Fine Particles on Both Sides of the Taiwan Strait, \*Scientific Reports\*,](#)  
528 [6, 22956, 10.1038/srep22956 <https://www.nature.com/articles/srep22956#supplementary-information>, 2016.](#)
- 529 Li, Z., Guo, J., Ding, A., Liao, H., Liu, J., Sun, Y., Wang, T., Xue, H., Zhang, H., and Zhu, B.: Aerosol and boundary-layer  
530 interactions and impact on air quality, *National Science Review*, 4, 810-833, 10.1093/nsr/nwx117 %J National Science  
531 Review, 2017.
- 532 Liang, P. F., Zhu, T., Fang, Y. H., Li, Y. R., Han, Y. Q., Wu, Y. S., Hu, M., and Wang, J. X.: The role of meteorological conditions  
533 and pollution control strategies in reducing air pollution in Beijing during APEC 2014 and Victory Parade 2015, *Atmos Chem*  
534 *Phys*, 17, 2017.
- 535 Liu, M. M., Bi, J., and Ma, Z. W.: Visibility-Based PM<sub>2.5</sub> Concentrations in China: 1957-1964 and 1973-2014, *Environmental*  
536 *Science & Technology*, 51, 13161-13169, 2017.
- 537 Liu, M. X., Song, Y., Zhou, T., Xu, Z. Y., Yan, C. Q., Zheng, M., Wu, Z. J., Hu, M., Wu, Y. S., and Zhu, T.: Fine particle pH  
538 during severe haze episodes in northern China, *Geophys Res Lett*, 44, 5213-5221, 2017.
- 539 Liu, M. X., Huang, X., Song, Y., Tang, J., Cao, J., Zhang, X., Zhang, Q., Wang, S., Xu, T., Kang, L., Cai, X., Zhang, H., Yang, F.,  
540 Wang, H., Yu, J., Lau, Alexis K. H., He, L., Huang, X., Duan, L., Ding A., Xue, L., Gao, J., Liu, B., and Zhu, T.: Ammonia  
541 emission control in China would mitigate haze pollution and nitrogen deposition, but worsen acid rain, *PANS*, 116 (16) 7760-  
542 7765, <https://doi.org/10.1073/pnas.1814880116>, 2019.
- 543 [Meng, Z. Y., Lin, W. L., Jiang, X. M., Yan, P., Wang, Y., Zhang, Y. M., Jia, X. F., and Yu, X. L.: Characteristics of atmospheric](#)  
544 [ammonia over Beijing, China, \*Atmos. Chem. Phys.\*, 11, 6139-6151, <https://doi.org/10.5194/acp-11-6139-2011>, 2011.](#)
- 545 Middlebrook, A. M., Bahreini, R., Jimenez, J. L., and Canagaratna, M. R.: Evaluation of Composition-Dependent Collection  
546 Efficiencies for the Aerodyne Aerosol Mass Spectrometer using Field Data, *Aerosol Sci Tech*, 46, 258-271, 2012. Ng, N. L.,  
547 Herndon, S. C., Trimborn, A., Canagaratna, M. R., Croteau, P. L., Onasch, T. B., Sueper, D., Worsnop, D. R., Zhang, Q., Sun,

- 548 Y. L., and Jayne, J. T.: An Aerosol Chemical Speciation Monitor (ACSM) for Routine Monitoring of the Composition and  
549 Mass Concentrations of Ambient Aerosol, *Aerosol Sci Tech*, 45, 780-794, 2011a.
- 550 Ng, N. L., Canagaratna, M. R., Jimenez, J. L., Zhang, Q., Ulbrich, I. M., and Worsnop, D. R.: Real-Time Methods for Estimating  
551 Organic Component Mass Concentrations from Aerosol Mass Spectrometer Data, *Environmental Science & Technology*, 45,  
552 910-916, 2011b.
- 553 Paatero, P.: The multilinear engine - A table-driven, least squares program for solving multilinear problems, including the n-way  
554 parallel factor analysis model, *J Comput Graph Stat*, 8, 854-888, 1999.
- 555 Petäjä, T., Järvi, L., Kerminen, V. M., Ding, A. J., Sun, J. N., Nie, W., Kujansuu, J., Virkkula, A., Yang, X., Fu, C. B., Zilitinkevich,  
556 S., and Kulmala, M.: Enhanced air pollution via aerosol-boundary layer feedback in China, *Scientific Reports*, 6, 18998,  
557 10.1038/srep18998 <https://www.nature.com/articles/srep18998#supplementary-information>, 2016.
- 558 Petzold, A., and Schonlinner, M.: Multi-angle absorption photometry - a new method for the measurement of aerosol light  
559 absorption and atmospheric black carbon, *J Aerosol Sci*, 35, 421-441, 2004.
- 560 Pope, C. A., Ezzati, M., and Dockery, D. W.: Fine-Particulate Air Pollution and Life Expectancy in the United States., *New Engl*  
561 *J Med*, 360, 376-386, 2009.
- 562 Pui, D. Y. H., Chen, S. C., and Zuo, Z. L.: PM<sub>2.5</sub> in China: Measurements, sources, visibility and health effects, and mitigation,  
563 *Particuology*, 13, 1-26, 2014.
- 564 Roelofs, G.-J. A. N., Lelieveld, J. O. S., and Ganzeveld, L.: Simulation of global sulfate distribution and the influence on effective  
565 cloud drop radii with a coupled photochemistry sulfur cycle model, *Tellus B*, 50, 224-242, 10.1034/j.1600-0889.1998.t01-2-  
566 00002.x, 1998.
- 567 Seinfeld, J. H. and Pandis, S. N.: Atmospheric chemistry and physics: from air pollution to climate change, 2nd Edition, John  
568 Wiley & Sons, New York, USA, 2012.
- 569 Shah, V., Jaegle, L., Thornton, J. A., Lopez-Hilfiker, F. D., Lee, B. H., Schroder, J. C., Campuzano-Jost, P., Jimenez, J. L., Guo,  
570 H. Y., Sullivan, A. P., Weber, R. J., Green, J. R., Fiddler, M. N., Bililign, S., Campos, T. L., Stell, M., Weinheimer, A. J.,  
571 Montzka, D. D., and Brown, S. S.: Chemical feedbacks weaken the wintertime response of particulate sulfate and nitrate to  
572 emissions reductions over the eastern United States, *P Natl Acad Sci USA*, 115, 8110-8115, 2018.
- 573 [Song, S., Gao, M., Xu, W., Shao, J., Shi, G., Wang, S., Wang, Y., Sun, Y., and McElroy, M. B.: Fine-particle pH for Beijing winter](#)  
574 [haze as inferred from different thermodynamic equilibrium models, \*Atmos. Chem. Phys.\*, 18, 7423-7438, 10.5194/acp-18-  
575 \[7423-2018, 2018.\]\(#\)](#)
- 576 Squizzato, S., Masiol, M., Brunelli, A., Pistollato, S., Tarabotti, E., Rampazzo, G., and Pavoni, B.: Factors determining the  
577 formation of secondary inorganic aerosol: a case study in the Po Valley (Italy), *Atmos Chem Phys*, 13, 1927-1939, 2013.
- 578 Su, X., Tie, X. X., Li, G. H., Cao, J. J., Huang, R. J., Feng, T., Long, X., and Xu, R. G.: Effect of hydrolysis of N<sub>2</sub>O<sub>5</sub> on nitrate  
579 and ammonium formation in Beijing China: WRF-Chem model simulation, *Sci Total Environ*, 579, 221-229, 2017.
- 580 Sun, J., Liang, M., Shi, Z., Shen, F., Li, J., Huang, L., Ge, X., Chen, Q., Sun, Y., Zhang, Y., Chang, Y., Ji, D., Ying, Q., Zhang,  
581 H., Kota, S. H., and Hu, J.: Investigating the PM<sub>2.5</sub> mass concentration growth processes during 2013–2016 in Beijing and  
582 Shanghai, *Chemosphere*, 221, 452-463, <https://doi.org/10.1016/j.chemosphere.2018.12.200>, 2019.
- 583 [Sun, K., Qu, Y., Wu, Q., Han, T., Gu, J., Zhao, J., Sun, Y., Jiang, Q., Gao, Z., Hu, M., Zhang, Y., Lu, K., Nordmann, S., Cheng,](#)  
584 [Y., Hou, L., Ge, H., Furuuchi, M., Hata, M., and Liu, X.: Chemical characteristics of size-resolved aerosols in winter in](#)  
585 [Beijing, \*Journal of Environmental Sciences\*, 26, 1641-1650, <https://doi.org/10.1016/j.jes.2014.06.004>, 2014.](#)
- 586 Sun, Y. L., Zhuang, G. S., Tang, A. H., Wang, Y., and An, Z. S.: Chemical characteristics of PM<sub>2.5</sub> and PM<sub>10</sub> in haze-fog episodes  
587 in Beijing, *Environmental Science & Technology*, 40, 3148-3155, 10.1021/es051533g, 2006.
- 588 Sun, Y., Jiang, Q., Wang, Z., Fu, P., Li, J., Yang, T., and Yin, Y.: Investigation of the sources and evolution processes of severe  
589 haze pollution in Beijing in January 2013, *Journal of Geophysical Research: Atmospheres*, 119, 4380-4398,  
590 10.1002/2014JD021641, 2014.
- 591 Sun, Y. L., Wang, Z. F., Du, W., Zhang, Q., Wang, Q. Q., Fu, P. Q., Pan, X. L., Li, J., Jayne, J., and Worsnop, D. R.: Long-term  
592 real-time measurements of aerosol particle composition in Beijing, China: seasonal variations, meteorological effects, and  
593 source analysis, *Atmos. Chem. Phys.*, 15, 10149-10165, 10.5194/acp-15-10149-2015, 2015.

- 594 Sun, Y. L., Du, W., Fu, P. Q., Wang, Q. Q., Li, J., Ge, X. L., Zhang, Q., Zhu, C. M., Ren, L. J., Xu, W. Q., Zhao, J., Han, T. T.,  
595 Worsnop, D. R., and Wang, Z. F.: Primary and secondary aerosols in Beijing in winter: sources, variations and processes,  
596 *Atmos Chem Phys*, 16, 8309-8329, 2016.
- 597 Tang, I. N., and Munkelwitz, H. R.: Aerosol Phase-Transformation and Growth in the Atmosphere, *J Appl Meteorol*, 33, 791-796,  
598 1994.
- 599 Ulbrich, I. M., Canagaratna, M. R., Zhang, Q., Worsnop, D. R., and Jimenez, J. L.: Interpretation of organic components from  
600 Positive Matrix Factorization of aerosol mass spectrometric data, *Atmos Chem Phys*, 9, 2891-2918, 2009.
- 601 van Donkelaar, A., Martin, R. V., Li, C., and Burnett, R. T.: Regional Estimates of Chemical Composition of Fine Particulate  
602 Matter Using a Combined Geoscience-Statistical Method with Information from Satellites, Models, and Monitors,  
603 *Environmental Science & Technology*, 10.1021/acs.est.8b06392, 2019. Wang, G. H., Zhang, R. Y., Gomez, M. E., Yang, L.  
604 X., Zamora, M. L., Hu, M., Lin, Y., Peng, J. F., Guo, S., Meng, J. J., Li, J. J., Cheng, C. L., Hu, T. F., Ren, Y. Q., Wang, Y.  
605 S., Gao, J., Cao, J. J., An, Z. S., Zhou, W. J., Li, G. H., Wang, J. Y., Tian, P. F., Marrero-Ortiz, W., Secrest, J., Du, Z. F.,  
606 Zheng, J., Shang, D. J., Zeng, L. M., Shao, M., Wang, W. G., Huang, Y., Wang, Y., Zhu, Y. J., Li, Y. X., Hu, J. X., Pan, B.,  
607 Cai, L., Cheng, Y. T., Ji, Y. M., Zhang, F., Rosenfeld, D., Liss, P. S., Duce, R. A., Kolb, C. E., and Molina, M. J.: Persistent  
608 sulfate formation from London Fog to Chinese haze, *P Natl Acad Sci USA*, 113, 13630-13635, 2016.
- 609 Wang, X. Y., Wang, K. C., and Su, L. Y.: Contribution of Atmospheric Diffusion Conditions to the Recent Improvement in Air  
610 Quality in China, *Scientific Reports*, 6, 2016.
- 611 Wang, Y., Zhang, Q., Jiang, J., Zhou, W., Wang, B., He, K., Duan, F., Zhang, Q., Philip, S., and Xie, Y.: Enhanced sulfate formation  
612 during China's severe winter haze episode in January 2013 missing from current models, 119, 10,425-410,440,  
613 doi:10.1002/2013JD021426, 2014.
- 614 Weber, R. J., Guo, H. Y., Russell, A. G., and Nenes, A.: High aerosol acidity despite declining atmospheric sulfate concentrations  
615 over the past 15 years, *Nat Geosci*, 9, 282-+, 2016.
- 616 Wu, Z. J., Wang, Y., Tan, T. Y., Zhu, Y. S., Li, M. R., Shang, D. J., Wang, H. C., Lu, K. D., Guo, S., Zeng, L. M., and Zhang, Y.  
617 H.: Aerosol Liquid Water Driven by Anthropogenic Inorganic Salts: Implying Its Key Role in Haze Formation over the North  
618 China Plain, *Environ Sci Tech Let*, 5, 160-166, 2018.
- 619 Xu, W. Q., Sun, Y. L., Chen, C., Du, W., Han, T. T., Wang, Q. Q., Fu, P. Q., Wang, Z. F., Zhao, X. J., Zhou, L. B., Ji, D. S., Wang,  
620 P. C., and Worsnop, D. R.: Aerosol composition, oxidation properties, and sources in Beijing: results from the 2014 Asia-  
621 Pacific Economic Cooperation summit study, *Atmos. Chem. Phys.*, 15, 13681-13698, 10.5194/acp-15-13681-2015, 2015.
- 622 [Xu, W., Sun, Y., Wang, Q., Zhao, J., Wang, J., Ge, X., Xie, C., Zhou, W., Du, W., Li, J., Fu, P., Wang, Z., Worsnop, D. R., and](#)  
623 [Coe, H.: Changes in Aerosol Chemistry from 2014 to 2016 in Winter in Beijing: Insights from High Resolution Aerosol Mass](#)  
624 [Spectrometry](#), 0, doi:10.1029/2018JD029245, 2018.
- 625 [Xu, W., Sun, Y., Wang, Q., Zhao, J., Wang, J., Ge, X., Xie, C., Zhou, W., Du, W., Li, J., Fu, P., Wang, Z., Worsnop, D. R., and](#)  
626 [Coe, H.: Changes in Aerosol Chemistry From 2014 to 2016 in Winter in Beijing: Insights From High-Resolution Aerosol](#)  
627 [Mass Spectrometry](#), *Journal of Geophysical Research: Atmospheres*, 124, 1132-1147, 10.1029/2018JD029245, 2019.
- 628 Yun, H., Wang, W. H., Wang, T., Xia, M., Yu, C., Wang, Z., Poon, S. C. N., Yue, D. L., and Zhou, Y.: Nitrate formation from  
629 heterogeneous uptake of dinitrogen pentoxide during a severe winter haze in southern China, *Atmos Chem Phys*, 18, 17515-  
630 17527, 2018.
- 631 Zhang, Q., Jimenez, J. L., Canagaratna, M. R., Ulbrich, I. M., Ng, N. L., Worsnop, D. R., and Sun, Y. L.: Understanding  
632 atmospheric organic aerosols via factor analysis of aerosol mass spectrometry: a review, *Anal Bioanal Chem*, 401, 3045-3067,  
633 2011.
- 634 [Zhang, Y., Tang, A., Wang, D., Wang, Q., Benedict, K., Zhang, L., Liu, D., Li, Y., Collett Jr., J. L., Sun, Y., and Liu, X.: The](#)  
635 [vertical variability of ammonia in urban Beijing, China](#), *Atmos. Chem. Phys.*, 18, 16385-16398, [https://doi.org/10.5194/acp-](https://doi.org/10.5194/acp-18-16385-2018)  
636 [18-16385-2018](#), 2018.
- 637 [Zhao, M., Wang, S., Tan, J., Hua, Y., Wu, D., and Hao, J.: Variation of Urban Atmospheric Ammonia Pollution and its Relation](#)  
638 [with PM2.5 Chemical Property in Winter of Beijing, China](#), *Aerosol Air Qual Res*, 16, 1378-1389, 10.4209/aaqr.2015.12.0699,  
639 2016.
- 640 [Zhao, P., Chen, Y., and Su, J.: Size-resolved carbonaceous components and water-soluble ions measurements of ambient aerosol](#)  
641 [in Beijing](#), *Journal of Environmental Sciences*, 54, 298-313, <https://doi.org/10.1016/j.jes.2016.08.027>, 2017.

- 642 Zhao, X. J., Zhang, X. L., Xu, X. F., Xu, J., Meng, W., and Pu, W. W.: Seasonal and diurnal variations of ambient PM<sub>2.5</sub>  
643 concentration in urban and rural environments in Beijing, *Atmos Environ*, 43, 2893-2900, 10.1016/j.atmosenv.2009.03.009,  
644 2009.
- 645 Zheng, B., Zhang, Q., Zhang, Y., He, K. B., Wang, K., Zheng, G. J., Duan, F. K., Ma, Y. L., and Kimoto, T.: Heterogeneous  
646 chemistry: a mechanism missing in current models to explain secondary inorganic aerosol formation during the January 2013  
647 haze episode in North China, *Atmos Chem Phys*, 15, 2031-2049, 2015.
- 648 Zheng, B., Tong, D., Li, M., Liu, F., Hong, C., Geng, G., Li, H., Li, X., Peng, L., Qi, J., Yan, L., Zhang, Y., Zhao, H., Zheng, Y.,  
649 He, K., and Zhang, Q.: Trends in China's anthropogenic emissions since 2010 as the consequence of clean air actions, *Atmos.*  
650 *Chem. Phys.*, 18, 14095-14111, <https://doi.org/10.5194/acp-18-14095-2018>, 2018.
- 651 Zheng, J., Hu, M., Peng, J. F., Wu, Z. J., Kumar, P., Li, M. R., Wang, Y. J., and Guo, S.: Spatial distributions and chemical  
652 properties of PM<sub>2.5</sub> based on 21 field campaigns at 17 sites in China, *Chemosphere*, 159, 480-487, 2016.
- 653 Zheng, G. J., Duan, F. K., Su, H., Ma, Y. L., Cheng, Y., Zheng, B., Zhang, Q., Huang, T., Kimoto, T., Chang, D., Poschl, U.,  
654 Cheng, Y. F., and He, K. B.: Exploring the severe winter haze in Beijing: the impact of synoptic weather, regional transport  
655 and heterogeneous reactions, *Atmos Chem Phys*, 15, 2969-2983, 2015.

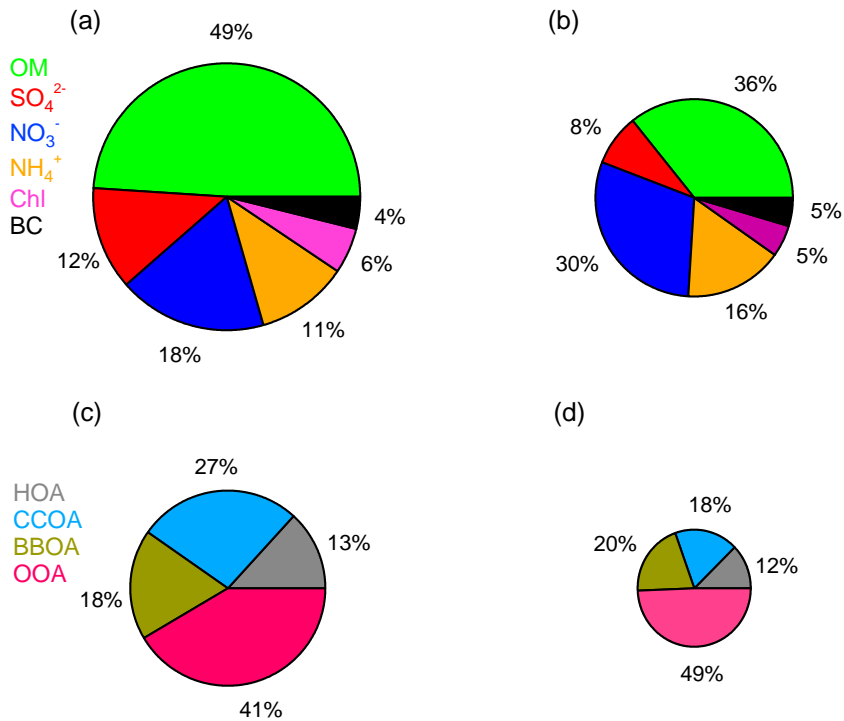
656 **Table 1** Summary of the average meteorological parameters, mixing ratios of gaseous species, and mass concentrations of the PM<sub>1</sub> chemical  
 657 components observed during the winters of 2014 and 2017.

Sampling period		2014 winter	2017 winter
Meteorological parameters	T (°C)	1.70	-2.26
	RH (%)	29.6	33.9
	WS (m s <sup>-1</sup> )	1.58	1.73
Gaseous species	SO <sub>2</sub> (ppb)	15.5	2.8
	NO <sub>2</sub> (ppb)	26.0	24.9
	CO (ppm)	1.6	0.7
	O <sub>3</sub> (ppb)	14.4	15.5
Aerosol species (µg m <sup>-3</sup> )	Org	30.4	11.9
	HOA	4.1	1.5
	BBOA	5.6	2.4
	CCOA	8.2	2.2
	OOA	12.6	5.8
	SO <sub>4</sub> <sup>2-</sup>	7.8	2.8
	NO <sub>3</sub> <sup>-</sup>	11.2	9.9
	NH <sub>4</sub> <sup>±</sup>	6.9	5.4
	Cl <sup>-</sup>	3.4	1.7
	BC	2.4	1.5
	PM <sub>1</sub>	66.2	33.4

658

2014

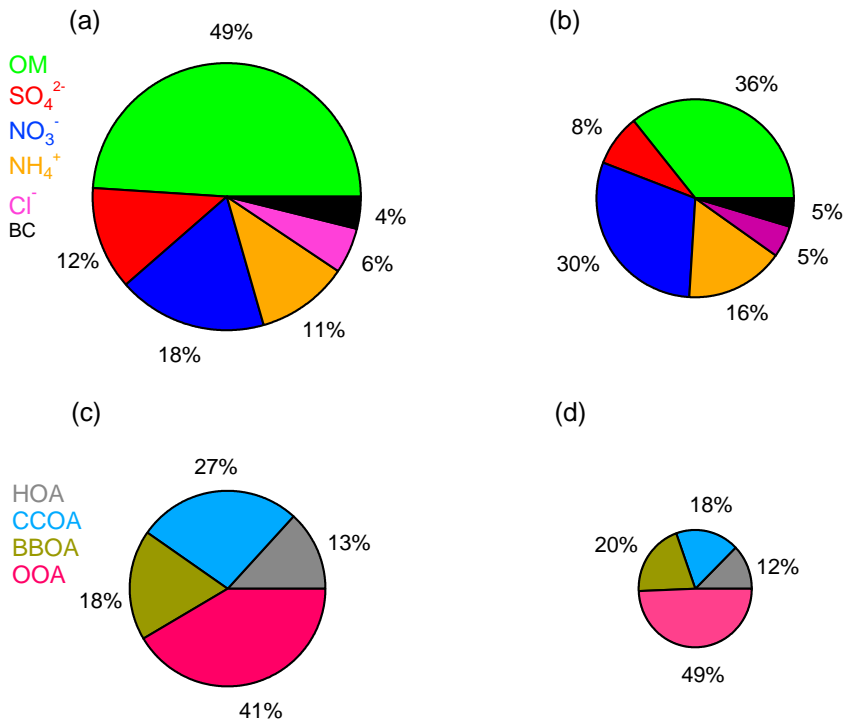
2017



659

2014

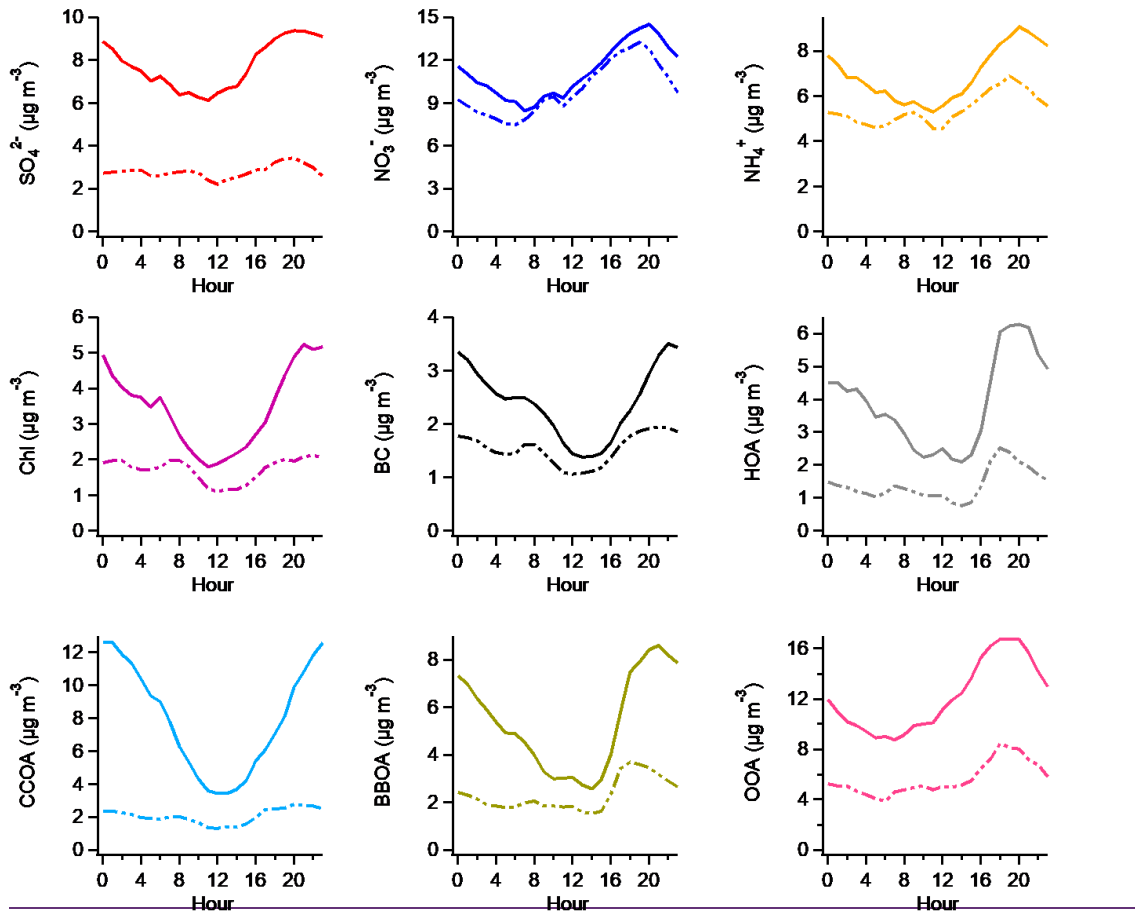
2017

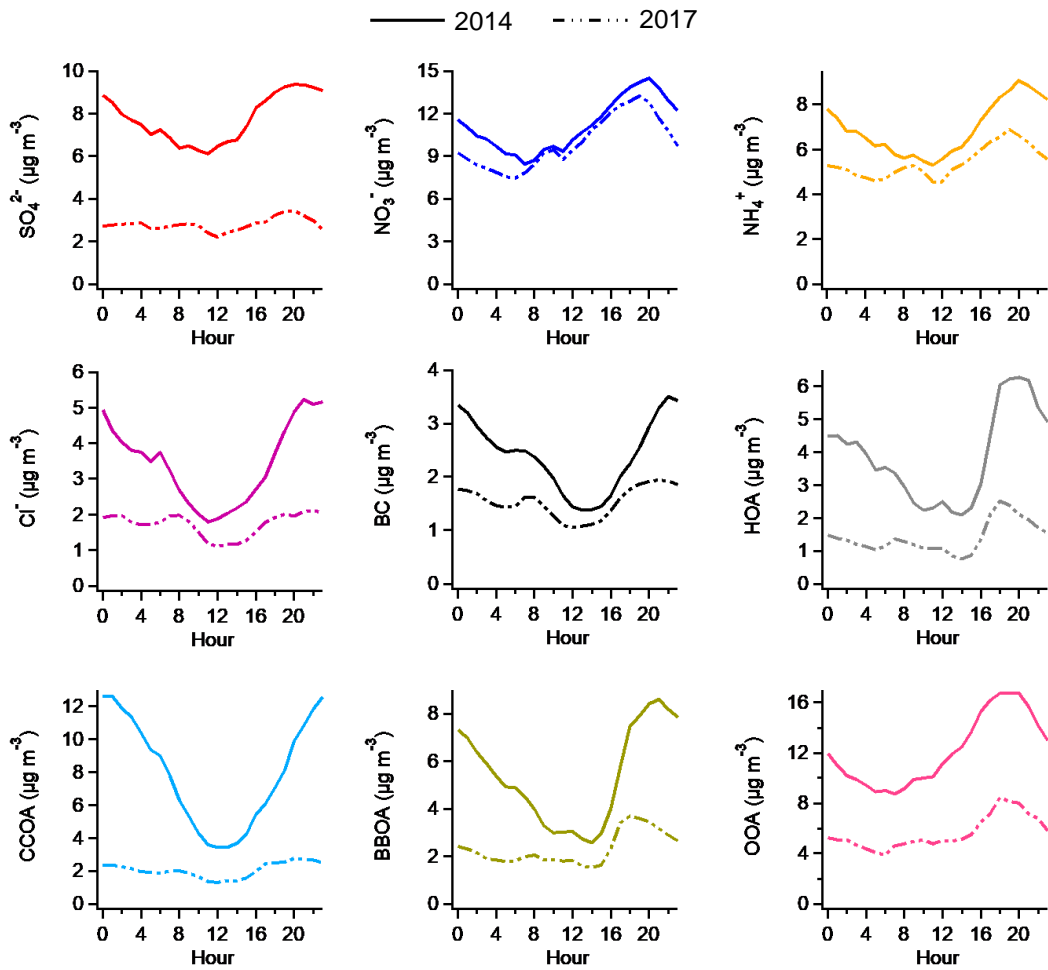


660

661 Figure 1. Average chemical compositions of PM<sub>1</sub> and OA in (a, c) winter of 2014 and (b, d) winter of 2017. The ~~decreasing rates~~  
662 ~~of decreases in the mass concentrations of~~ different components from 2014 to 2017 are as follows: 60.9% for organics, 64.1% for sulfate,  
663 11.6% for nitrate, 21.7% for ammonium, 50.0% for chloride, and 37.5% for BC.

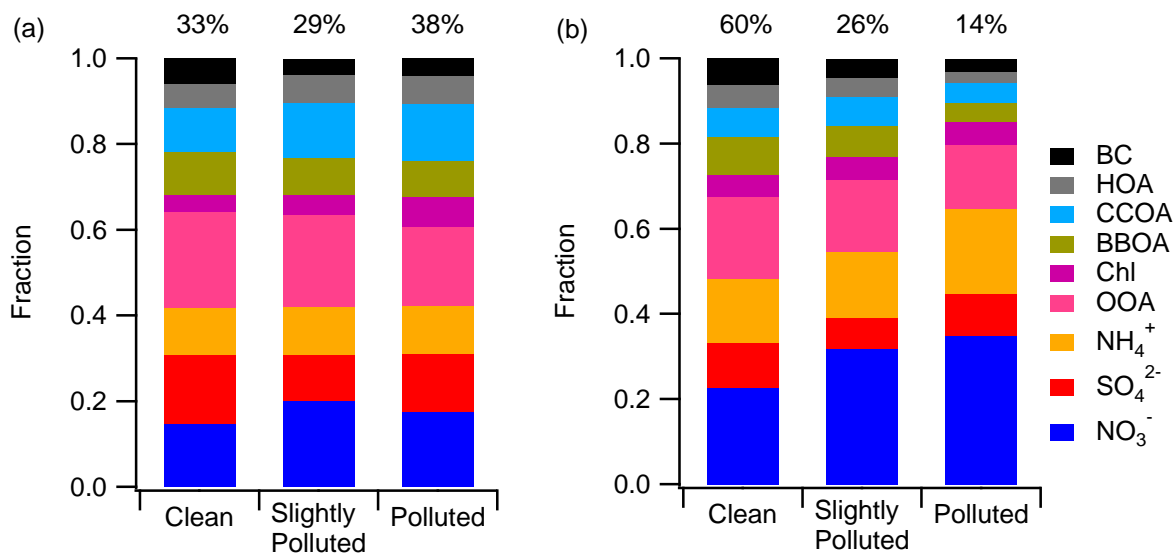
— 2014    - - - 2017



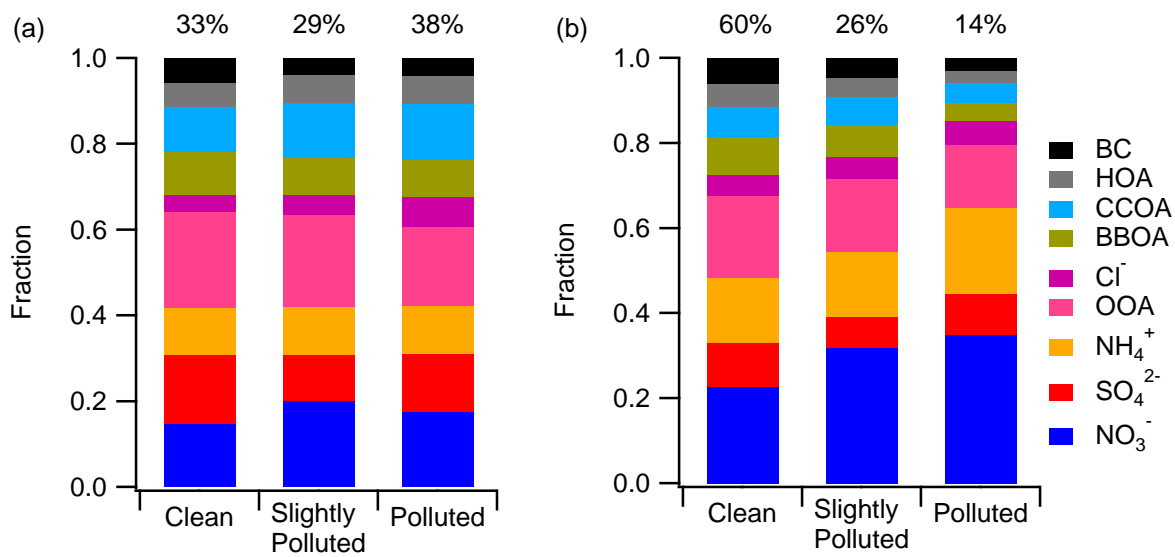


665

666 Figure 2. Average diurnal cycles of different aerosol species in the winter of 2014 (solid line) and winter of 2017 (dashed line).



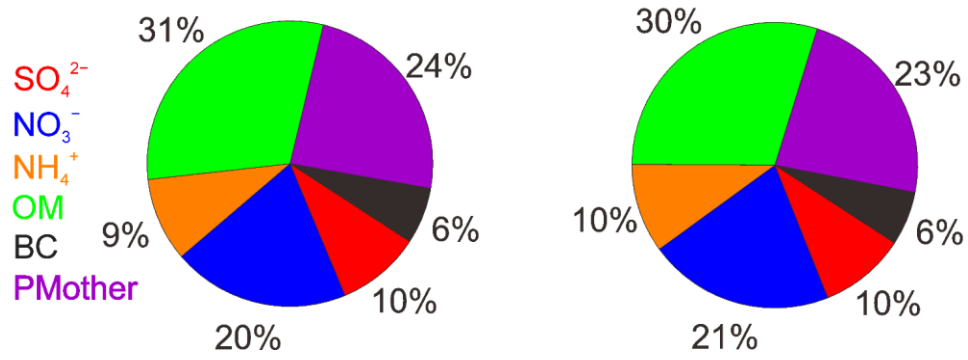
667



668

669 **Figure 3. Aerosol chemical composition at different pollution levels in the (a) winter of 2014 and (b) winter of 2017. The contributions of**  
 670 **each pollution level are shown at the top of each bar.**

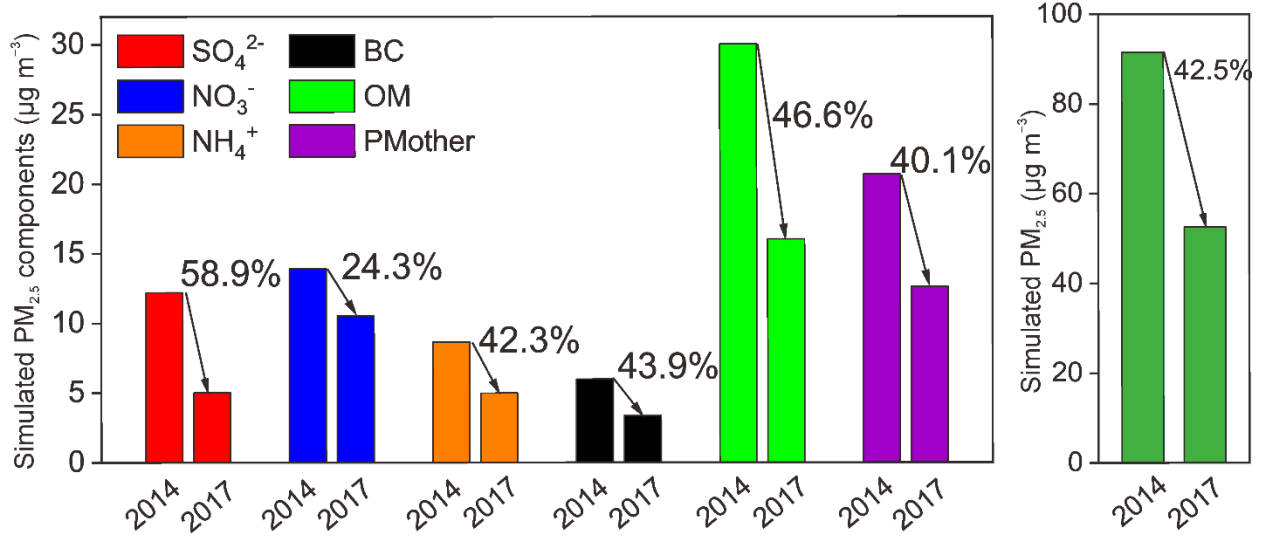
(a) 2017 Emission+2017 Meteorology (b) 2017 Emission+2014 Meteorology



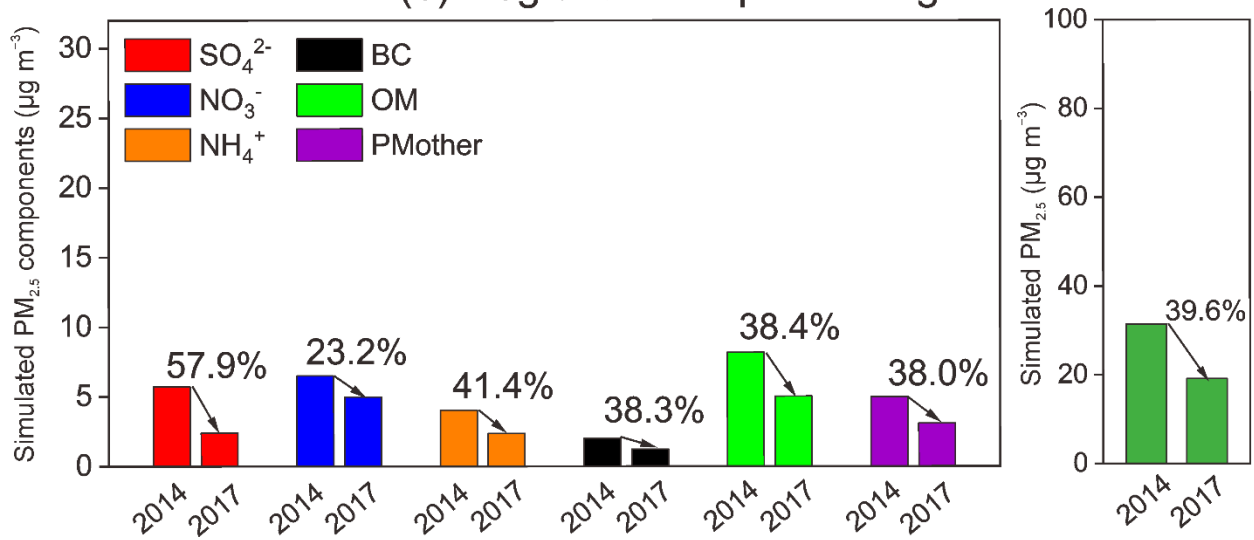
671

672 **Figure 4. The average PM<sub>2.5</sub> chemical composition simulated by the WRF-CMAQ model for the observation periods in 2017: (a) base**  
673 **scenario with the 2017 emissions and the 2017 meteorological conditions; (b) simulation with the 2017 emissions and 2014 meteorological**  
674 **conditions.**

(a) Total change

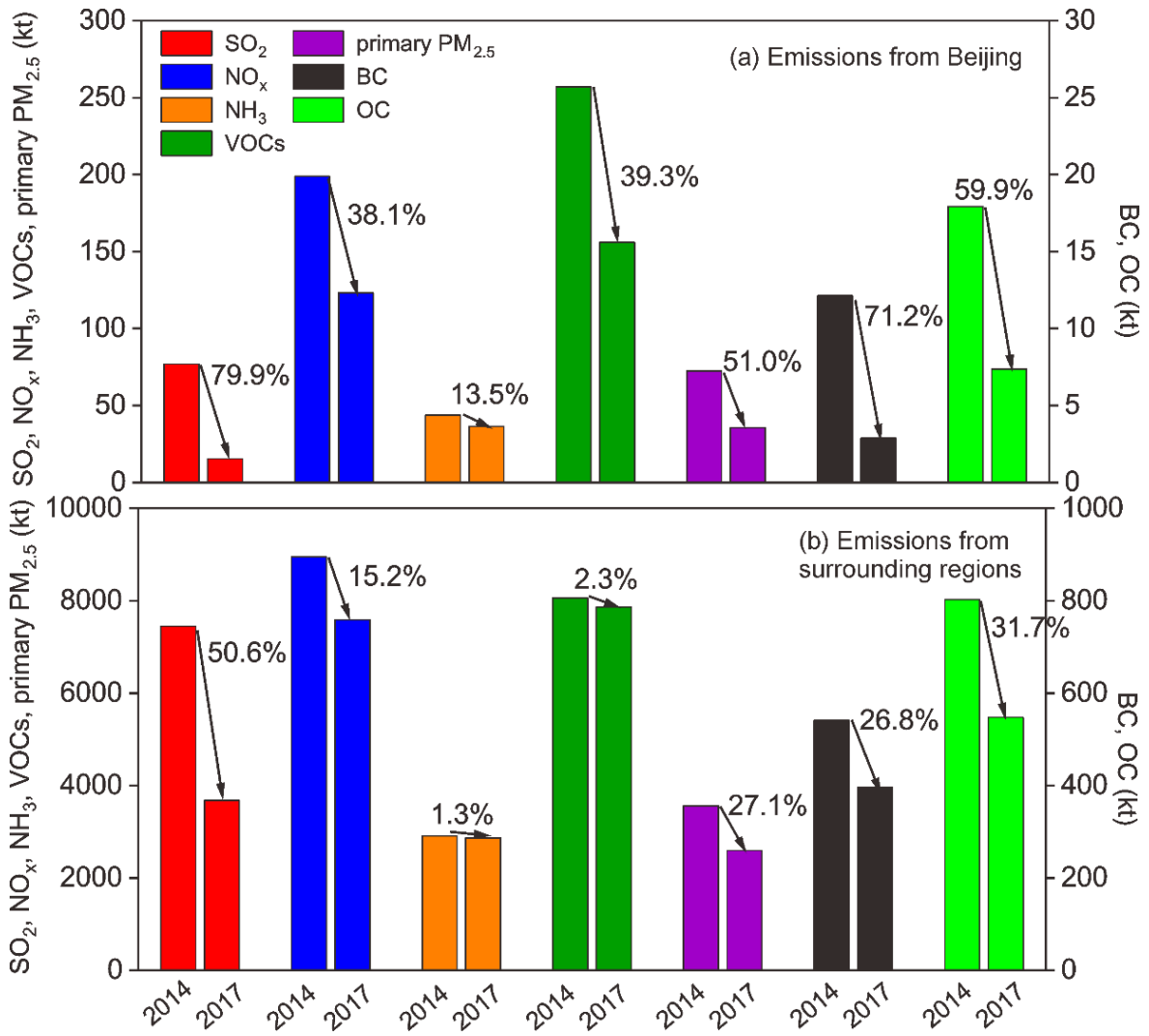


(b) Regional transport change



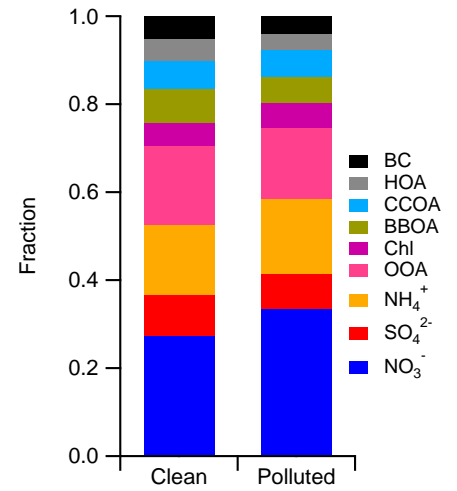
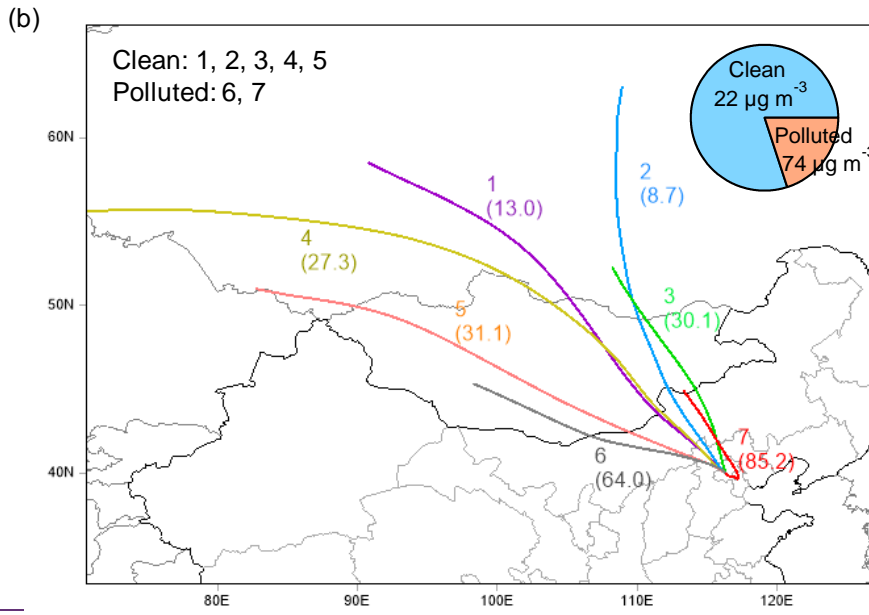
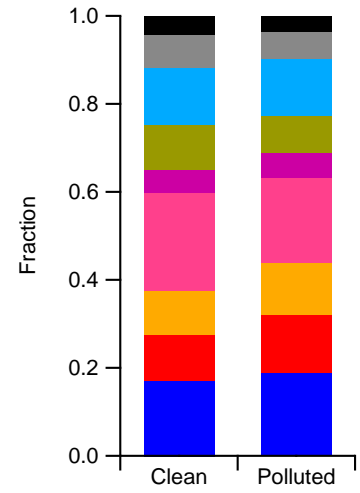
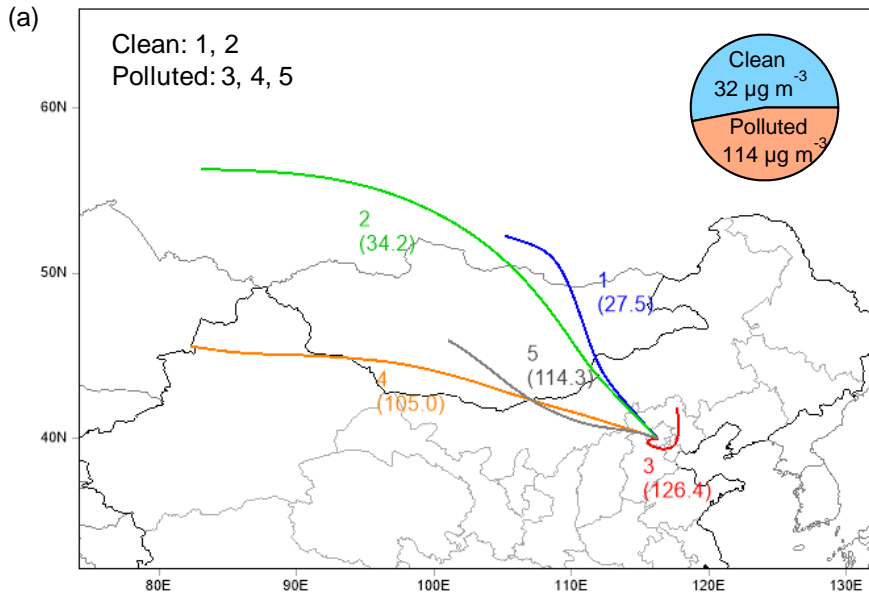
675

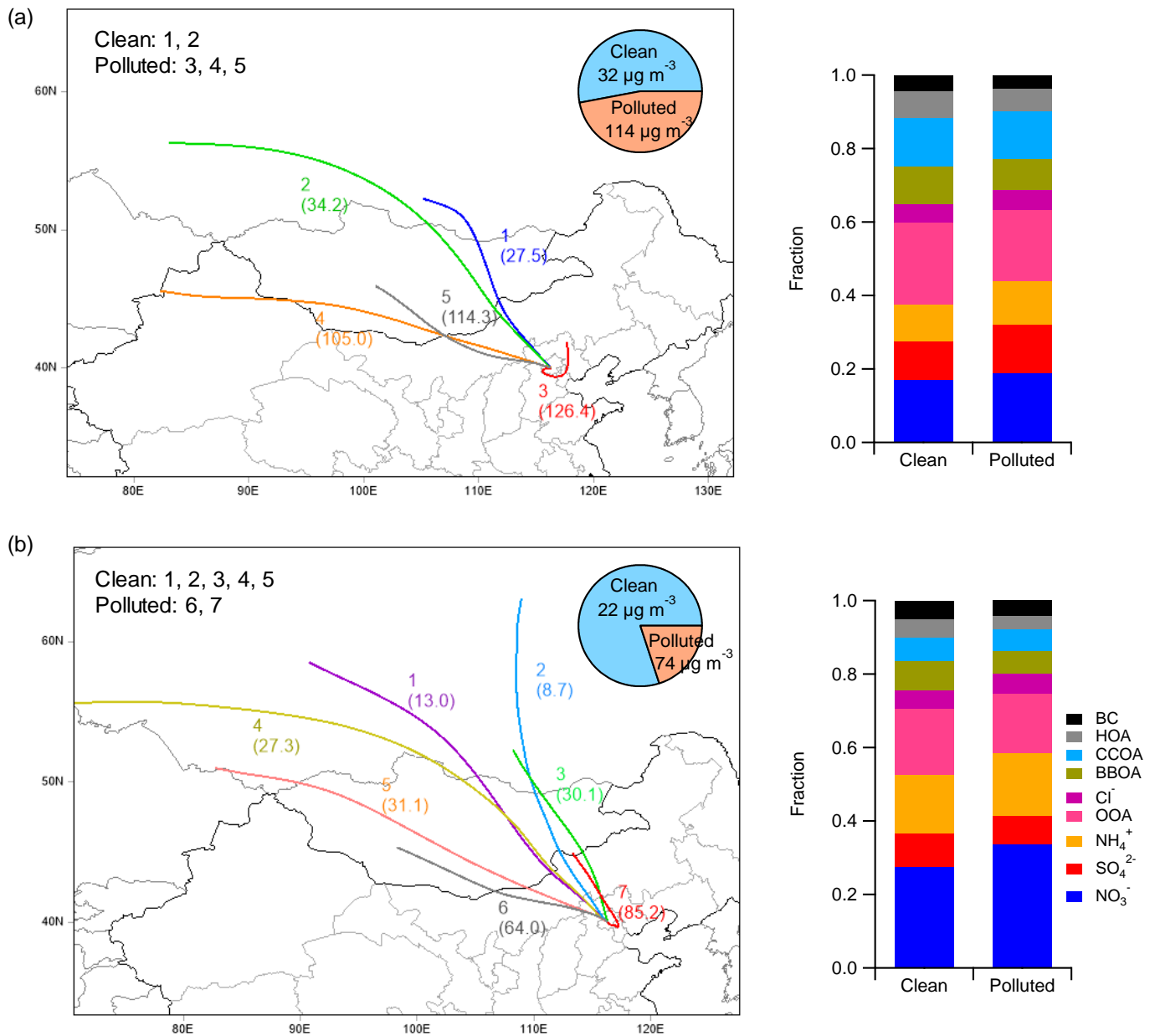
676 Figure 5. Simulated concentrations of PM<sub>2.5</sub> and its chemical components during the observation periods of 2014 and 2017: (a) total  
677 changes in Beijing and (b) changes due to regional transport.



678

679 **Figure 6.** Changes in the anthropogenic emissions of SO<sub>2</sub>, NO<sub>x</sub>, NH<sub>3</sub>, VOCs, primary PM<sub>2.5</sub>, BC, and OC in (a) Beijing and (b) its  
 680 surrounding regions from 2014 to 2017.





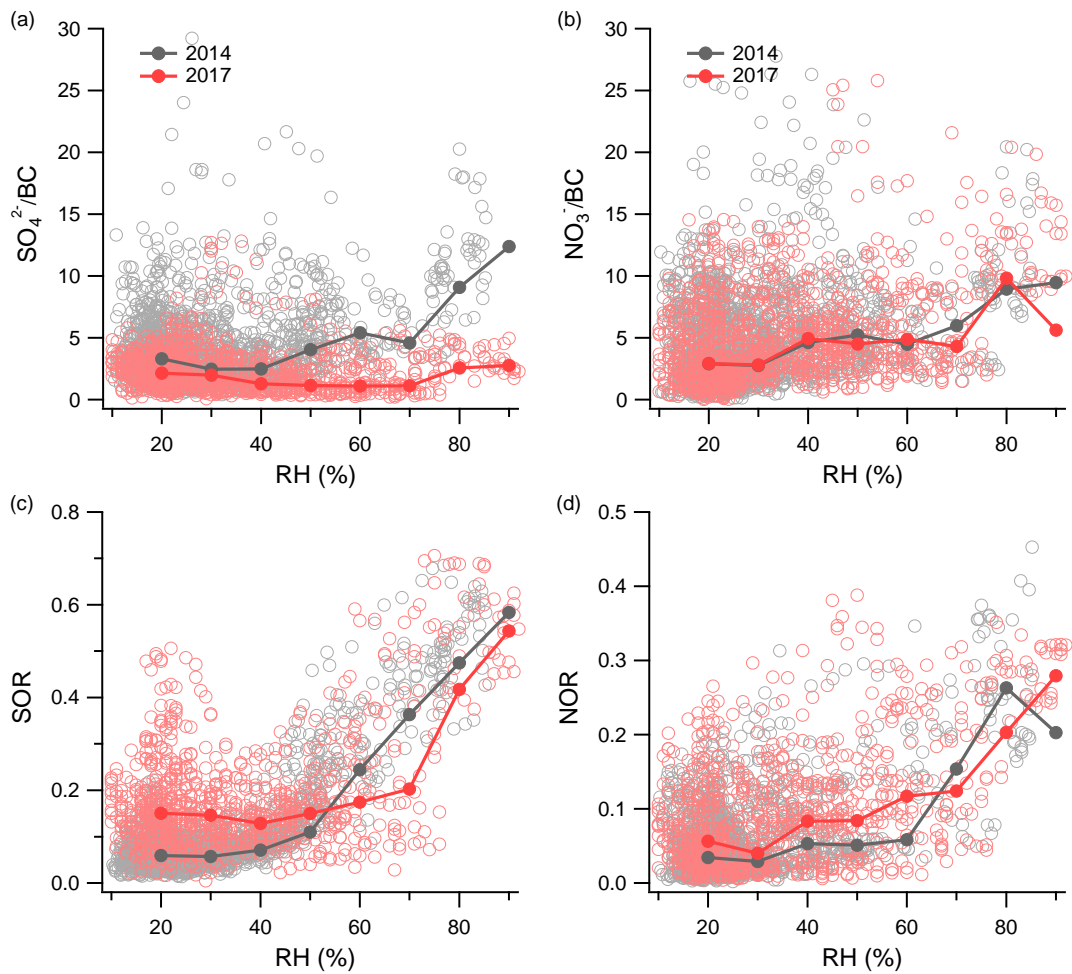
682

683

684

685

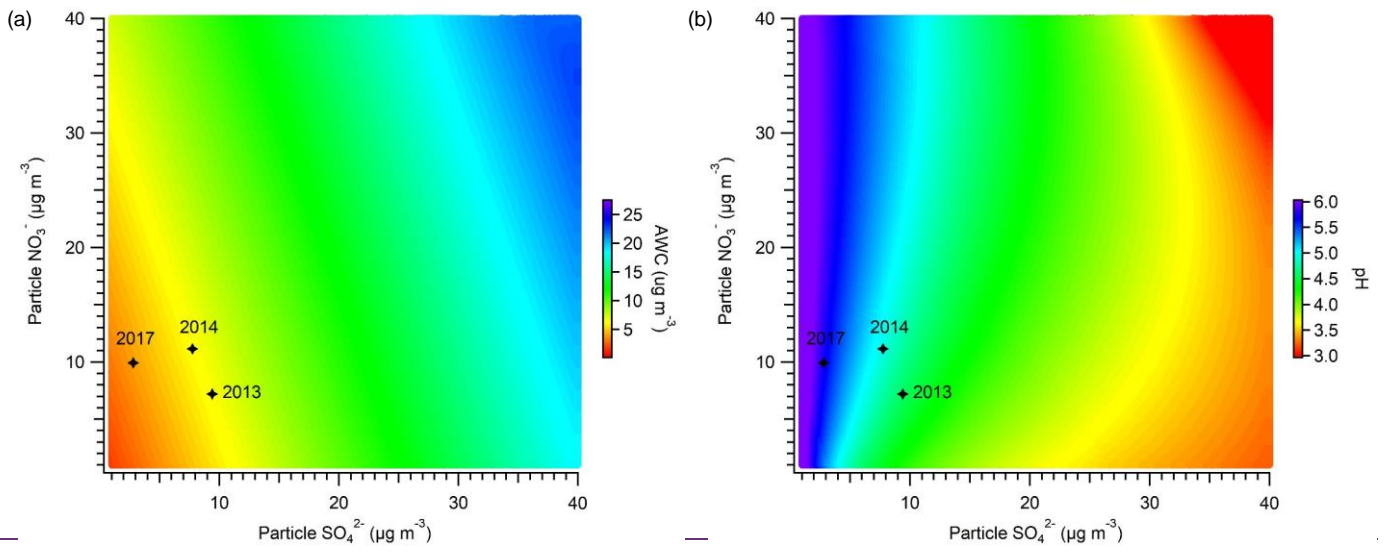
**Figure 7. Comparison of the air masses arriving in Beijing between 2014 and 2017. (a) and (b) show the clustering analysis of the back trajectories in the winters of 2014 and 2017, respectively, with pie charts displaying the contributions of the clean and polluted air masses. The stacked bar charts on the right show the average aerosol compositions for the clean and polluted clusters.**



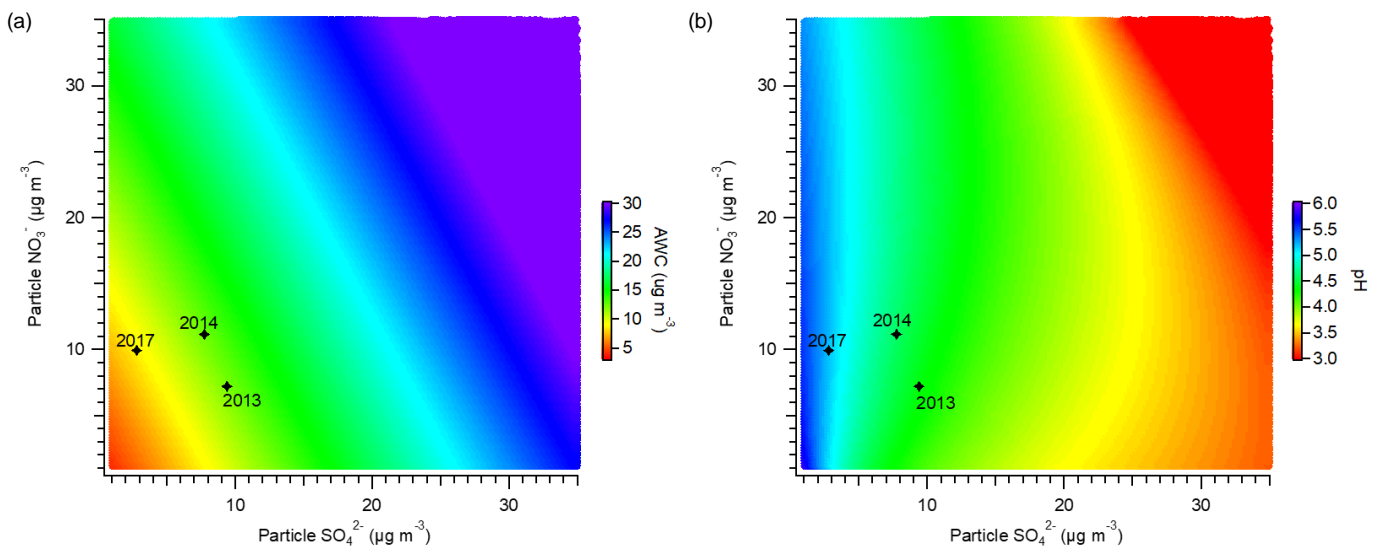
686

687 **Figure 8. Variations in (a)  $\text{SO}_4/\text{BC}$ , (b)  $\text{NO}_3/\text{BC}$ , (c) SOR, and (d) NOR plotted against increasing RH. The data are also binned according**  
 688 **to RH values, with the median value shown for each bin.**

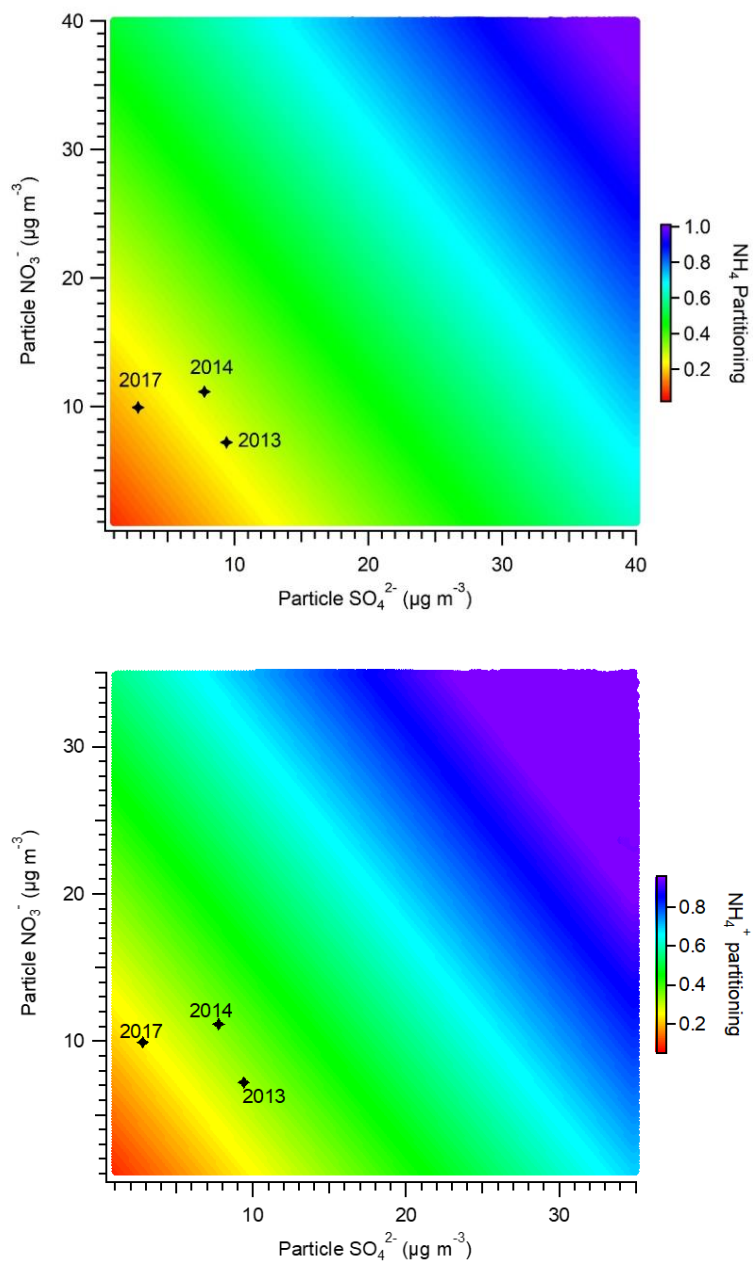
689



690



691 **Figure 9. Sensitivity of (a) AWC and (b) particle pH to the mass concentrations of particulate sulfate and nitrate. The stars indicate the**  
692 **average winter conditions for the years 2013, 2014, and 2017.**



693

694

695 **Figure 10. Sensitivity of the ammonium partitioning ratio to the mass concentrations of particulate sulfate and nitrate. The stars indicate**  
 696 **the average winter conditions for the years 2013, 2014, and 2017.**

1 *Supplementary information*

2 **Rapid transition in winter aerosol composition in Beijing from**  
3 **2014 to 2017: response to clean air actions**

4 Haiyan Li<sup>1,a</sup>, Jing Cheng<sup>2</sup>, Qiang Zhang<sup>2</sup>, Bo Zheng<sup>3</sup>, Yuxuan Zhang<sup>2</sup>, Guangjie Zheng<sup>1</sup>, Kebin  
5 He<sup>1,3</sup>

6 <sup>1</sup> State Key Joint Laboratory of Environment Simulation and Pollution Control, School of Environment, Tsinghua  
7 University, Beijing 100084, China

8 <sup>2</sup> Ministry of Education Key Laboratory for Earth System Modeling, Department of Earth System Science, Tsinghua  
9 University, Beijing 100084, China

10 <sup>3</sup> State Environmental Protection Key Laboratory of Sources and Control of Air Pollution Complex, Tsinghua  
11 University, Beijing 100084, China

12 <sup>a</sup>present address: Institute for Atmospheric and Earth System Research/Physics, Faculty of Science, University of  
13 Helsinki, 00014 Helsinki, Finland

14 *Correspondence:* Qiang Zhang ([qiangzhang@tsinghua.edu.cn](mailto:qiangzhang@tsinghua.edu.cn))

15 **Table S1.** Monthly descriptive statistic of the comparison between the observational PM<sub>2.5</sub>  
 16 concentrations and CMAQ-simulated PM<sub>2.5</sub> concentrations in Beijing during the winters of 2014  
 17 and 2017. Concentration values are all reported in  $\mu\text{g m}^{-3}$ .  
 18

<u>Year</u>	<u>Month</u>	<u>Mean_obs</u>	<u>Mean_sim</u>	<u>R</u>	<u>MB</u>	<u>ME</u>	<u>RMSE</u>	<u>NMB(%)</u>	<u>NME(%)</u>
<u>2014</u>	<u>12</u>	<u>58.75</u>	<u>77.87</u>	<u>0.91</u>	<u>19.12</u>	<u>24.53</u>	<u>39.57</u>	<u>13.73</u>	<u>31.24</u>
<u>2015</u>	<u>1</u>	<u>97.76</u>	<u>104.05</u>	<u>0.75</u>	<u>6.29</u>	<u>32.27</u>	<u>34.84</u>	<u>15.14</u>	<u>37.29</u>
	<u>2</u>	<u>93.36</u>	<u>92.66</u>	<u>0.86</u>	<u>-0.70</u>	<u>21.26</u>	<u>31.47</u>	<u>-1.29</u>	<u>29.34</u>
<u>2017</u>	<u>12</u>	<u>43.35</u>	<u>47.80</u>	<u>0.90</u>	<u>4.45</u>	<u>19.86</u>	<u>25.17</u>	<u>12.01</u>	<u>28.06</u>
<u>2018</u>	<u>1</u>	<u>33.87</u>	<u>55.76</u>	<u>0.79</u>	<u>21.89</u>	<u>35.97</u>	<u>36.41</u>	<u>29.45</u>	<u>44.45</u>
	<u>2</u>	<u>50.14</u>	<u>54.28</u>	<u>0.83</u>	<u>4.14</u>	<u>34.55</u>	<u>32.83</u>	<u>14.08</u>	<u>27.39</u>

19  
 20  
 21 **Table S2 (a).** Correlations between simulated PM<sub>2.5</sub> compositions and observed PM<sub>1</sub> compositions  
 22 in this study.  
 23

<u>Period</u>	<u>OM</u>	<u>SO<sub>4</sub><sup>2-</sup></u>	<u>NO<sub>3</sub><sup>-</sup></u>	<u>NH<sub>4</sub><sup>+</sup></u>	<u>BC</u>
<u>2014 Winter</u>	<u>0.83</u>	<u>0.76</u>	<u>0.82</u>	<u>0.84</u>	<u>0.76</u>
<u>2017 Winter</u>	<u>0.72</u>	<u>0.81</u>	<u>0.89</u>	<u>0.90</u>	<u>0.73</u>

24

**Table S2 (b).** Comparison of the simulation and observations of PM<sub>2.5</sub> compositions. The observation data was collected from the SPARTAN, Beijing Site (40.01°N, 116.207°E) (<https://www.spartan-network.org/beijing-china>); while the simulated data was extracted from the same grid where the Beijing Site located in the third domain. Concentration values are all reported in µg m<sup>-3</sup>.

year	Date_range (dd/mm)	PM <sub>2.5</sub>			SIA			SO <sub>4</sub> <sup>2-</sup>			NO <sub>3</sub>		
		Obs	Sim	MB	Obs	Sim	MB	Obs	Sim	MB	Obs	Sim	MB
2014	01/12-28/12	64.12	70.31	6.19	15.14	18.90	3.75	5.56	6.38	0.82	6.41	8.05	1.64
2015	22/01-27/02	95.38	97.64	2.26	18.55	21.39	2.84	9.81	10.02	0.21	4.13	6.14	2.01
2017	27/11-12/12	39.14	42.70	3.56	14.21	15.56	1.35	2.29	3.49	1.20	8.72	9.72	1.00

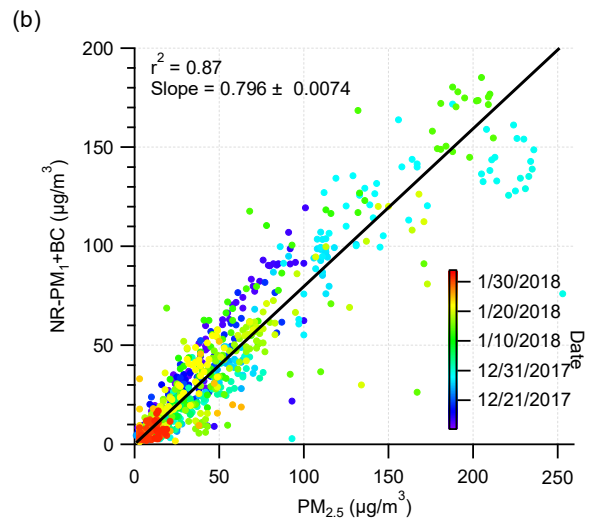
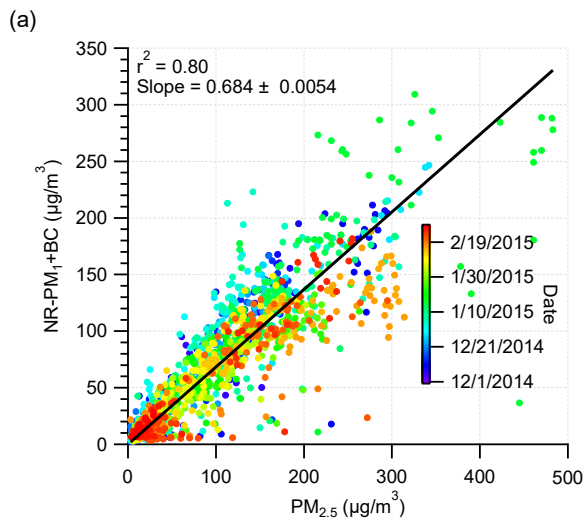
year	Date_range (dd/mm)	NH <sub>4</sub> <sup>+</sup>			RM/OM			BC			OTHER		
		Obs	Sim	MB	Obs	Sim	MB	Obs	Sim	MB	Obs	Sim	MB
2014	01/12-28/12	3.17	4.46	1.29	30.64	24.30	-6.34	7.92	9.20	1.27	20.38	17.92	-2.46
2015	22/01-27/02	4.61	5.23	0.62	30.00	28.90	-1.10	8.82	12.57	3.74	42.59	34.79	-7.80
2017	27/11-12/12	3.20	2.35	-0.85	14.25	13.72	-0.53	3.31	3.37	0.06	6.56	10.04	3.48

<sup>a</sup>SIA represents the total amount of secondary inorganic aerosol, that the sum of SO<sub>4</sub><sup>2-</sup>, NO<sub>3</sub><sup>-</sup> and NH<sub>4</sub><sup>+</sup>.

<sup>b</sup>RM represents the residual matter in SPARTAN observations. There is no direct organic composition in SPARTAN, however RM in SPARTAN measurements is dominated by organics, and has been used to evaluate the organic mass simulations (Weagle et al., 2018). OM represents the organic mass in CMAQ simulations.

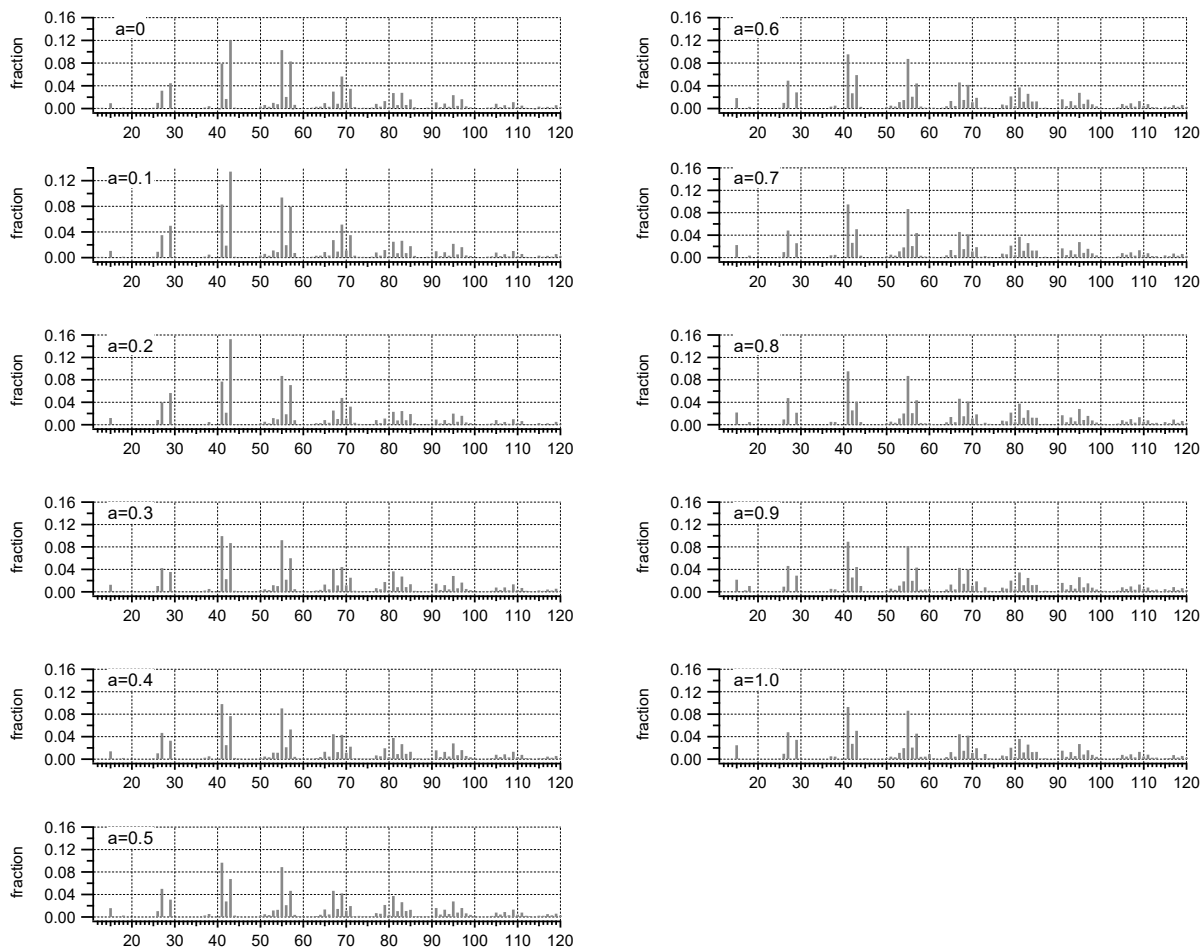
<sup>c</sup>BC represents the black carbon.

<sup>d</sup>Other represents the rest of the PM<sub>2.5</sub> compositions, such as crustal matter, sea salt.



37

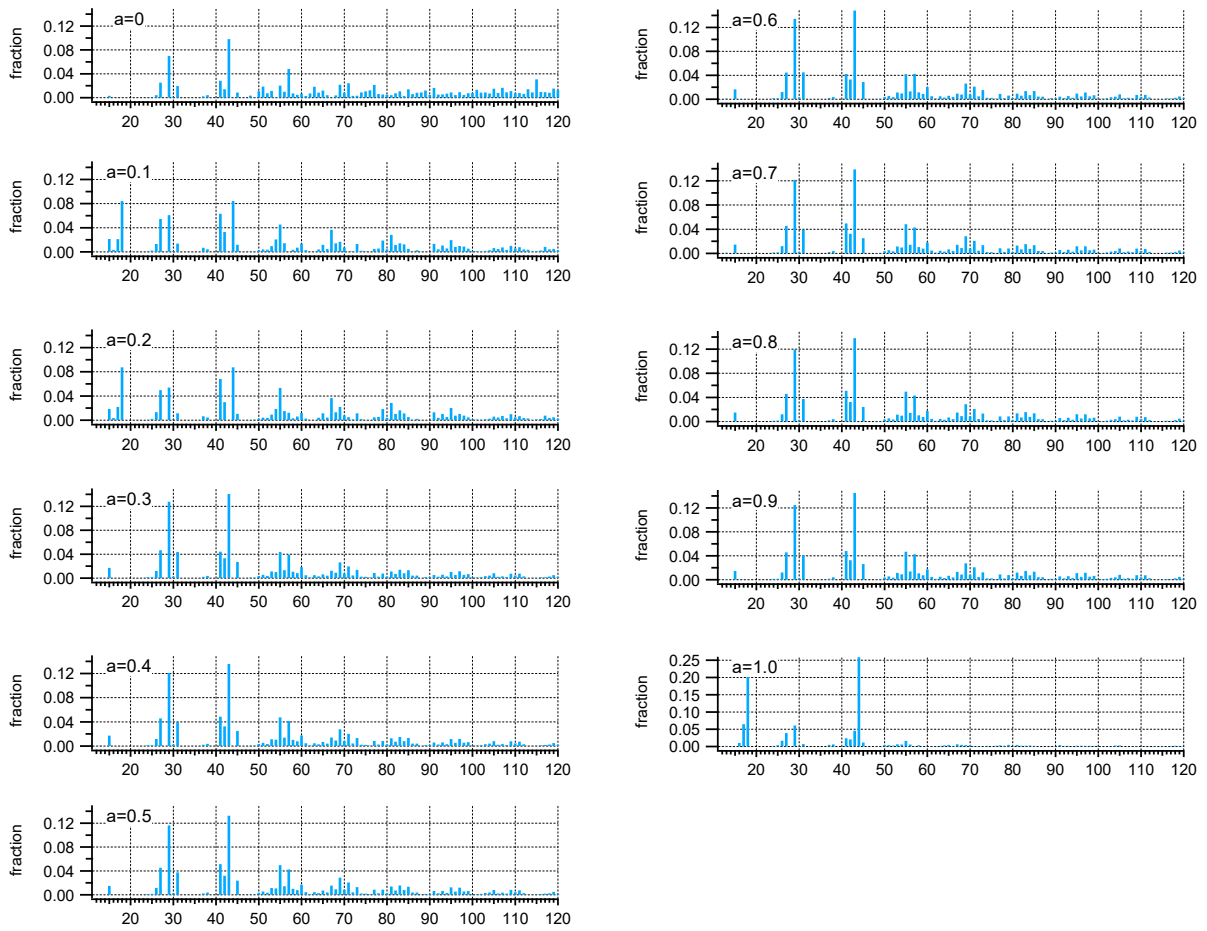
38 **Figure S1.** Correlation of total PM<sub>1</sub> concentration (NR-PM<sub>1</sub> plus BC) with PM<sub>2.5</sub> concentration  
39 during the winter of (a) 2014 and (b) 2017.



40

41 **Figure S2.** Factor profiles of HOA with different  $a$  values of ME-2 analysis.

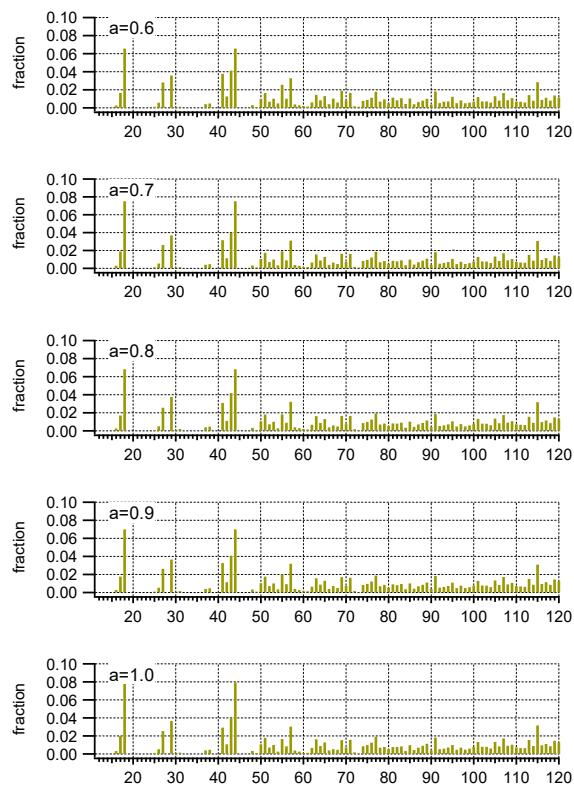
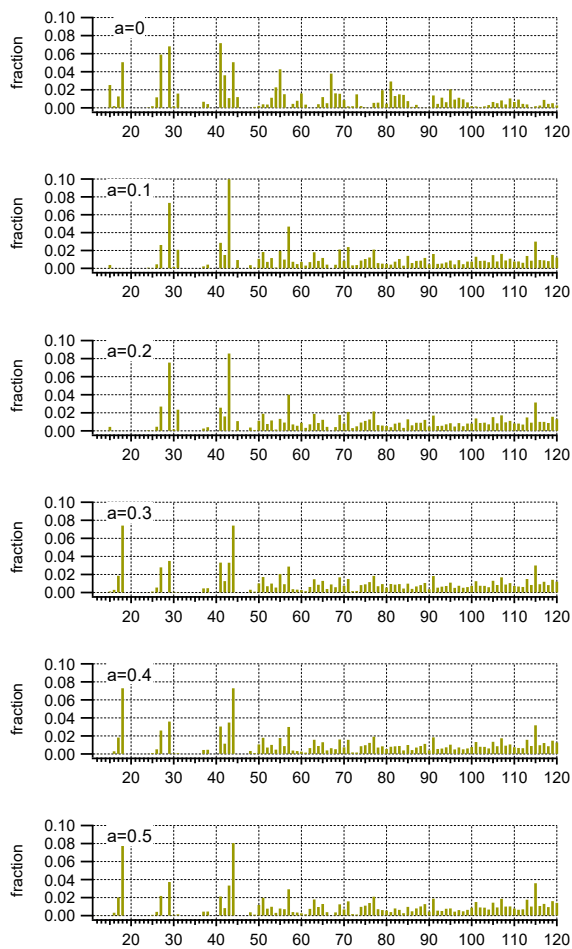
42



43

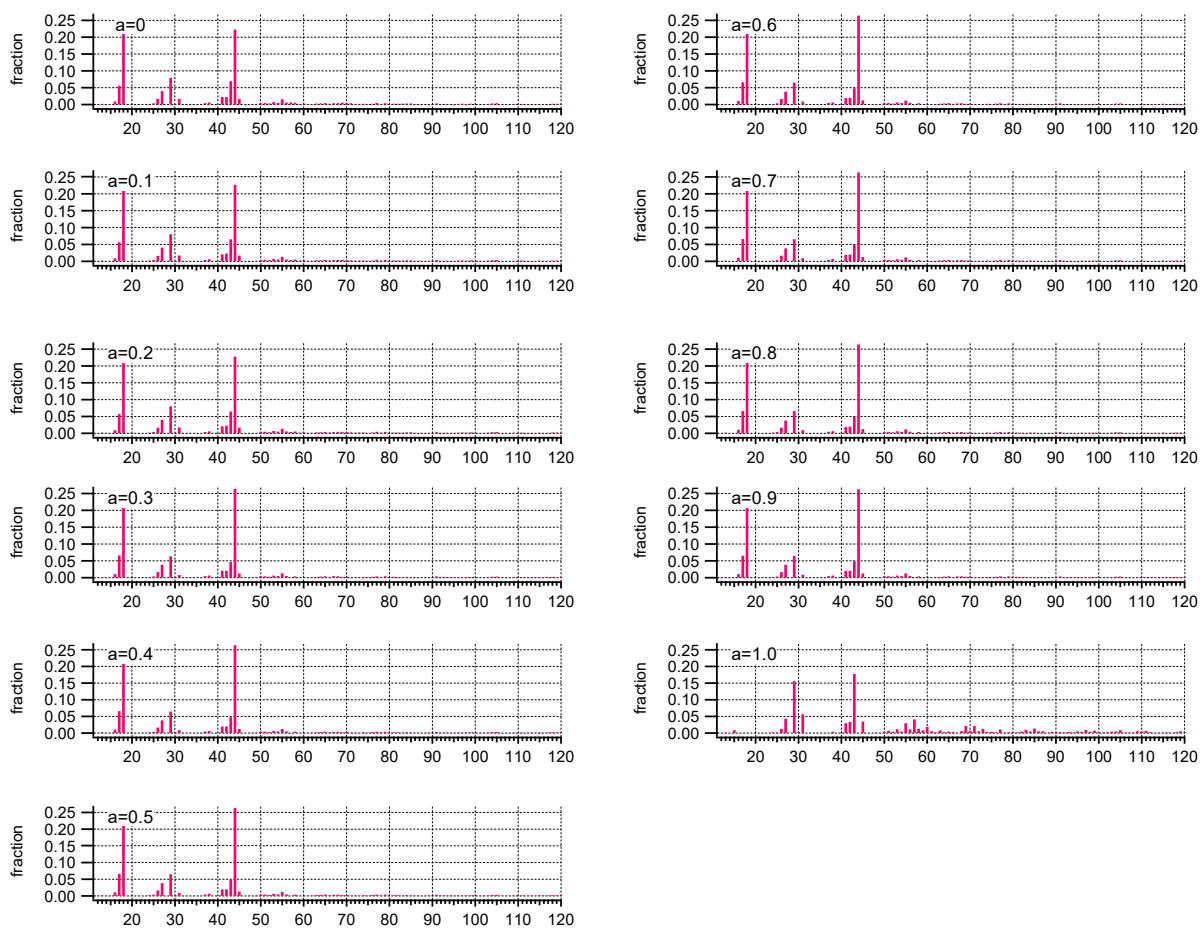
44

**Figure S3.** Factor profiles of CCOA with different  $a$  values of ME-2 analysis.



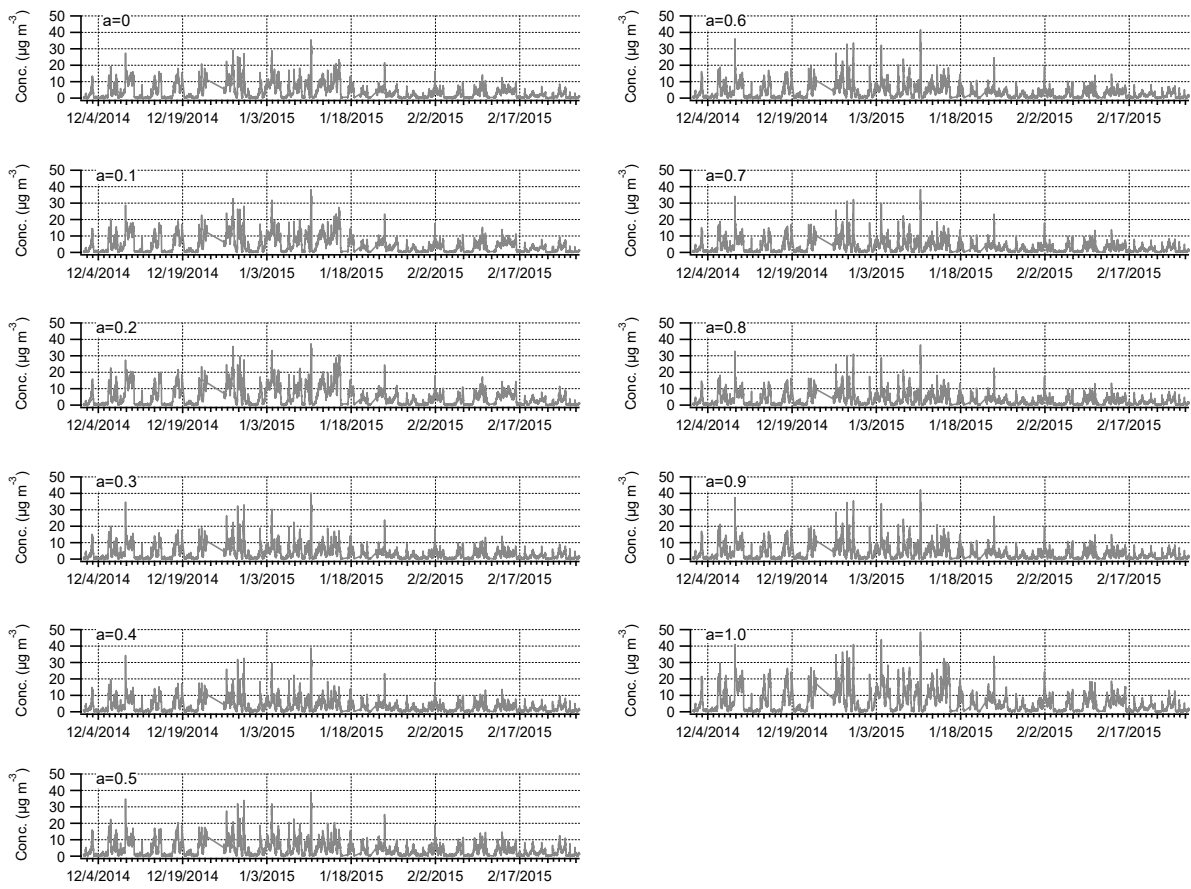
45

46 **Figure S4.** Factor profiles of BBOA with different  $a$  values of ME-2 analysis.



47

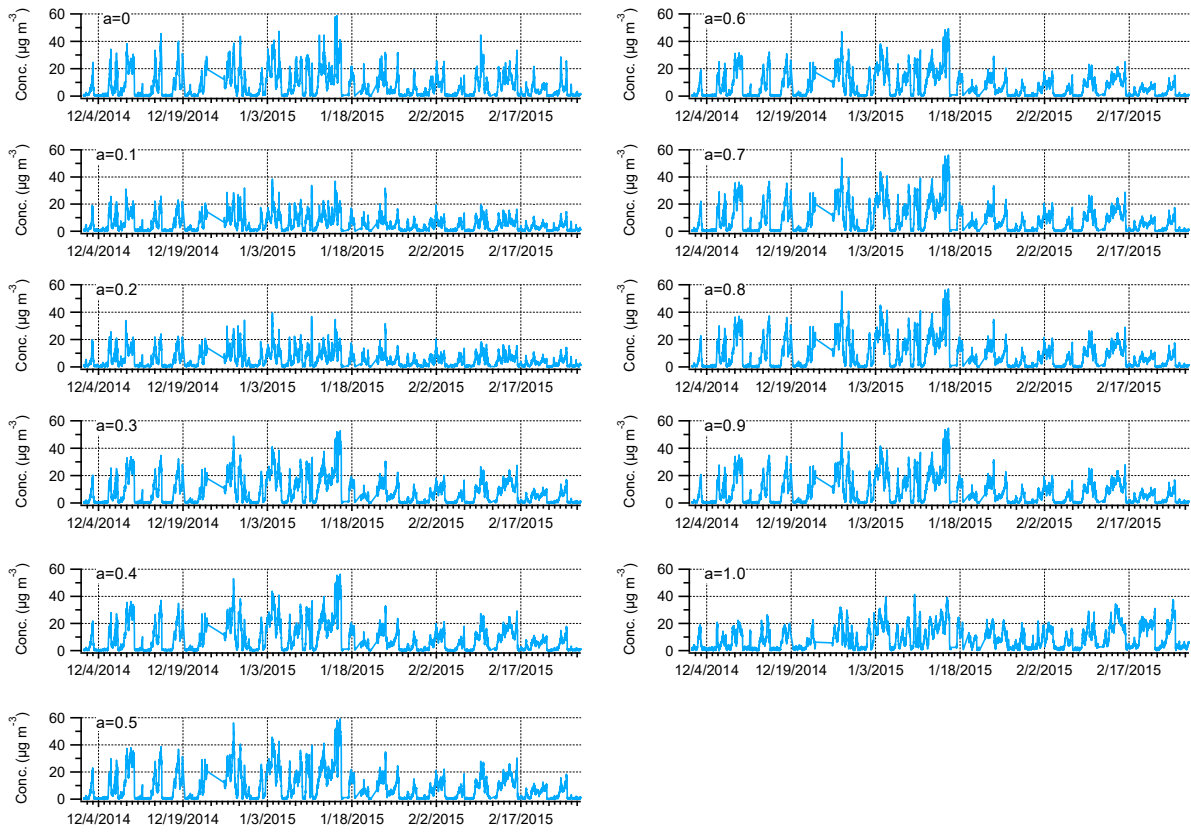
48 **Figure S5.** Factor profiles of OOA with different  $a$  values of ME-2 analysis.



49

50

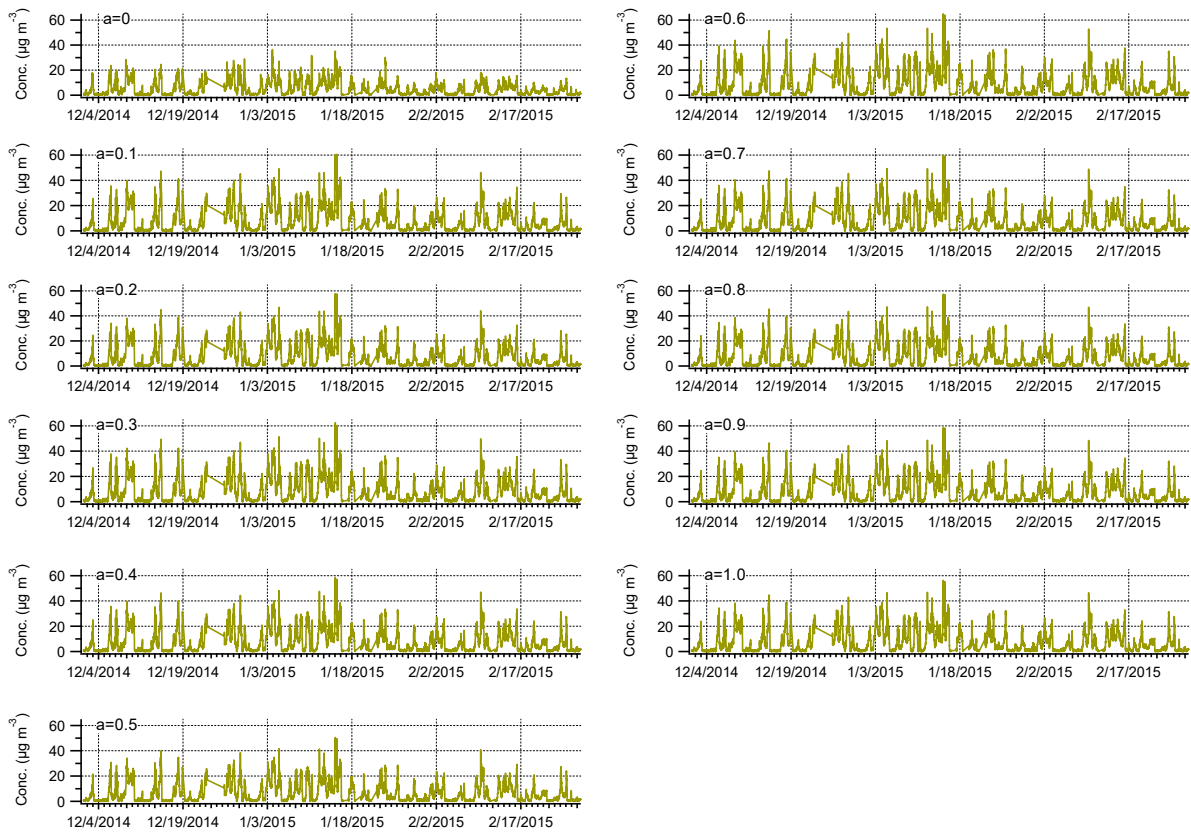
**Figure S6.** Time series of HOA with different  $\alpha$  values of ME-2 analysis.



51

52

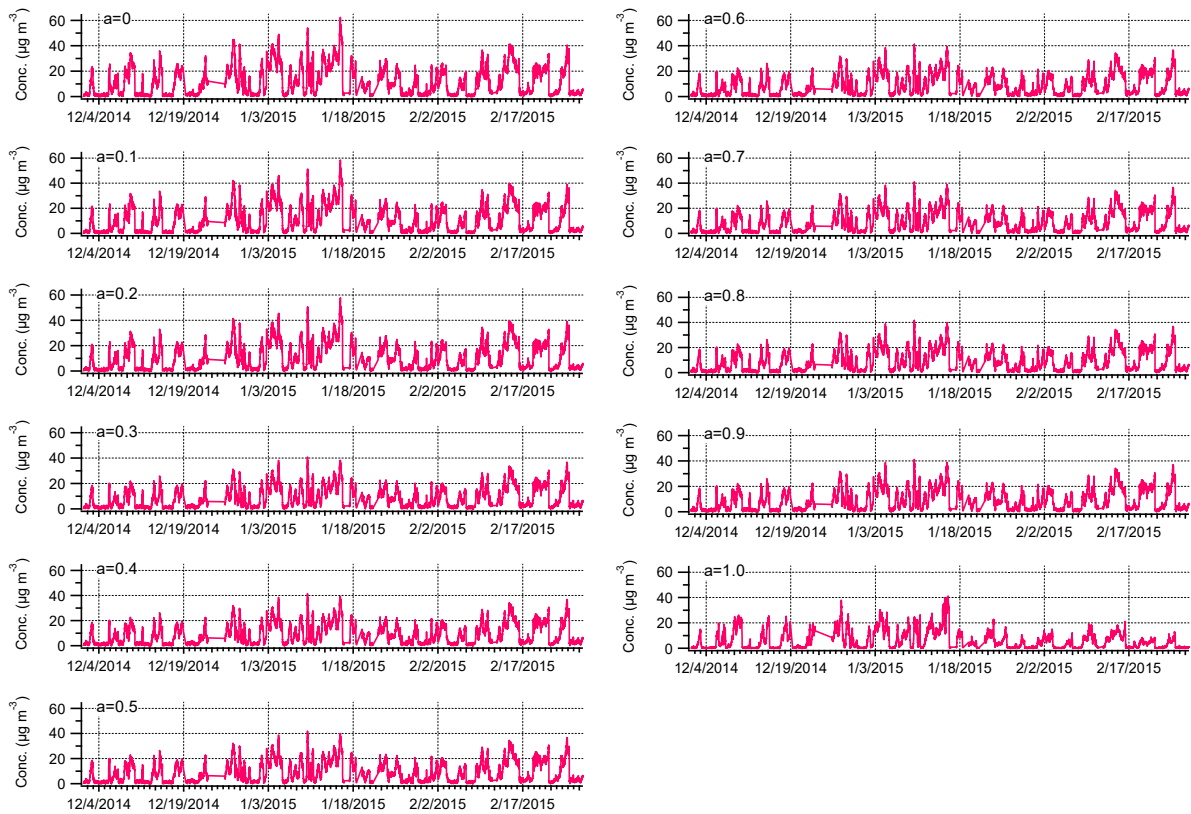
**Figure S7.** Time series of CCOA with different  $a$  values of ME-2 analysis.



53

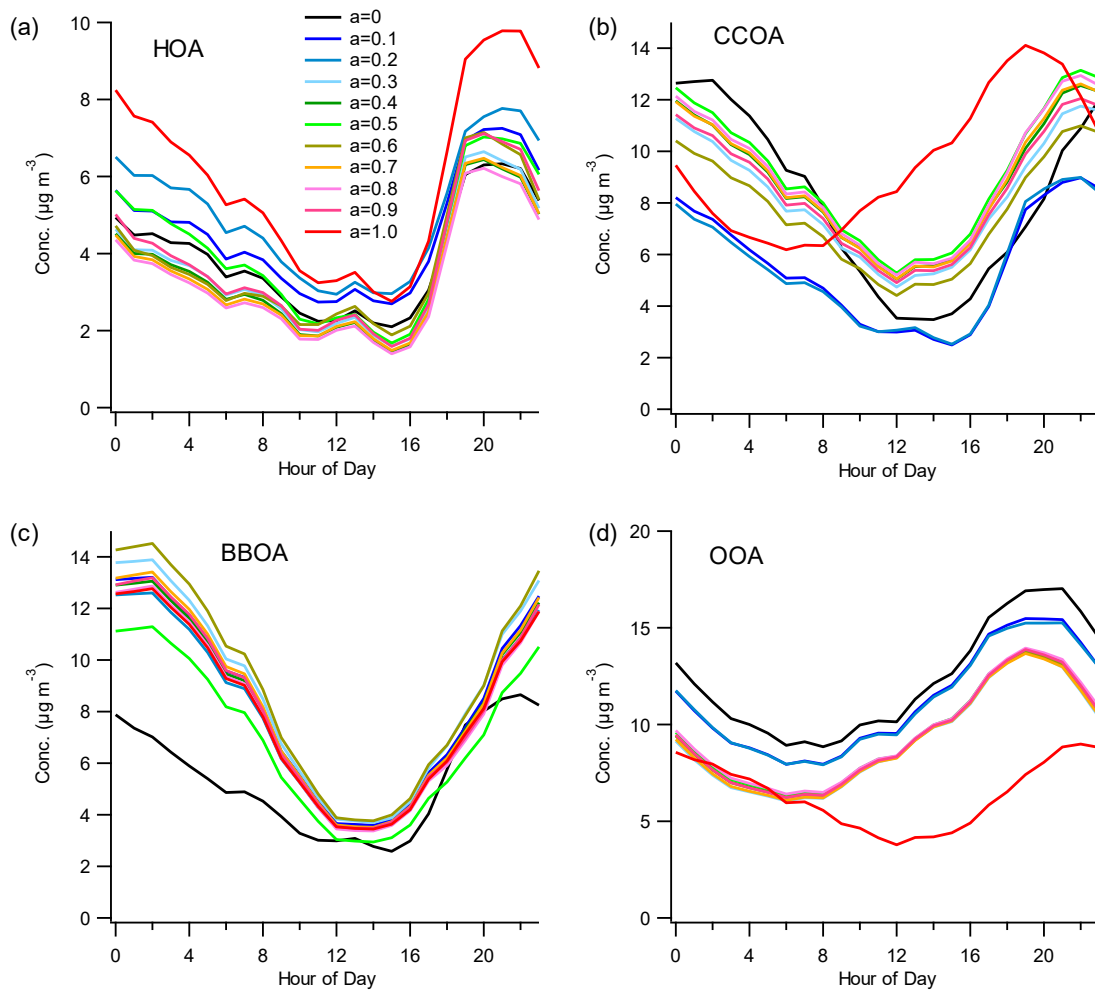
54

**Figure S8.** Time series of BBOA with different  $a$  values of ME-2 analysis.



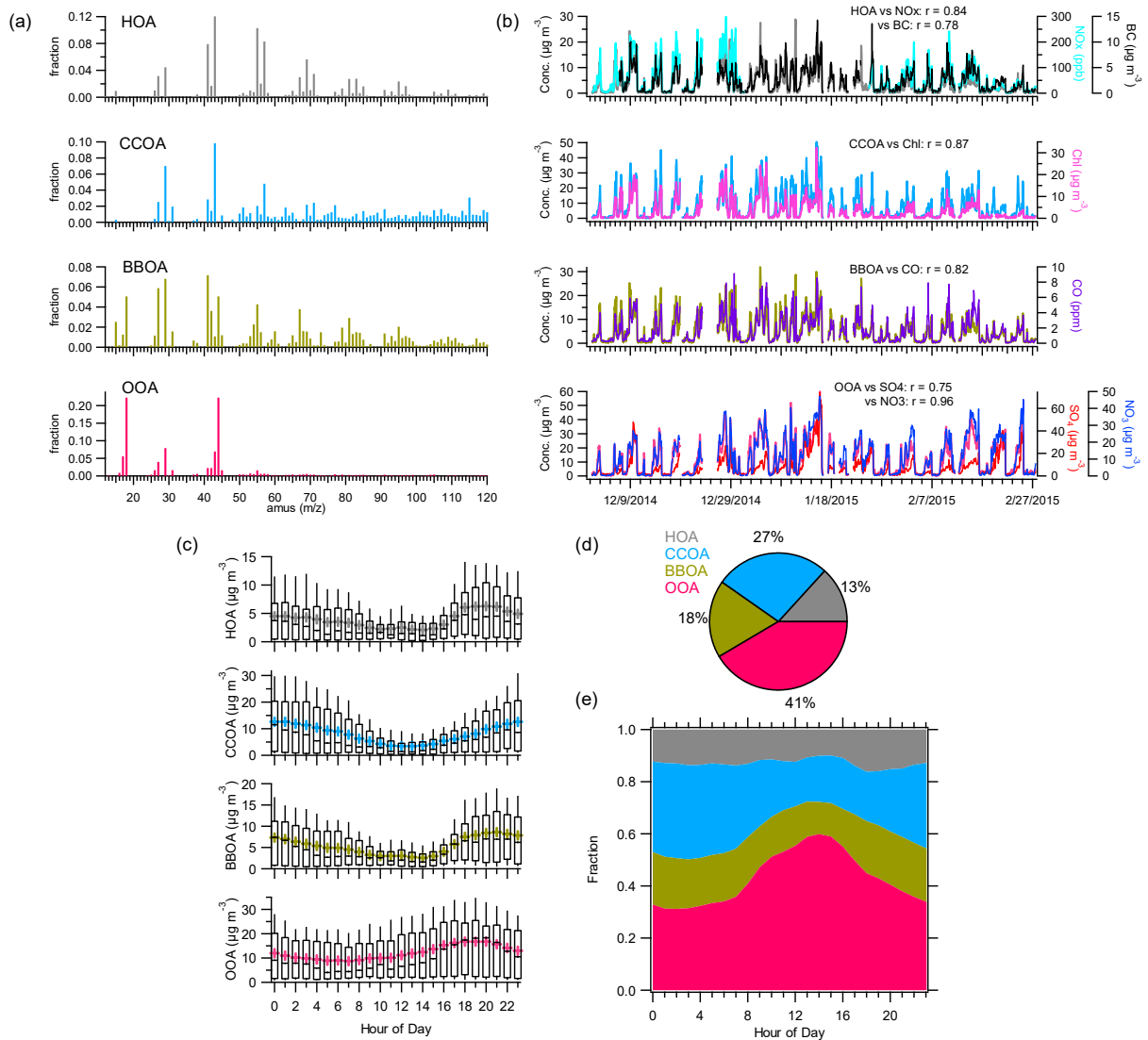
55

56 Figure S9. Time series of OOA with different  $a$  values of ME-2 analysis.



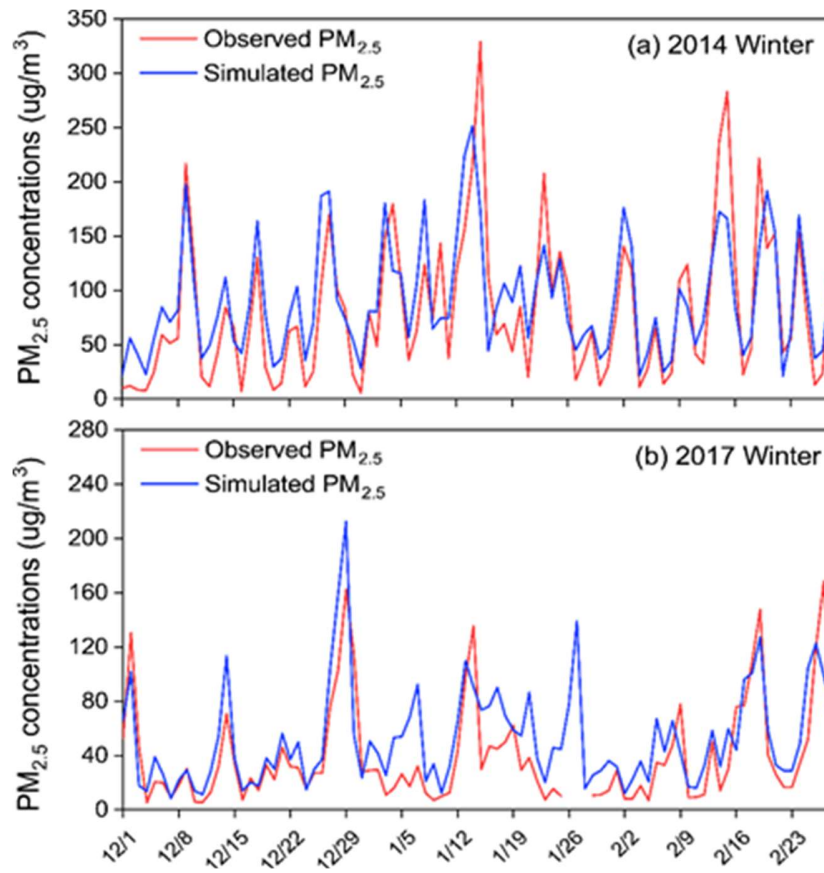
57

58 **Figure S10.** Diurnal cycles of (a) HOA, (b) CCOA, (d) BBOA, and (d) OOA with different *a*  
 59 values of ME-2 analysis.



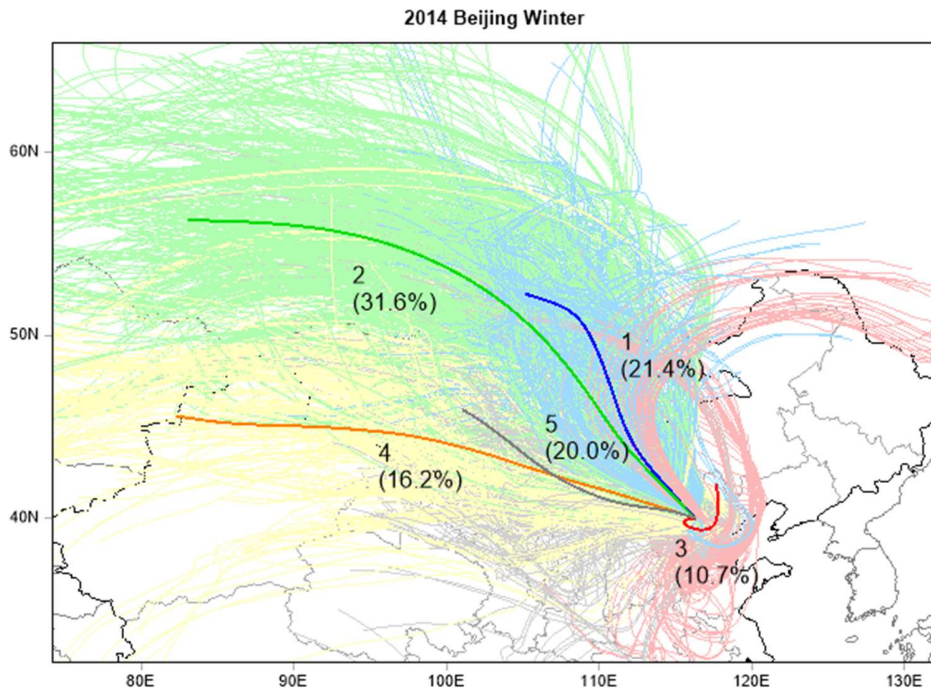
60

61 **Figure S112.** Source apportionment results of OA during the winter of 2014. (a) Mass spectra of  
 62 HOA, CCOA, BBOA, and OOA. (b) Time series of different OA factors and their corresponding  
 63 tracers. The correlation coefficients of OA factors with the tracers are also shown. (c) Diurnal  
 64 cycles of OA factors. (d) The average fractional pie chart of OA factors to total OA. (e) The  
 65 average diurnal mass contributions of OA factors to total OA.

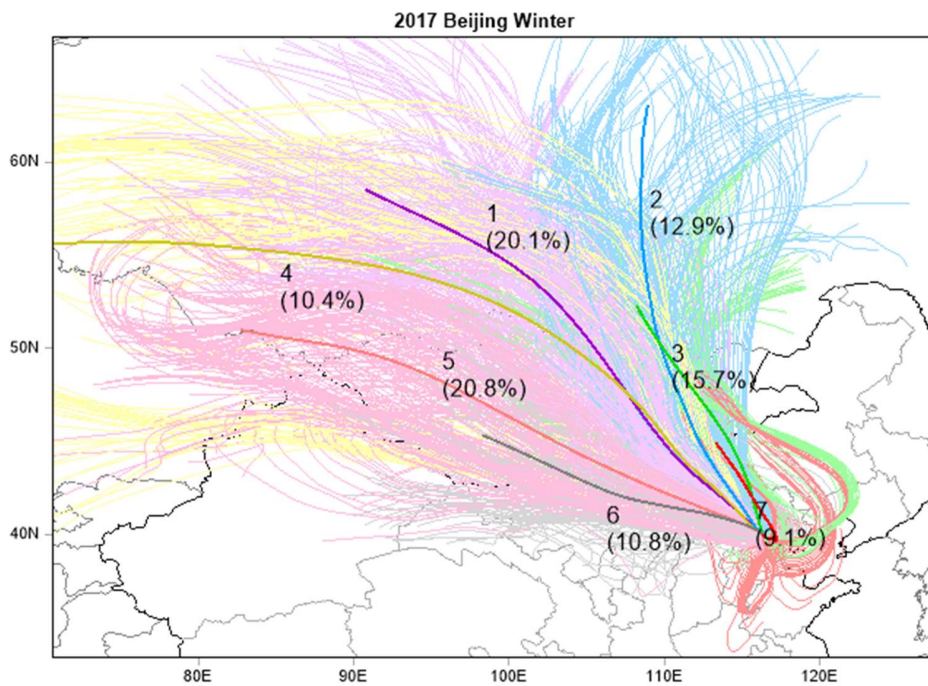


66

67 **Figure S12.** Comparison of observed (red) and CMAQ-simulated (blue) daily mean PM<sub>2.5</sub>  
 68 concentrations over Beijing during the winters of 2014 (a) and 2017 (b). Observation data was  
 69 obtained and averaged from 12 national observation stations in Beijing. Simulated concentrations  
 70 were extracted from the grids corresponding to the station locations.

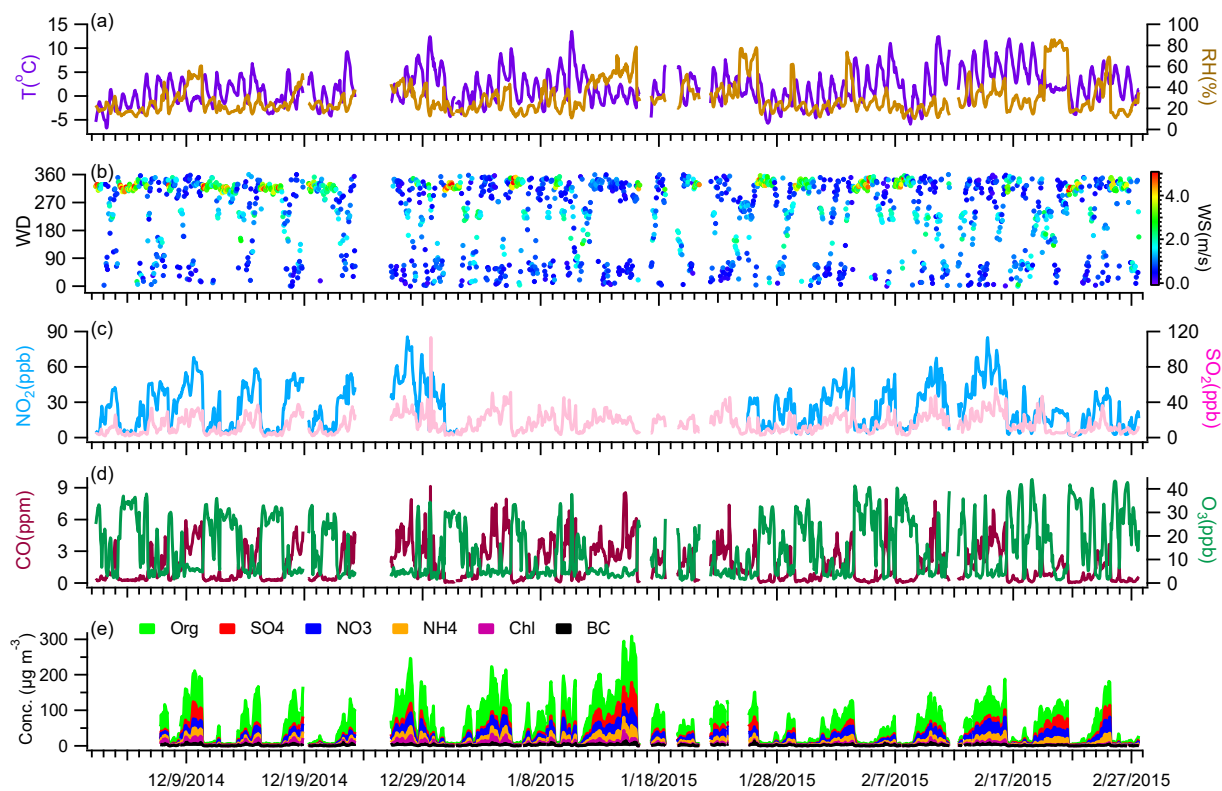


71



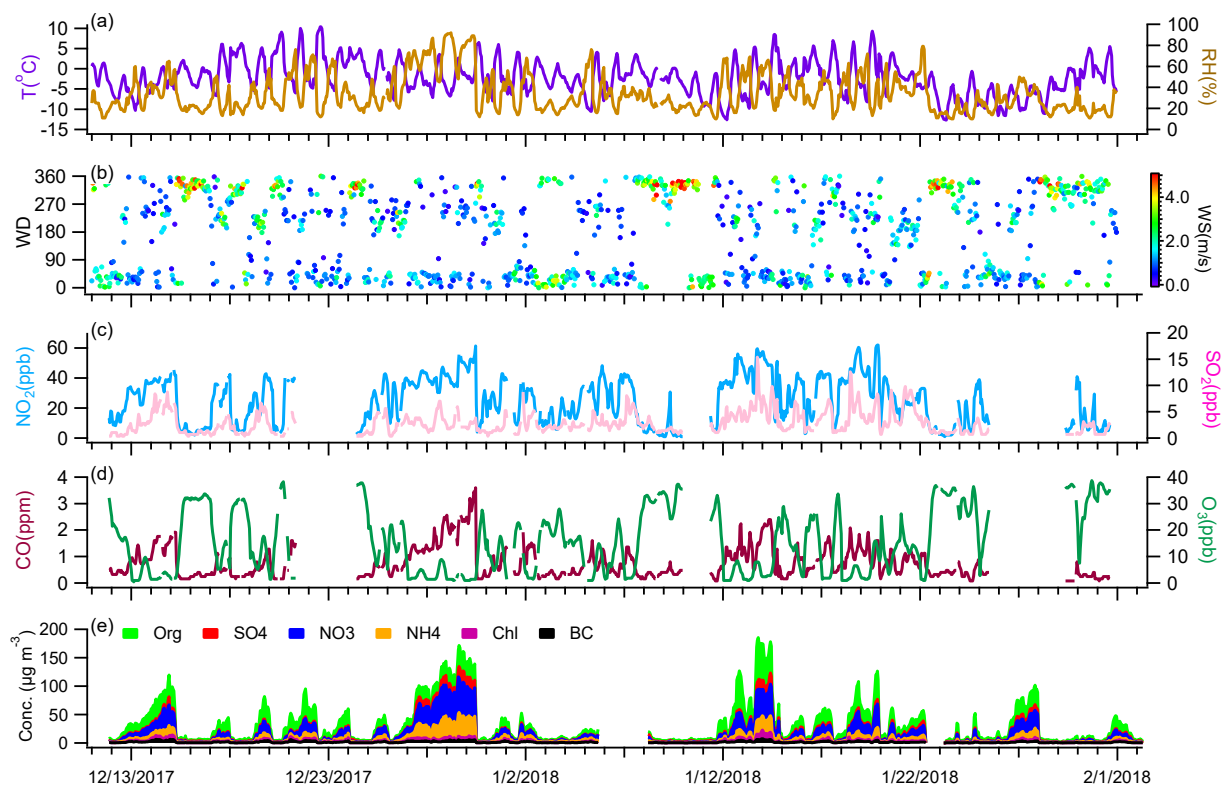
72

73 **Figure S13.** Back trajectories of air masses arriving in Beijing in winter 2014 and winter 2017  
 74 with unique colors for different clusters. The average percentage of each cluster is shown.



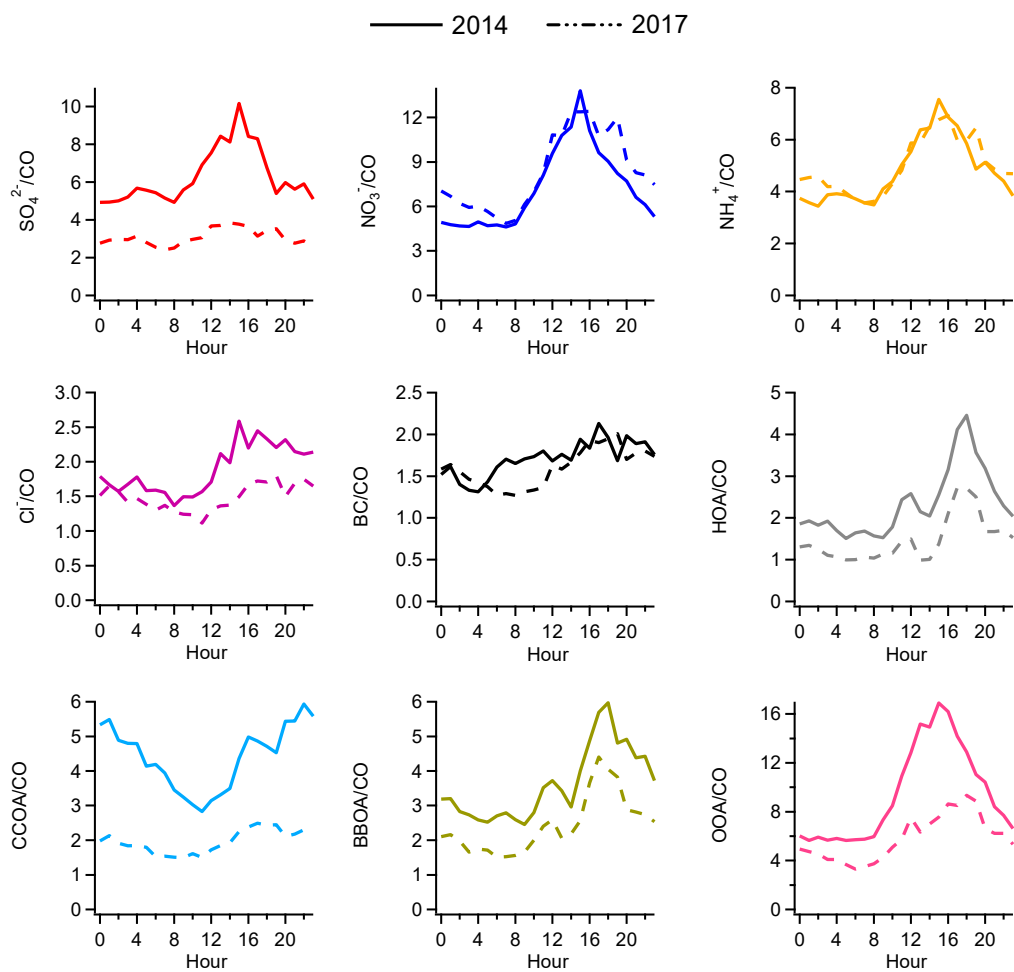
75

76 **Figure S14.** Temporal variations of (a, b) meteorological parameters, (c, d) gaseous species, and  
 77 (e) aerosol species during the winter of 2014.



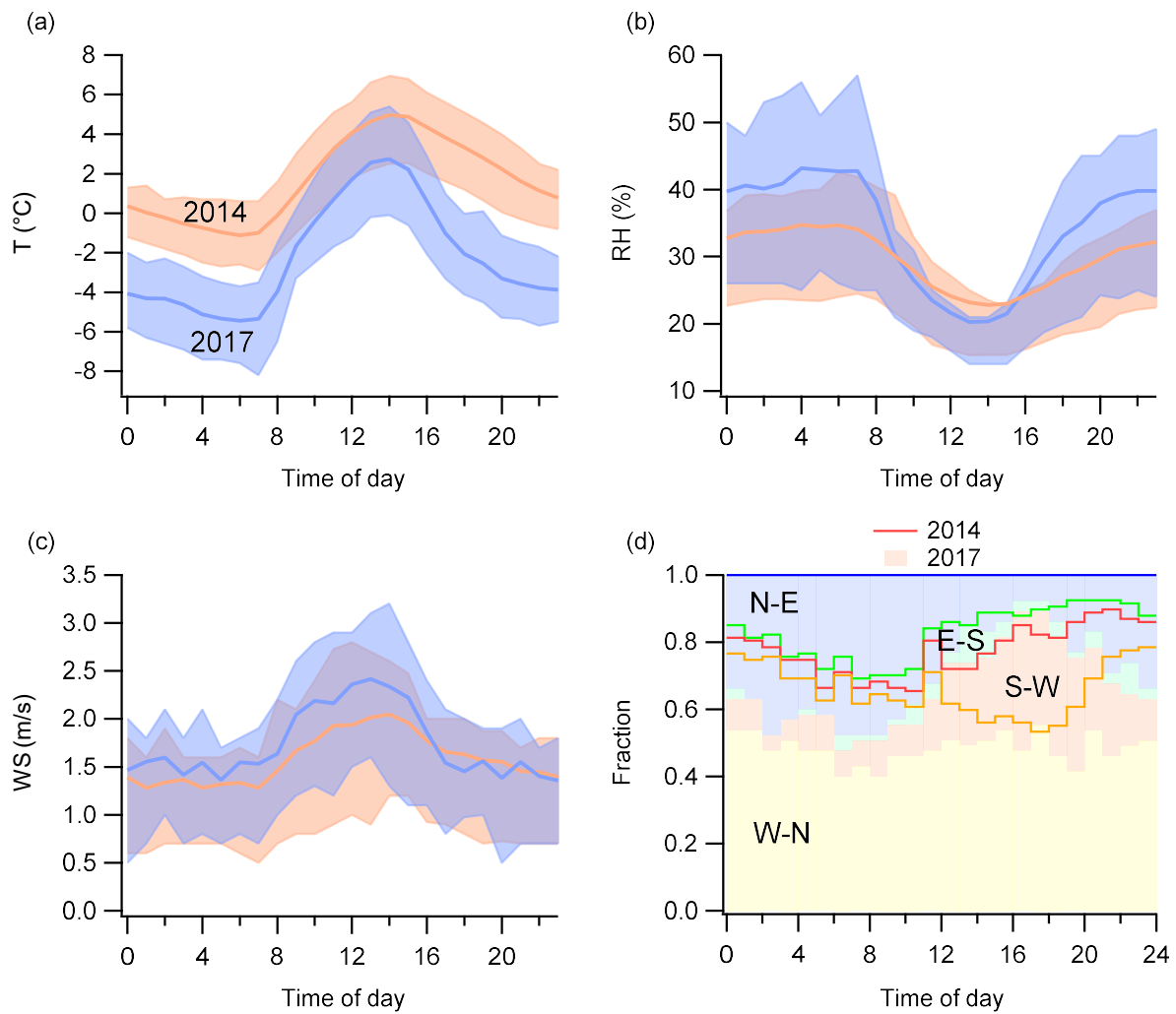
78

79 **Figure S15.** Temporal variations of (a, b) meteorological parameters, (c, d) gaseous species, and  
 80 (e) aerosol species during the winter of 2017.



81

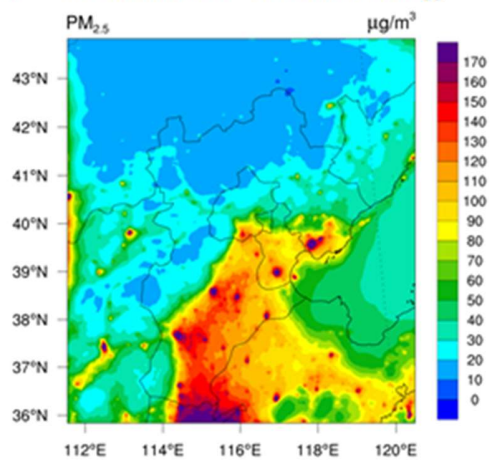
82 **Figure S16. Average diurnal cycles of CO-scaled aerosol species in the winter of 2014 (solid line)**  
 83 **and winter of 2017 (dashed line).**



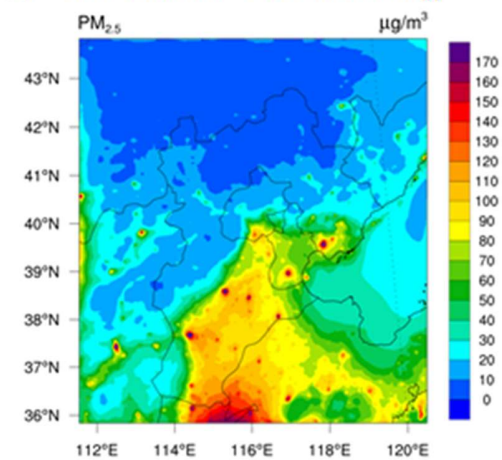
84

85 **Figure S176.** Diurnal cycles of meteorological parameters in 2014 and 2017. (a-c) The average  
 86 variations of temperature, relative humidity (RH), and wind speed (WS). The shaded areas indicate  
 87 25<sup>th</sup> and 75<sup>th</sup> percentiles. (d) The distribution of different wind directions through the day. The  
 88 lines and the stacked areas represent the year of 2014 and 2017, respectively.

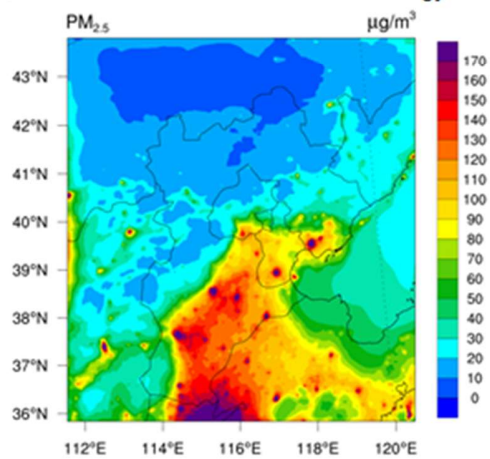
(a) 2014 Emission + 2014 Meteorology



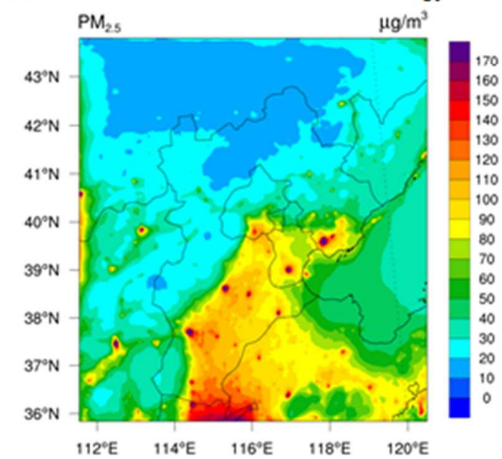
(b) 2017 Emission + 2017 Meteorology



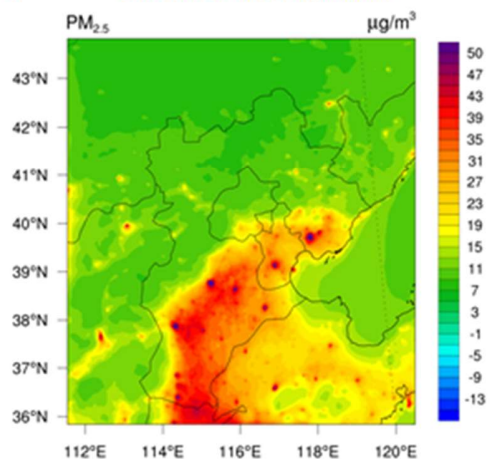
(c) 2014 Emission + 2017 Meteorology



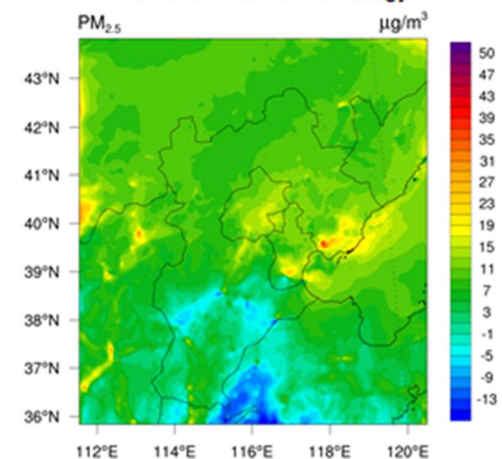
(d) 2017 Emission + 2014 Meteorology



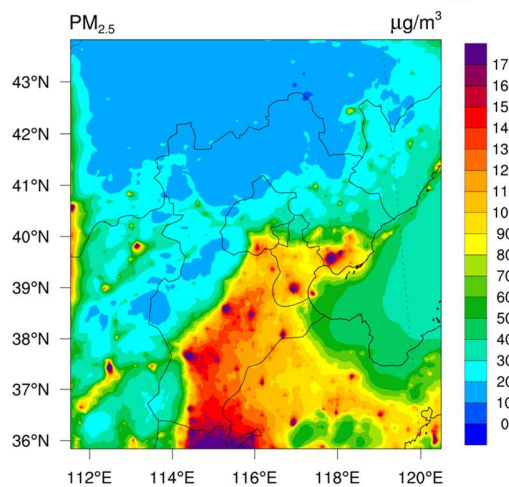
(e) Difference from Emission



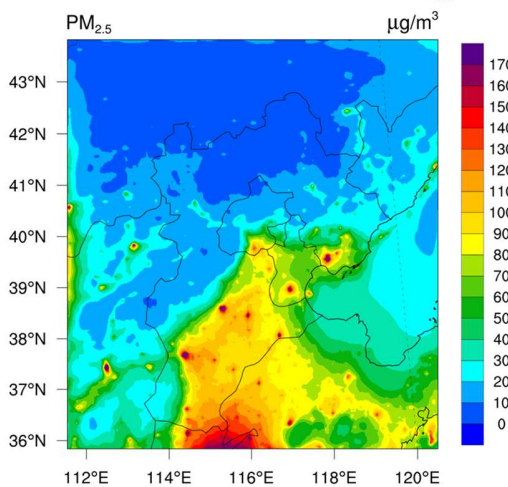
(f) Difference from Meteorology



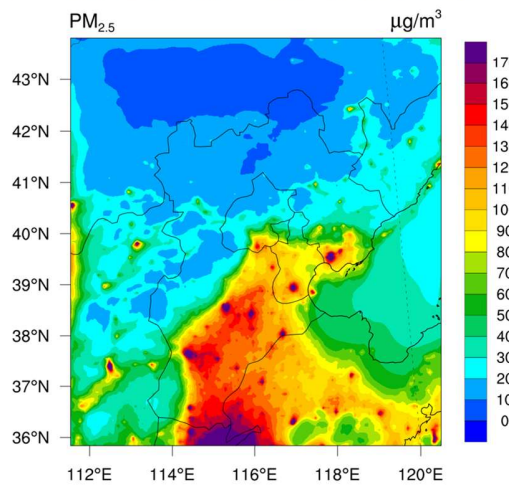
(a) 2014 Emission + 2014 Meteorology



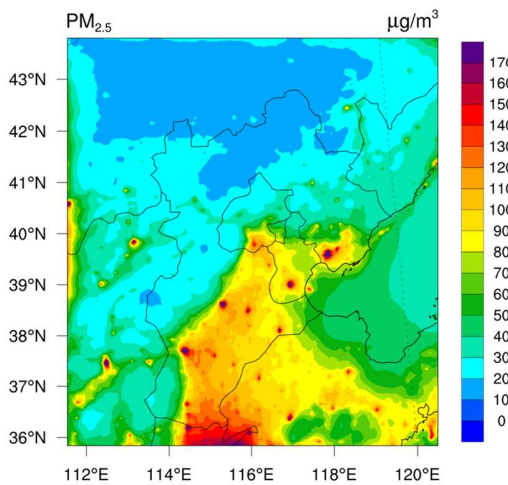
(b) 2017 Emission + 2017 Meteorology



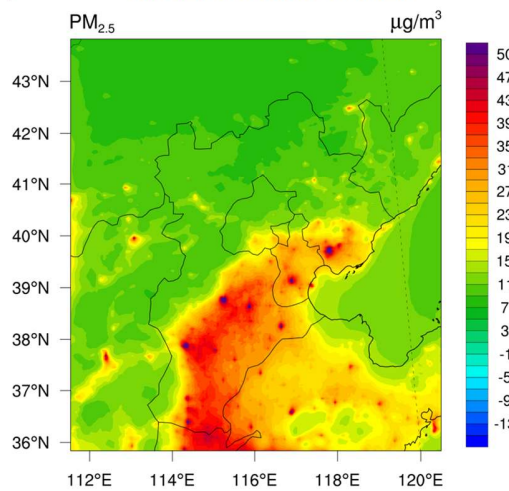
(c) 2014 Emission + 2017 Meteorology



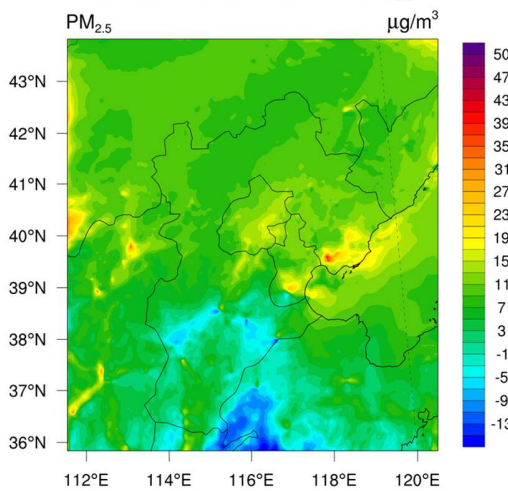
(d) 2017 Emission + 2014 Meteorology



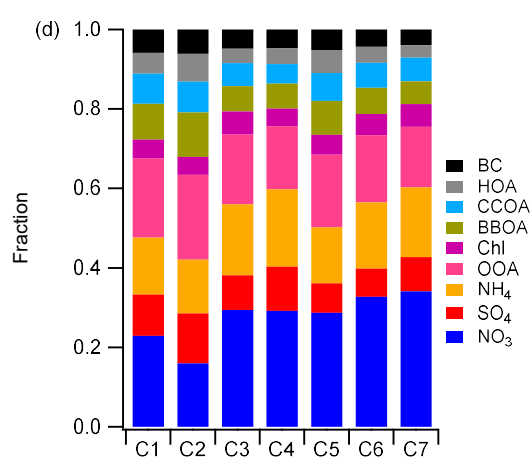
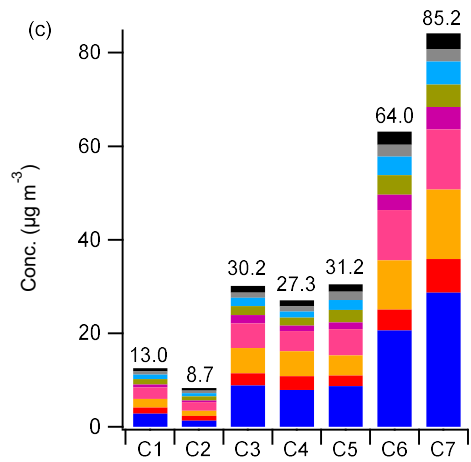
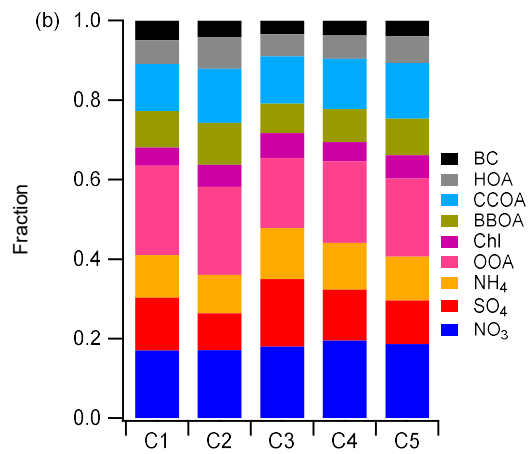
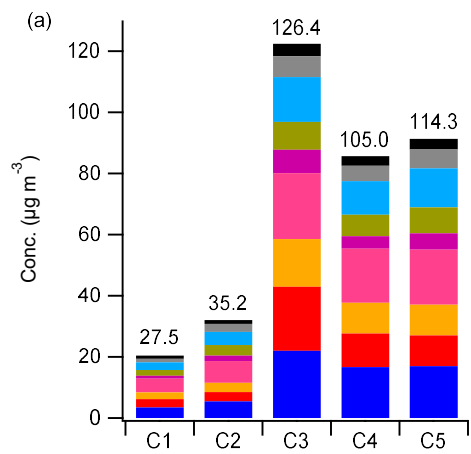
(e) Difference from Emission

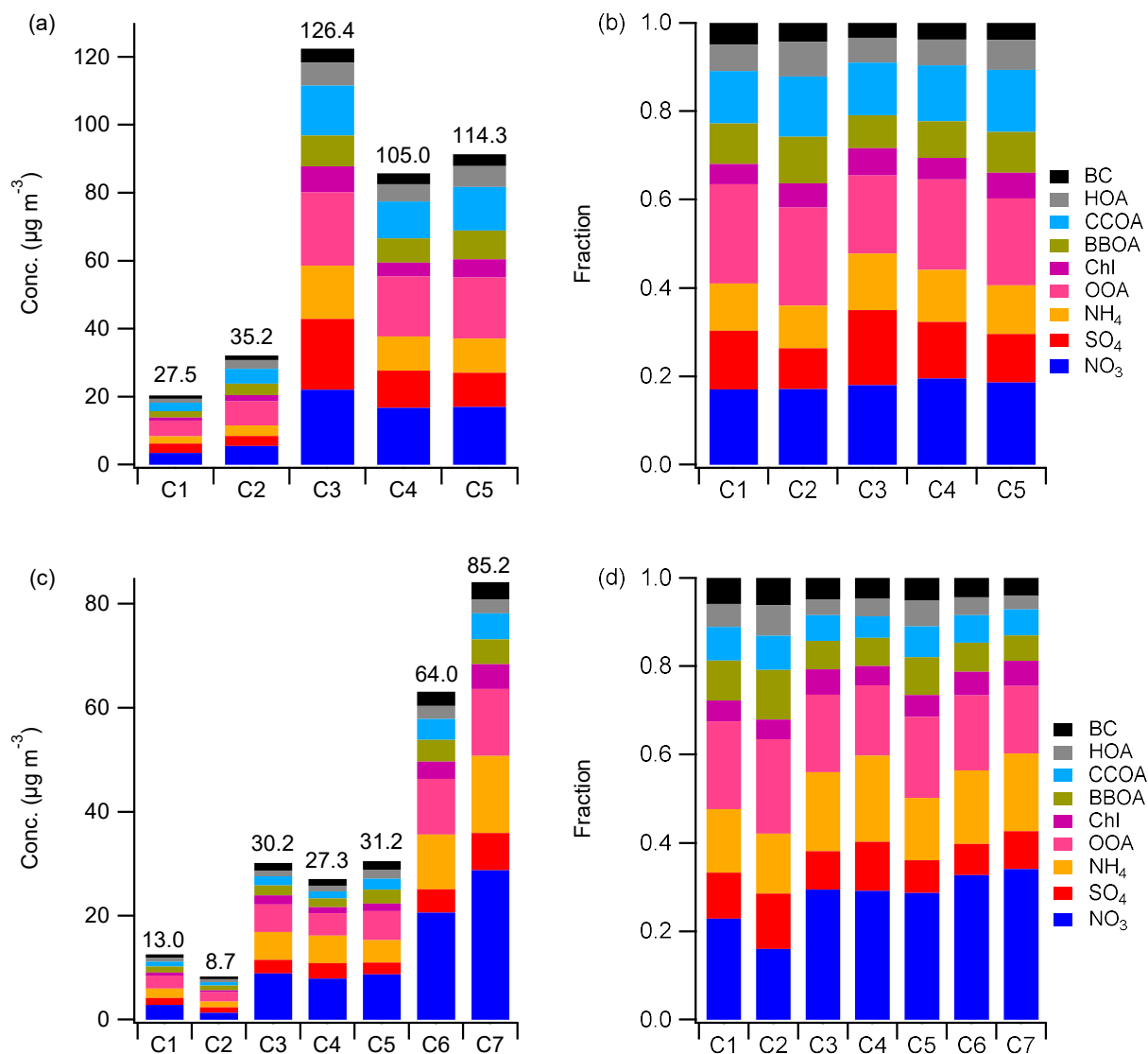


(f) Difference from Meteorology



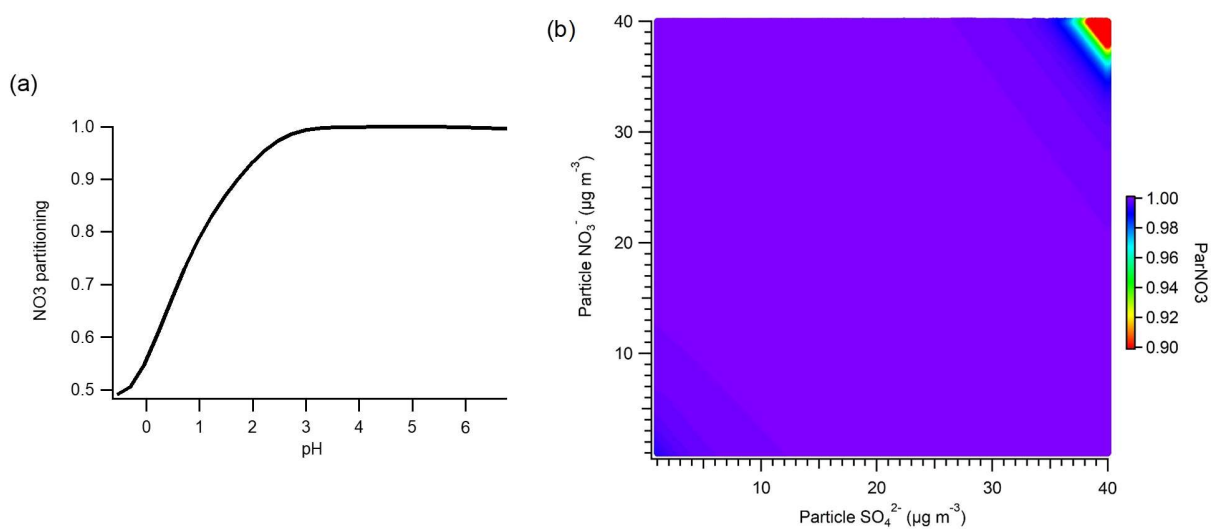
91 **Figure S187.** WRF-CMAQ simulated PM<sub>2.5</sub> concentration under different scenarios for the  
92 observation periods of 2014 and 2017.





94

95 **Figure S198.** The mass concentrations of aerosol species and their fractional contributions in total  
 96  $PM_{10}$  for different clusters in (a, b) winter 2014 and (c, d) winter 2017. The average  $PM_{10}$   
 97 concentration of each cluster is shown on the top of the bar.



98

99 **Figure S209.** (a) Variation of  $\epsilon(\text{NO}_3^-)$  as a function of particle pH. (b) Sensitivity of the fraction  
 100 of particulate nitrate to the mass concentrations of particulate sulfate.